

Editor-in-Chief B.E.Paton

Editorial board:

Yu.S.Borisov	V.F.Khorunov
A.Ya.Ishchenko	I.V.Krivtsun
B.V.Khitrovskaya	L.M.Lobanov
V.I.Kirian	A.A.Mazur
S.I.Kuchuk	Yatsenko
Yu.N.Lankin	I.K.Pokhodnya
V.N.Lipodaev	V.D.Poznyakov
V.I.Makhnenko	K.A.Yushchenko
O.K.Nazarenko	A.T.Zelnichenko
I.A.Ryabtsev	

International editorial council:

N.P.Alyoshin	(Russia)
U.Diltay	(Germany)
Guan Qiao	(China)
D. von Hofe	(Germany)
V.I.Lysak	(Russia)
N.I.Nikiforov	(Russia)
B.E.Paton	(Ukraine)
Ya.Pilarczyk	(Poland)
P.Seyffarth	(Germany)
G.A.Turichin	(Russia)
Zhang Yanmin	(China)
A.S.Zubchenko	(Russia)

Promotion group:

V.N.Lipodaev, V.I.Lokteva
A.T.Zelnichenko (exec. director)

Translators:

A.A.Fomin, O.S.Kurochko,
I.N.Kutianova, T.K.Vasilenko
PE «Melnik A.M.»

Editor

N.A.Dmitrieva
Electron galley:
D.I.Sereda, T.Yu.Snegiryova

Address:

E.O. Paton Electric Welding Institute,
International Association «Welding»,
11, Bozhenko str., 03680, Kyiv, Ukraine

Tel.: (38044) 287 67 57

Fax: (38044) 528 04 86

E-mail: journal@paton.kiev.ua

http://www.nas.gov.ua/pwj

State Registration Certificate
KV 4790 of 09.01.2001

Subscriptions:

\$324, 12 issues per year,
postage and packaging included.
Back issues available.

All rights reserved.

This publication and each of the articles
contained herein are protected by copyright.
Permission to reproduce material contained in
this journal must be obtained in writing from
the Publisher.

Copies of individual articles may be obtained
from the Publisher.

CONTENTS

Boris Paton — Laureate of the Global Energy Prize 2

SCIENTIFIC AND TECHNICAL

Kuchuk-Yatsenko S.I., Shvets V.I., Shvets Yu.V., Taranova T.G.
and *Gordan G.N.* Causes of crack formation in the HAZ of
cast high-manganese steel in flash-butt welding 4

Makhnenko V.I. and *Romanova I.Yu.* Probabilistic
characteristics of high-cycle fatigue resistance of structural
steel welded joints 7

Ryabtsev I.A., Kondratiev I.A., Vasiliev G.V., Zhdanov V.A. and
Babinets A.A. Investigation of structure and service properties
of deposited metal for reconditioning and strengthening of
rolling mill rolls 12

Khorunov V.F., Maksymova S.V. and *Stefaniv B.V.* Effect of tin
additions on structure and technological properties of brazing
filler metals of the Ag-Cu-Zn system 16

Pismenny A.S., Prokofiev A.S., Pismenny A.A., Novikova D.P.,
Yukhimenko R.V., Polukhin V.V., Ptashinskaya I.I. and
Polukhin Yu.V. Properties of the welded joints of tubular billets
produced by pressure braze-welding with a forming device 22

Gedrovich A.I., Tkachenko S.A. and *Galtsov I.A.* Evaluation of
stress-strain state of dissimilar welded joints from
10KH13G18D + 09G2S steels 25

INDUSTRIAL

Kuchuk-Yatsenko S.I., Kachinsky V.S., Ignatenko V.Yu.,
Goncharenko E.I. and *Koval M.P.* Magnetically-impelled arc
butt welding of pipes of steel X70 29

Savitsky M.M., Pismenny A.S., Savitskaya E.M., Pritula S.I.
and *Babenko S.K.* Technology and equipment for manufacture
of high-pressure cylinder bodies of sheet rolled steel 32

Seyffarth P. Modern equipment for shipbuilding 38

Pervukhin L.B., Pervukhina O.L. and *Bondarenko S.Yu.*
Cleaning and activation of welded surfaces during explosion
welding 41

NEWS

8th International Conference on Beam Technology-2010 44

XIV International Specialised Exhibition «Welding-2010» 46

Fifth International Conference «Mathematical Modelling and
Information Technologies in Welding and Related Processes» 48

Session of the Scientific Council on New Materials at the
Natural Sciences Committee of the International Association
of the Academies of Sciences 49

Specialized Forum «Paton Expo 2010» 51

BORIS PATON — LAUREATE OF THE GLOBAL ENERGY PRIZE

The Global Energy Prize was instituted in 2002. The idea of introducing it was put forward by a group of known Russian scientists, supported by the largest energy companies, and approved by the President of Russia. It is one of the most prestigious prizes, which has been awarded annually since 2003 for outstanding scientific achievements in the field power engineering.

On the 18th of June, the President of Russia Dmitry Medvedev in St-Petersburg presented the Global Energy Prize to academicians Boris Paton and Alexander Leontyev. The ceremony took place within the framework of the Petersburg International Economic Forum.

Boris Paton received the honorary award for his «contribution in solving scientific and technological problems of pipeline transport of energy sources and machinery», and Russian scientist Alexander Leontyev — for «fundamental research in the intensification of processes of heat exchange at power installations».

Prof. Boris Paton was recognised to be the prominent research leader by Ukrainian, Russian and world scientists. Upon graduating from the Kiev Polytechnic Institute in 1941 in speciality of electrical engineer, he immediately started working in the defence industry, first at the «Krasnoe Sormovo» plant in Gorky (now Nizhny Novgorod), and then in Kiev at the Electric Welding Institute, which was evacuated to Nizhny Tagil to the Ural Car Building Plant (Uralvagonzavod).



Boris Paton is speaking at the awarding ceremony

By continuing the work of his father, the legendary Evgeny Paton, he made several fundamental inventions in the field of electric welding, took an active part in upgrading and application of high-speed automatic submerged arc welding in tank construction and arms production, and laid the basis for a new scientific direction — automatic control of welding processes. Boris Paton developed a fundamentally new welding method — electroslag welding, which was used to solve the problem of production of unique pressure vessels for heat, nuclear and hydraulic power generation, chemical engineering and manufacture of large-size units of seagoing ships.



The President of Russia Dmitry Medvedev is presenting the Global Energy Prize to academician Boris Paton



Academicians Boris Paton and Alexander Leontyev — laureates of the 2010 Global Energy Prize

As early as 10 years after graduating from the institute, Boris Paton became a corresponding member, after another 7 years — academician of the Ukr. SSR Academy of Sciences, and after another 4 years — academician of the USSR Academy of Sciences.

For 48 years Prof. Boris Paton has been heading the National Academy of Sciences of Ukraine, and since 1993 — the International Association of Academies of Sciences.

«Academician Paton made a vast contribution in all aspects of power engineering, — said Academician Nikolai Laverov, the Vice President of the Russian Academy of Sciences. — His activity plays

an exceptional role in power generation of the CIS countries and, on the whole, in feeding fuel to different countries all over the world. Owing to his work in welding of pipes, the energy is reliably supplied to millions of people».

Results of the research, engineering and organisational activities of Boris Paton are a major contribution to addressing the global problems in power generation, such as pipeline transportation of power supplies, heat, nuclear and hydraulic power engineering, defence industry, and utilisation of non-conventional energy types. The results he achieved are unique in their technical level and scales of application to supply energy to many countries, and serve to improve the human health and habitat.

We are heartily congratulating our dear Boris Evgenievich with a high appraisal of his work, and wishing him strong health, new creative achievements, success and happiness.

Editorial Board



CAUSES OF CRACK FORMATION IN THE HAZ OF CAST HIGH-MANGANESE STEEL IN FLASH-BUTT WELDING

S.I. KUCHUK-YATSENKO, V.I. SHVETS, Yu.V. SHVETS, T.G. TARANOVA and G.N. GORDAN

E.O. Paton Electric Welding Institute, NASU, Kiev, Ukraine

Results of investigations of the causes of cracks forming in the HAZ of cast high-manganese steel 110G13L in its flash-butt welding to austenitic steel 08Kh18N10T are presented. It is shown that cracking is caused by segregational heterogeneity of distribution of phosphorus, which occurs both in solidification of castings and in the solid solution under thermal deformation conditions of welding. To prevent cracking, it is recommended to pay special attention to the process of homogenizing annealing of 110G13L castings.

Keywords: flash-butt welding, pulsed flashing, high-manganese steel 110G13L, austenitic insert, frog, HAZ, phosphorus segregation, cracks

Frogs are one of the most critical elements of railway tracks. Welded structures are widely used in their manufacture in the world. PWI developed technology and equipment for welding railway frogs in the shop [1]. This technology is based on the process of pulsed flash-butt welding [2], when a core of high-manganese 110G13L steel is joined to rail steel M76 through an intermediate insert from chromium-nickel austenitic steel 08Kh18N10T.

Outgoing inspection of some batches of welded frogs in a number of cases revealed cracks in the toe section in the near-weld zone of 110G13L steel after final machining (Figure 1), which were the cause for rejection of the finished product.

The objective of this work is establishing the causes for crack initiation in 110G13L steel and development of measures to prevent them.

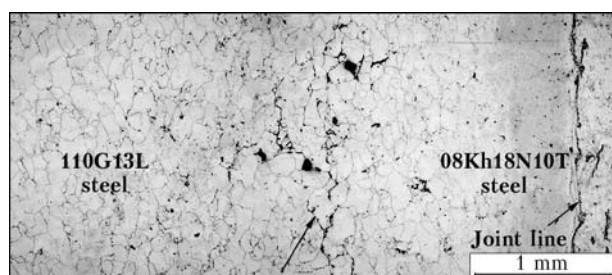


Figure 1. Macrostructure of fusion zone of 110G13L steel with 08Kh18N10T steel in the frog welded joint

Table 1. Composition of 110G13L steel (wt.%)

Source	C	Mn	Si	S	P	Cr	Ni	Cu
GOST 2176-77	0.9-1.4	11.5-15.0	0.3-1.0	≤0.05	≤0.12	≤3.8	≤0.7	≤0.3
X-ray microprobe analysis	0.92-0.95	12.3-12.7	0.46	0.021-0.023	0.033-0.036	N/D	N/D	N/D

Flash-butt welding was performed in K924M welding machine, developed at PWI, in the mode accepted for industrial production. Welding process duration was 90-110 s, welding allowance was (3.0 + 1.5) mm, insert width in the welded joint was 18-20 mm.

Analysis of microstructure and chemical heterogeneity of the HAZ of 110G13L steel joint was performed to reveal the causes for cracking. The cracked area and adjacent area without cracks were analyzed. Investigations were conducted in optical microscope «Neophot-32», microscope-microanalyser SX-50 of Camebax, scanning electron microscope JSM-840 with «Link-systems» microanalyser. Microstructure was revealed by electrolytic etching in 10 % water solution of ammonium triosulphate.

Spectral analysis of chemical composition of 110G13L steel, used in frog manufacture, corresponded to GOST 2176-77 (Table 1). Phosphorus and sulphur content was much lower than the standard requirement.

Macrostructure analysis showed (see Figure 1) that metal fracture in all the cases runs in a layer about 0.5 mm wide, which is located in parallel to the joint line at about 1.5-2.0 mm distance. Cracking is of intergranular nature, i.e. is concentrated on the boundaries of austenitic grains of 110G13L steel.

Investigations showed that metal of 110G13L steel joint has a stable austenitic structure with unit carbide inclusions and a considerable quantity of nonmetallic inclusions. Under the impact of thermal cycle of welding first a refinement of austenite grains occurs in the HAZ metal, and in the near-contact layer austenite grain size increases as a result of collective recrystallization. An austenitic structure with strength prop-

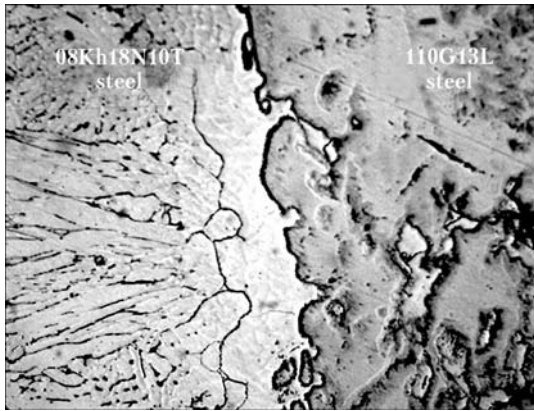


Figure 2. Microstructure ($\times 400$) of the transition zone on the contact line of fusion of 110G13L steel with 08Kh18N10T steel

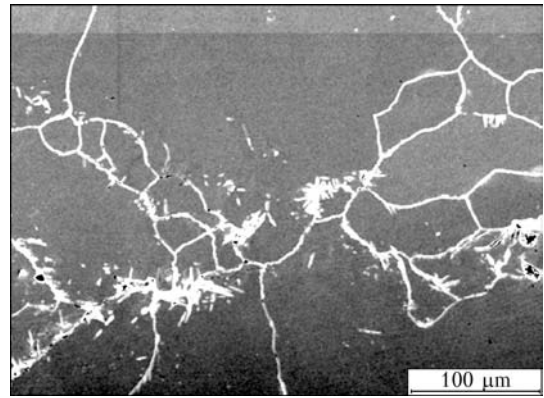


Figure 3. HAZ microstructure of 110G13L steel in the section with phosphide eutectics

erties on the level of those of base metal forms in the transition zone on the contact boundary of 110G13L steel with 08Kh18N10T steel (Figure 2). In the HAZ region at approximately 1.5–2.0 mm distance from the joint line, a certain structural component is present along the grain boundaries, which, obviously, is what causes the cracking. In areas with a high content of this structure an acicular phase forms from the grain boundaries (Figure 3).

Analysis of nonmetallic inclusions of 110G13L steel was performed to clarify the nature of formation of this structural component. It is established that the steel contains a considerable volume fraction of complex sulphides (Figure 4, *a, b*), the central part of which is made of aluminium sulphide, and the peripheral part are manganese and iron sulphides. There are also individual inclusions of aluminium sulphide. Clusters of fine nitride inclusions of a regular geometrical shape, as well as, possibly, titanium carbonitrides, non-uniformly distributed in the bulk, are also observed (Figure 4, *c*). Phosphide inclusions are absent. This is in agreement with the results of earlier investigations, which showed that phosphides could not be found even at 0.1 wt.% P in 110G13L steel [3].

Analysis of transformation of nonmetallic inclusions in the HAS showed that high-temperature nitrides remain stable up to steel melting temperature. Sulphide inclusions change only slightly compared to those in the base metal, at least in the section of the layer with the newly formed structural component. Thus, contamination of 110G13L steel by nonmetallic inclusions is not a source of formation of the above component.

According to the curves of chemical element distribution (Figure 5), an increase of manganese and phosphorus content is found at transition through grain boundaries with the new structural component. At analysis of the composition of accessible for study microvolumes at the junction of three grains, it is established that phosphorus and manganese content is equal to 12.040 and 29.826 wt.%, respectively (Table 2, No.1). This gives rise to the conclusion that cracking is caused by the described in literature proc-

ess of formation of a low-melting phosphide (carbo-phosphide at high carbon content) eutectic in manganese steels, embrittling the grain boundaries [4].

At 0.033–0.043 wt.% P content in 110G13L steel the cause for phosphide eutectic formation, evidently, is a local increase of this element concentration, caused by its non-uniform distribution. The latter can result,

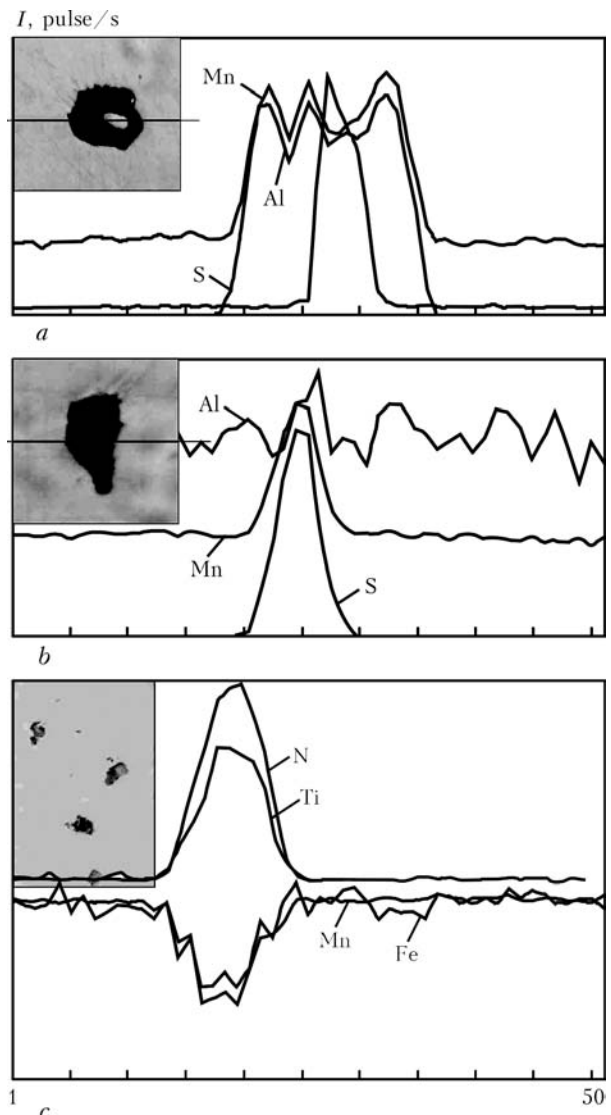


Figure 4. Distribution of chemical elements in sulphides (*a, b*) and nitrides (*c*) of 110G13L steel (I – radiation pulse; 1.02 μm step)

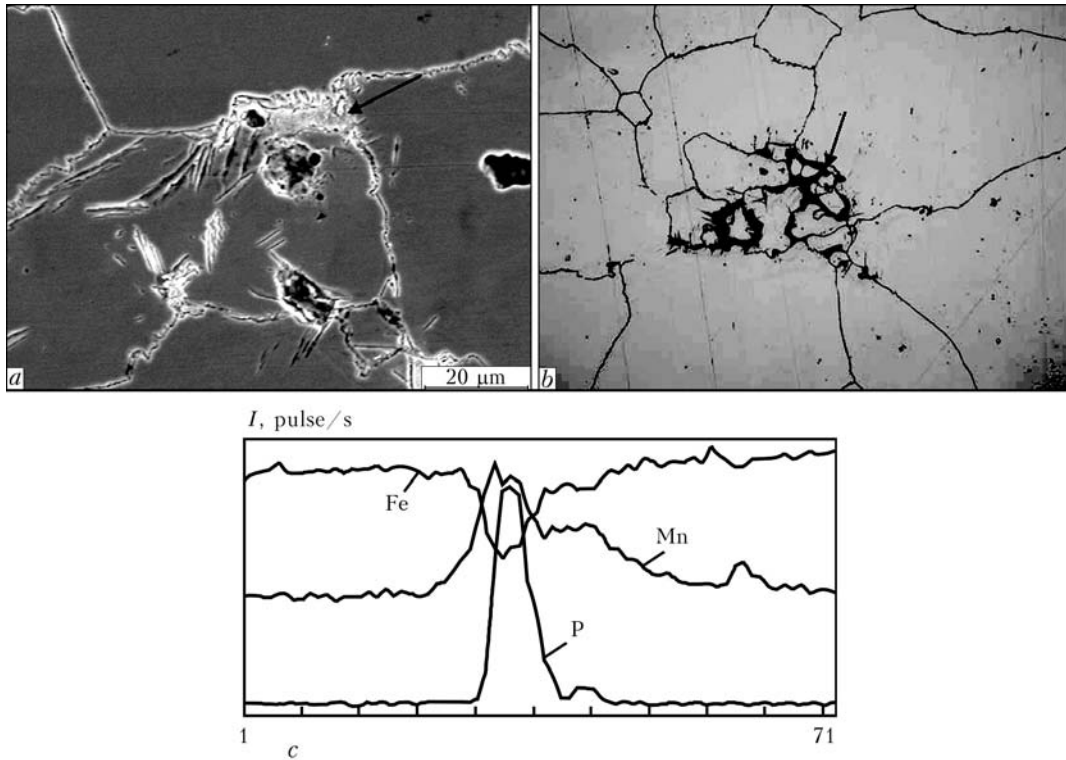


Figure 5. Carbophosphide eutectics in microstructure of 110G13L steel (marked by arrows): *a* – electron microscopy image; *b* – optical image (×400); *c* – distribution of chemical elements in the zone of carbophosphide eutectic (2 μm step)

primarily, from primary segregation – phosphorus greatly widens the temperature interval of steel solidification. Moreover, in welding segregation of surface-active phosphorus in the solid phase and grain boundary enrichment in it are possible in iron in the thermodeformational impact zone. This, obviously, occurs in the HAZ layer at 1.5–2.5 mm distance from the joint line, where the temperature is approximately equal to 900–1000 °C in welding.

It is known that the temperature of eutectic reaction $l \rightarrow \gamma\text{-Fe} + (\text{Fe}, \text{Mn})_2\text{P}$ in Fe–Mn–P system is equal to about 950 °C [5]. Increase of phosphorus and manganese content on grain boundaries causes their concentration melting, which leads to development of the process of eutectic phase formation. Manganese, phosphorus, as well as carbon, actively diffuse into the melt, as their solubility in the liquid phase is by several orders of magnitude higher than in the solid phase.

Solidification of the formed intergranular melt occurs with formation of phosphide eutectics and acicular carbides growing from grain boundaries.

In the HAZ layer of 110G13L steel up to 1.5 mm wide adjacent to the joint line, the thermal impact corresponds to homogenizing annealing. Concentrational heterogeneity of phosphorus and manganese in this region is eliminated – intergranular eutectic interlayers are absent in the microstructure.

In the more remote HAZ regions diffusion mobility is insufficient to achieve phosphorus concentration on grain boundaries, at which partial melting occurs.

Thus, investigation results showed that in flash-butt welding conditions for formation of phosphide eutectics are in place in the HAZ metal of 110G13L steel at 1.5–2.0 mm distance from the joint line. As its formation occurs in an irregular manner, it is anticipated that the main cause for its appearance at average phosphorus content of 0.033–0.036 wt.% in steel is the non-uniformity of its distribution. Achievement of a uniform distribution of phosphorus in 110G13L steel is difficult because of its low diffusion mobility in iron. One of the ways to achieve a uniform distribution of phosphorus is to strictly follow the specified mode of homogenizing annealing of 110G13L

Table 2. Results of X-ray microprobe analysis of composition (wt.%) of the new structural component of the layer with microcracks in 110G13L steel

No	P	Si	Mn	Cr	Fe	C
1	12.040	0.434	29.826	0.438	52.182	5.054
2	2.234	0.659	21.361	0.213	73.352	2.181
3	1.298	0.634	18.148	0.163	78.561	1.195
4	3.534	0.672	21.936	0.214	71.428	2.204



steel castings; another one is to lower phosphorus content. In order to prevent cracks in manganese steels the recommended phosphorus content should be less than 0.02 wt.% [4, 5].

CONCLUSIONS

1. In manufacture of rail frogs by flash-butt welding low-melting intergranular interlayers of phosphide eutectics causing cracking, can form at the distance of 1.5–2.5 mm from the joint line in the HAZ metal of 110G13L steel.

2. Formation of intergranular interlayers of phosphide eutectics at phosphorus content of 0.033–0.036 wt.% is caused by segregational heterogeneity of its distribution at solidification of castings.

3. To prevent formation of intergranular interlayers of phosphide eutectics in the HAZ of 110G13L steel it is necessary to strictly follow the established mode of homogenizing annealing of castings from 110G13L steel.

1. *TU U DP 32-4520.13.500-007-2002:2006*: Crossing and frogs with welded rail ends of R65, R50 and USC60 type with and without insert. Test batch. Valid from 01.01.2003 to 01.01.2006.
2. Kuchuk-Yatsenko, S.I., Shvets, Yu.V., Dumchev, E.A. et al. (2005) Flash butt welding of railway frogs with rail ends using an intermediate insert. *The Paton Welding J.*, **1**, 2–4.
3. Ershov, G.S., Poznyak, L.A. (1998) *Formation of structure and properties of steels and alloys*. Kiev: Naukova Dumka.
4. Kondratyuk, S.E., Kasatkin, O.G. (1987) *Fracture of cast manganese steel*. Kiev: Naukova Dumka.
5. Goudremont, E. (1960) *Special steels*. Vol. 2. Moscow: Metallurgizdat.

PROBABILISTIC CHARACTERISTICS OF HIGH-CYCLE FATIGUE RESISTANCE OF STRUCTURAL STEEL WELDED JOINTS

V.I. MAKHNENKO and I.Yu. ROMANOVA

E.O. Paton Electric Welding Institute, NASU, Kiev, Ukraine

Issues of probabilistic determination of resistance of welded joints to high-cycle fatigue fracture are considered. The probability of failure-free performance of the joints for different types and variable values of applied loads is analysed.

Keywords: *welded joints, cyclic loading, high-cycle fatigue, fatigue resistance, probabilistic prediction methods, safe operation*

The growth of interest has been noted lately in probabilistic methods for estimation of beginning of the limiting state of welded joints under different loads, this being associated to a substantial degree with a large number of factors taking place within the joining zone and affecting the beginning of the limiting state. This is particularly important for alternating loads and fatigue fractures of welded joints. The presence of many factors, which are hard to describe in deterministic expressions, leads to a wide spread of data of fatigue tests of the welded joints.

The use of stochastic methods for calculation of fatigue of the welded joints requires clear ideas of the probabilistic characteristics of fatigue fracture resistance of welded joints on different structural materials. Such characteristics for certain welded joints and materials (mainly structural steels) in the form of a range of variations of normal rated stresses, $\Delta\sigma$, and probability of fracture were obtained experimentally [1–3, etc.].

The efforts of the International Institute of Welding (IIW) [4], dedicated to high-cycle fatigue of welded joints on ferritic-pearlitic structural steels with strength of up to 900 MPa showed that at failure

probability $Q_p = 5 \cdot 10^{-2}$ (no-fracture probability is $9.5 \cdot 10^{-1}$) the fatigue fracture resistance can be sufficiently reliably described by rated stress ranges *FAT* on a base of $N = 2 \cdot 10^6$ cycles. In this case, the permissible ranges under regular cyclic loading are determined by the following relationship [4]:

$$[\Delta\sigma] = FAT \frac{f_1(N)f_2(R)}{\gamma_m f_3(\delta)}, \quad (1)$$

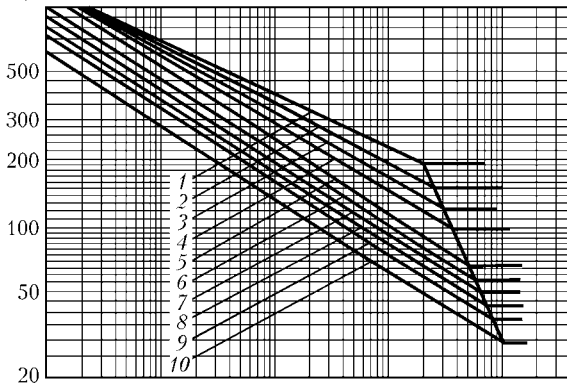
where $f_1(N)$, $f_2(R)$ and $f_3(\delta)$ are the corrections for durability N , cycle asymmetry R and thickness δ of a workpiece welded (at $N < 2 \cdot 10^6$ cycles, $R \geq 0.5$ and $\delta > 25$ mm, each of these corrections is more than 1); γ_m is the safety factor equal to 1.0–1.4, i.e. at $f_1 = f_2 = f_3 = 1$ and $\gamma_m = 1$ the failure probability is guaranteed at a level of approximately 0.05.

Naturally, safety grows at $\gamma_m > 1$, and the failure probability dramatically decreases as a result of fatigue fracture.

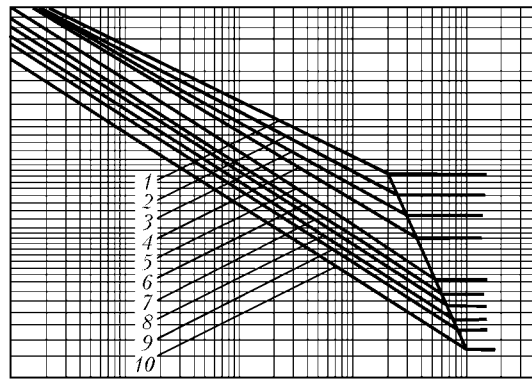
Considering the IIW recommendations [4], it is of high practical interest to supplement them with the data on fracture probability for different *FAT* values and classes K_x of the joints, depending on the required value of durability N and load level $\Delta\sigma$. For this purpose it is possible to use the already published experimental results on fracture probability of different types of the welded joints, by relating these data to the recommendations given in [4]. The search for



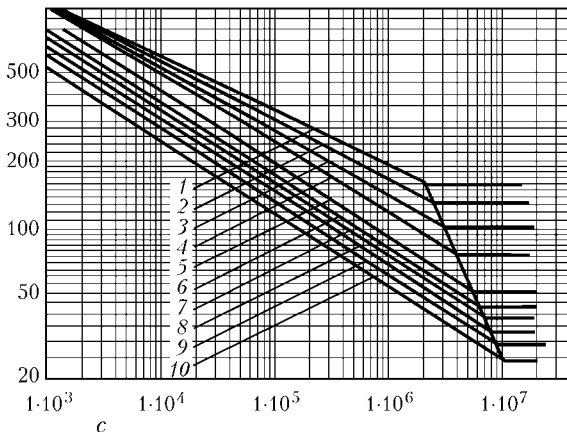
$\sigma_r, N/mm^2$



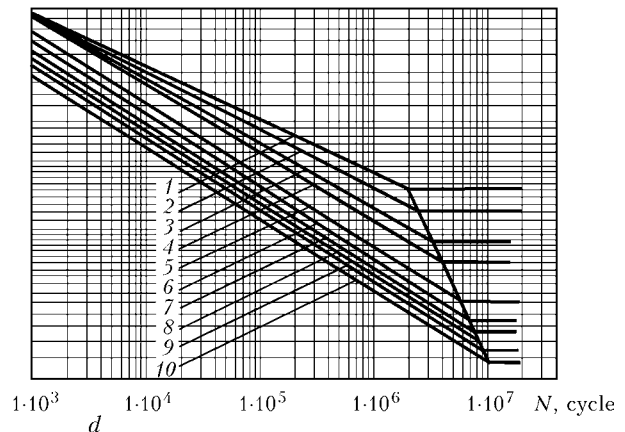
a



b



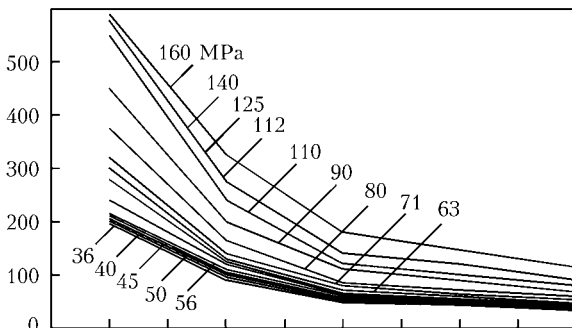
c



d

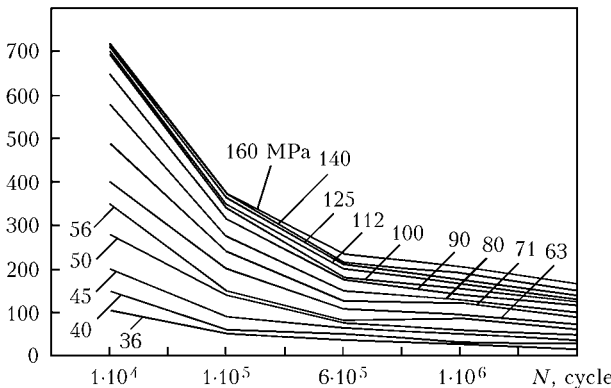
Figure 1. Experimental data [5] on fatigue resistance of different types of welded joints at failure probability $Q_p = 1 \cdot 10^{-2}$ (a), $1 \cdot 10^{-3}$ (b), $1 \cdot 10^{-4}$ (c), $1 \cdot 10^{-5}$ (d) and at $K_x = 1.3$ (1), 1.5 (2), 1.7 (3), 2.0 (4), 2.3 (5), 2.6 (6), 3.0 (7), 3.5 (8), 4.0 (9) and 5.0 (10)

A, MPa



a

B, MPa



b

Figure 2. Weibull equation parameters A (a) and B (b) versus durability N and class of a joint from 36 to 160 MPa

the corresponding published data led to a publication of the manual by Swedish Company «Svenkt Stal» in 1987, dedicated to design (strength calculation) of weldments of extra high-strength (EHS) and abrasion-resistant (AR) steels for equipment of the type of excavating machines, dump trucks, mining, felling and other machines [5]. The steels (especially EHS) correspond in full to those described in [4], and the set of the welded joints in [5] also corresponds to that considered in [4]. However, the classification employed is different. A class of the joint in [5] is determined by ratio $K_x = 315/\sigma_r$, where σ_r is the maximal stress at $R = 0$, i.e. $\sigma_r \approx \Delta\sigma$. Figure 1 and Table 1 give data on different values of failure probability Q_p , K_x , durability N and $\sigma_r = \Delta\sigma$ at $R = 0$, this corresponding to

$$\sigma_r = FAT f_2(R) f_4(Q_p), \quad (2)$$

where f_2 is the correction for cycle asymmetry coefficient R according to [4] at $R = 0$; $f_2(R) = 1.2$; and $f_4(Q_p)$ is the correction related to probability Q_p other than 0.05, corresponding to FAT according to [4].

To describe Q_p , we suggest using the three-parameter Weibull law in the form of

$$Q_p = \left(\frac{\Delta\sigma - A}{B} \right)^n, \quad (3)$$



Table 1. Maximal stress σ_r (N/mm^2) according to [5]

N, cycle	K_x									
	1.3	1.5	1.7	2.0	2.3	2.6	3.0	3.5	4.0	5.0
$Q_p = 1 \cdot 10^{-2}$										
$1 \cdot 10^3$	900	900	900	900	900	900	900	800	720	600
$1 \cdot 10^4$	690	680	620	580	540	460	420	370	340	280
$1 \cdot 10^5$	400	350	325	290	245	220	195	175	160	135
$6 \cdot 10^5$	260	220	195	170	138	120	110	100	87	74
$1 \cdot 10^6$	220	190	168	142	115	103	92	83	75	62
$2 \cdot 10^6$	185	160	138	115	93	80	73	65	58	48
$Q_p = 1 \cdot 10^{-3}$										
$1 \cdot 10^3$	900	900	900	900	900	856	781	705	655	554
$1 \cdot 10^4$	636	598	559	529	450	398	362	327	304	257
$1 \cdot 10^5$	357	321	289	258	209	184	168	152	141	119
$6 \cdot 10^5$	228	197	176	147	115	101	93	84	78	66
$1 \cdot 10^6$	201	172	149	125	97	86	78	71	66	55
$2 \cdot 10^6$	169	143	123	101	77	68	62	56	52	44
$Q_p = 1 \cdot 10^{-4}$										
$1 \cdot 10^3$	900	900	900	900	900	800	710	650	600	520
$1 \cdot 10^4$	600	560	520	490	410	360	340	300	280	240
$1 \cdot 10^5$	340	300	270	240	190	170	158	140	130	112
$6 \cdot 10^5$	215	185	160	137	107	95	87	78	70	63
$1 \cdot 10^6$	185	160	140	115	87	80	73	65	58	53
$2 \cdot 10^6$	160	135	114	94	70	64	57	52	47	42
$Q_p = 1 \cdot 10^{-5}$										
$1 \cdot 10^3$	900	900	900	900	781	692	642	592	554	491
$1 \cdot 10^4$	557	514	481	450	363	322	298	275	257	228
$1 \cdot 10^5$	312	276	249	219	168	149	138	128	119	106
$6 \cdot 10^5$	199	170	150	125	93	82	76	70	66	58
$1 \cdot 10^6$	176	148	129	107	78	69	64	59	55	49
$2 \cdot 10^6$	148	123	106	86	62	55	51	47	44	39

Table 2. Comparison of experimental data of Table 1 with calculated ones (3) for σ_r (MPa) at $N = 2 \cdot 10^6$ cycle and mean values of parameters A and B

Q_p	K_x									
	1.3	1.5	1.7	2.0	2.3	2.6	3.0	3.5	4.0	5.0
$1 \cdot 10^{-2}$	$\frac{185}{192}$	$\frac{160}{166}$	$\frac{138}{141}$	$\frac{115}{120}$	$\frac{93}{95}$	$\frac{80}{84}$	$\frac{73}{75}$	$\frac{65}{67}$	$\frac{58}{60}$	$\frac{48}{50}$
$1 \cdot 10^{-3}$	$\frac{169}{170}$	$\frac{143}{145}$	$\frac{123}{124}$	$\frac{101}{102}$	$\frac{77}{78}$	$\frac{68}{70}$	$\frac{62}{63}$	$\frac{56}{57}$	$\frac{52}{52}$	$\frac{44}{44}$
$1 \cdot 10^{-4}$	$\frac{160}{158}$	$\frac{135}{133}$	$\frac{114}{113}$	$\frac{94}{93}$	$\frac{70}{69}$	$\frac{64}{62}$	$\frac{57}{56}$	$\frac{52}{51}$	$\frac{47}{47}$	$\frac{42}{41}$
$1 \cdot 10^{-5}$	$\frac{148}{151}$	$\frac{123}{126}$	$\frac{106}{108}$	$\frac{86}{87}$	$\frac{62}{63}$	$\frac{55}{57}$	$\frac{51}{52}$	$\frac{47}{48}$	$\frac{44}{45}$	$\frac{39}{40}$

Note. The data according to [5] are given in numerator, and those calculated from (3) are given in denominator.



Table 3. Failure probability Q_p and corresponding values of safety factor γ_m for $N = 2 \cdot 10^6$ cycle at $R = 0$

K_x	FAT, MPa	$Q_p = 5 \cdot 10^{-2}$		$Q_p = 1 \cdot 10^{-2}$		$Q_p = 1 \cdot 10^{-3}$		$Q_p = 1 \cdot 10^{-4}$		$Q_p = 1 \cdot 10^{-5}$	
		$\Delta\sigma$, MPa	γ_m								
1.7	135	161.9	1.0	138	1.17	123	1.32	114	1.42	106	1.53
2.0	116	139.5	1.0	115	1.21	101	1.38	94	1.48	86	1.62
2.3	95	114.6	1.0	93	1.23	77	1.49	70	1.64	62	1.85
2.6	84	100.6	1.0	80	1.26	68	1.48	64	1.58	55	1.83
3.0	74	89.00	1.0	73	1.22	62	1.43	57	1.56	51	1.74
3.5	65	78.00	1.0	65	1.20	56	1.39	52	1.50	47	1.66
4.0	58	68.70	1.0	58	1.18	52	1.32	47	1.46	44	1.56
5.0	46	55.60	1.0	48	1.16	44	1.26	42	1.32	39	1.42

Table 4. Examples of calculation of durability of weldments with 15 welded joints for different N

FAT, MPa	A, MPa	B, MPa	n	$\Delta\sigma$, MPa	$Q(1)$	$Q(n)$
$N = 2 \cdot 10^6$ cycle						
71	44	88	5	70	$7.59 \cdot 10^{-3}$	$3.79 \cdot 10^{-2}$
63	42	73	5	60	$3.68 \cdot 10^{-3}$	$1.84 \cdot 10^{-2}$
45	36	36	2	50	$2.26 \cdot 10^{-2}$	$4.52 \cdot 10^{-2}$
36	32	15	3	40	$7.77 \cdot 10^{-2}$	$2.33 \cdot 10^{-1}$
						$\Sigma Q_p = 2.84 \cdot 10^{-1}$
$N = 1 \cdot 10^6$ cycle						
71	55	120	5	70	$2.44 \cdot 10^{-4}$	$1.22 \cdot 10^{-3}$
63	52	95	5	70	$1.29 \cdot 10^{-3}$	$6.44 \cdot 10^{-3}$
45	46	49	2	60	$6.64 \cdot 10^{-3}$	$1.33 \cdot 10^{-2}$
36	43	25	3	45	$4.09 \cdot 10^{-5}$	$1.23 \cdot 10^{-4}$
						$\Sigma Q_p = 2.1 \cdot 10^{-2}$
$N = 6 \cdot 10^5$ cycle						
71	65	125	5	80	$2.07 \cdot 10^{-4}$	$1.03 \cdot 10^{-3}$
63	62	108	5	80	$7.71 \cdot 10^{-4}$	$3.85 \cdot 10^{-3}$
45	53	64	2	70	$4.96 \cdot 10^{-3}$	$9.93 \cdot 10^{-3}$
36	48	35	3	60	$1.37 \cdot 10^{-2}$	$4.12 \cdot 10^{-2}$
						$\Sigma Q_p = 5.44 \cdot 10^{-2}$
$N = 1 \cdot 10^5$ cycle						
71	125	240	5	140	$1.52 \cdot 10^{-5}$	$7.63 \cdot 10^{-5}$
63	120	200	5	140	$9.99 \cdot 10^{-5}$	$5.00 \cdot 10^{-4}$
45	100	90	2	110	$1.52 \cdot 10^{-4}$	$3.05 \cdot 10^{-4}$
36	90	50	3	100	$1.60 \cdot 10^{-3}$	$4.79 \cdot 10^{-3}$
						$\Sigma Q_p = 5.66 \cdot 10^{-3}$
$N = 1 \cdot 10^4$ cycle						
71	280	490	5	310	$1.40 \cdot 10^{-5}$	$7.02 \cdot 10^{-5}$
63	240	400	5	270	$3.16 \cdot 10^{-5}$	$1.58 \cdot 10^{-4}$
45	205	200	2	220	$3.16 \cdot 10^{-5}$	$6.33 \cdot 10^{-5}$
36	195	105	3	210	$4.16 \cdot 10^{-4}$	$1.25 \cdot 10^{-3}$
						$\Sigma Q_p = 1.54 \cdot 10^{-3}$

Note. n – quantity of joints of the same type at preset FAT; $Q(1)$ – failure probability for one joint; $Q(n)$ – failure probability for at least one of the n joints of the same type; ΣQ_p – failure probability for at least one of the joints in a weldment.



where $\Delta\sigma > A$. Here A , B and η are the law parameters depending on K_x (or FAT) and N . They can be determined from the data given in Table 1. Good agreement was achieved at $\eta = 4$. The calculations of the values of A and B depending on durability N and class of a joint FAT are shown in Figure 2.

Consider the degree of agreement of the calculation of Q_p from (2) with the experimental data of Table 1 by using the above relationship between K_x and FAT in the following form:

$$FAT(K_x) = \sigma_r(K_x, Q_p = 5 \cdot 10^{-2}, N = 2 \cdot 10^6) / 1.2, \quad (4)$$

as well as the data of Table 1 and relationship (3).

The results obtained are given in Table 2. They show that the experimental data according to [5] for σ_r from Table 1 and the calculated data based on (3) at different values of parameters A and B at $Q_p = 1 \cdot 10^{-2}$, $1 \cdot 10^{-3}$, $1 \cdot 10^{-4}$ and $1 \cdot 10^{-5}$ are in sufficiently good agreement.

Of special interest is the question how the calculation based on the permissible fracture probability agrees with the calculation based on the preset value of safety factor $\gamma_m = 1.0$ – 1.4 recommended in [4]. Table 3 gives such data obtained for welded joints with different values of K_x [5] and corresponding FAT [4] for durability $N = 2 \cdot 10^6$ cycles at cycle asymmetry coefficient $R = 0$.

It can be seen from Table 3 that a relatively small variation in γ_m has a dramatic effect on the Q_p values, i.e. at the reasonable risks of failure within $Q_p = 1 \cdot 10^{-4}$ the need for $\gamma_m > 1.64$ is low. Hence, at $\gamma_m = 1.4$ the failure probability for the conditions under consideration is $1 \cdot 10^{-3}$.

It should be noted that failure probability Q_p in the majority of cases determines the risk of initiation of a fatigue macrocrack, which is followed by its growth to critical sizes, at which transition to a spontaneous fracture takes place. Therefore, the values of $\gamma_m = 1.0$ – 1.4 recommended in [4] correspond to the probability of initiation of a fatigue crack equal to $Q_p = 5 \cdot 10^{-2}$ – $1 \cdot 10^{-3}$, which is quite reasonable, depending on how serious the anticipated consequences might be [4].

The possibility of obtaining more reasonable qualitative characteristics concerning the probability of initiation of fatigue cracks for individual welded joints allows estimating the possibility of safe operation of individual weldments with a large number of different types of welded joints (different FAT) and different stress ranges (Table 4).

The known relationships are used in the studies:

$$\begin{aligned} Q(n) &= 1 - \exp[-nQ(1)]; \\ \Sigma Q_p &= 1 - \exp[-\Sigma Q(n)]. \end{aligned} \quad (5)$$

It can be seen from Table 4 that probability ΣQ_p is always higher than probability $Q(n)$, which in turn is higher than $Q(1)$, i.e. ensuring safety of a weldment only from one of the weakest joints by ignoring characteristics of other joints is far from being always grounded.

CONCLUSIONS

1. Fatigue fracture resistance of a welded joint is a rather stochastic value. In this connection, the IIW recommendations [4] based on statistical processing of experimental data with a guaranteed failure probability of $5 \cdot 10^{-2}$, combined with recommendations for safety factor $\gamma_m = 1.0$ – 1.4 , are sufficiently well-grounded, according to the scheme of the weakest link for welded structures under high-cycle fatigue conditions.

2. Combining the experimental data generated by some institutions on probabilistic characteristics of fatigue resistance with the IIW recommendations for high-cycle fatigue of welded structures from ferritic-pearlitic (ferritic-bainitic) structural steels leads to expansion of the calculation capabilities for estimation of safety by using probabilistic approaches.

1. (1990) *Strength of welded joints at variable loads*. Ed. by V.I. Trufiyakov. Kiev: Naukova Dumka.
2. Kogaev, V.P. (1977) *Strength calculation at time variable stresses*. Moscow: Mashinostroenie.
3. Maddox, S.D. *Fatigue strength of transverse one-side welded joints*. www.svarkainfo.ru
4. (1996) Recommendation for fatigue design of welded joints and components. *IIW Doc. XIII-1539-96/XV-845-96*.
5. (1987) *Design with EHS and AR plate*. Oxeloesund: Svenskt Stal Heavy Plate Division.



INVESTIGATION OF STRUCTURE AND SERVICE PROPERTIES OF DEPOSITED METAL FOR RECONDITIONING AND STRENGTHENING OF ROLLING MILL ROLLS

I.A. RYABTSEV, I.A. KONDRATIEV, G.V. VASILIEV, V.A. ZHDANOV and A.A. BABINETS
E.O. Paton Electric Welding Institute, NASU, Kiev, Ukraine

Structure and service properties of deposited metal designed for strengthening and reconditioning of various-purpose forming rolls have been studied. Metal deposited with flux-cored wire PP-AN132 has the highest high-temperature resistance, hot hardness and wear resistance at metal-on-metal friction at high temperatures, however, it has the lowest thermal stability. Metal deposited with flux-cored wire PP-AN130 has the highest thermal stability, although it is inferior to other materials as to a number of other indices. Metal deposited with flux-cored wire PP-AN147 takes an intermediate position by all the indices.

Keywords: arc hardfacing, forming rolls, flux-cored wires, deposited metal, macrostructure, wear resistance, thermal stability, heat resistance

PWI developed flux-cored wires PP-AN130 (Fe-C-Cr-Mo-V alloying system), PP-AN132 (Fe-C-Cr-W-Mo-V) and PP-AN147 (Fe-C-Cr-Mo-Ni-V) used in arc hardfacing of tools and jigs for hot forming of metals, in particular, forming rolls for different purposes [1]. Some publications [2-4] give data on the structure and certain properties of metal deposited with these wires. However, this testing was often conducted by different procedures and in different scope, so that it did not seem possible to provide a sufficiently objective assessment of the advantages of a particular type of deposited metal and give substantiated recommendations on its application. This paper presents generalized results on studying the structure of metal deposited with these wires, as well as its service properties obtained at testing under the same conditions and by the same procedures.

To study the structure and properties of the deposited metal each of the three flux-cored wires was used to deposit four to five layers on blanks, from which samples were cut out for metallographic investigations, studying thermal stability, heat resistance, hot hardness and wear resistance at metal-on-metal friction at high temperatures.

It is known that the structure and properties of the deposited metal significantly depend on its cooling rate in the region of temperatures of the lowest stability of austenite. Arc hardfacing of forming rolls, which are usually made of carbon and high-carbon steels, is performed with preheating up to 300-350 °C and delayed cooling in a furnace or thermostat. It was experimentally established that at hardfacing without preheating and cooling in quiet air the cooling rate of the hardfaced part is equal to approximately 3-

4 °C/s, and in hardfacing with preheating and delayed cooling in a furnace or thermostat, it is equal to about 0.018-0.020 °C/s. Proceeding from that, the structure of the deposited metal of three types after heating up to 950 °C and cooling at the rate of 0.018 and 3 °C/s, respectively, was studied. Investigations were conducted in Chevenard dilatometer, which provides cooling of samples with such rates.

It is established that first bainite, and then martensite transformation is observed in the metal deposited with flux-cored wire PP-AN130 at cooling rates of 0.018 and 3 °C/s. The distinctive feature consists in that at a lower cooling rate the quantity of bainite is higher, and deposited metal hardness is lower. As a result, the structure of deposited metal of this type consists of martensite, bainite, residual austenite and carbides (Figure 1, *a, b*). Deposited metal hardness is *HRC* 44-47.

In the metal deposited with flux-cored wire PP-AN132 at cooling rate of 0.018 °C/s, first bainite transformation is observed, which is followed by martensite transformation. At cooling rate above 3 °C/s just the martensite transformation is observed as a result of a higher content of carbon and alloying elements (compared to PP-AN130 wire). Hardness of deposited metal of this type is equal to *HRC* 48-50, its structure consists of martensite, residual austenite, carbides and a small amount of bainite (Figure 1, *c, d*).

In the metal deposited with flux-cored wire PP-AN147 bainite and martensite transformations are also observed at these cooling rates. Deposited metal microstructure after cooling consists of martensite, bainite and residual austenite with carbides (Figure 1, *e, f*). Deposited metal hardness is equal to *HRC* 46-49.

Properties of deposited metal of three types were studied.

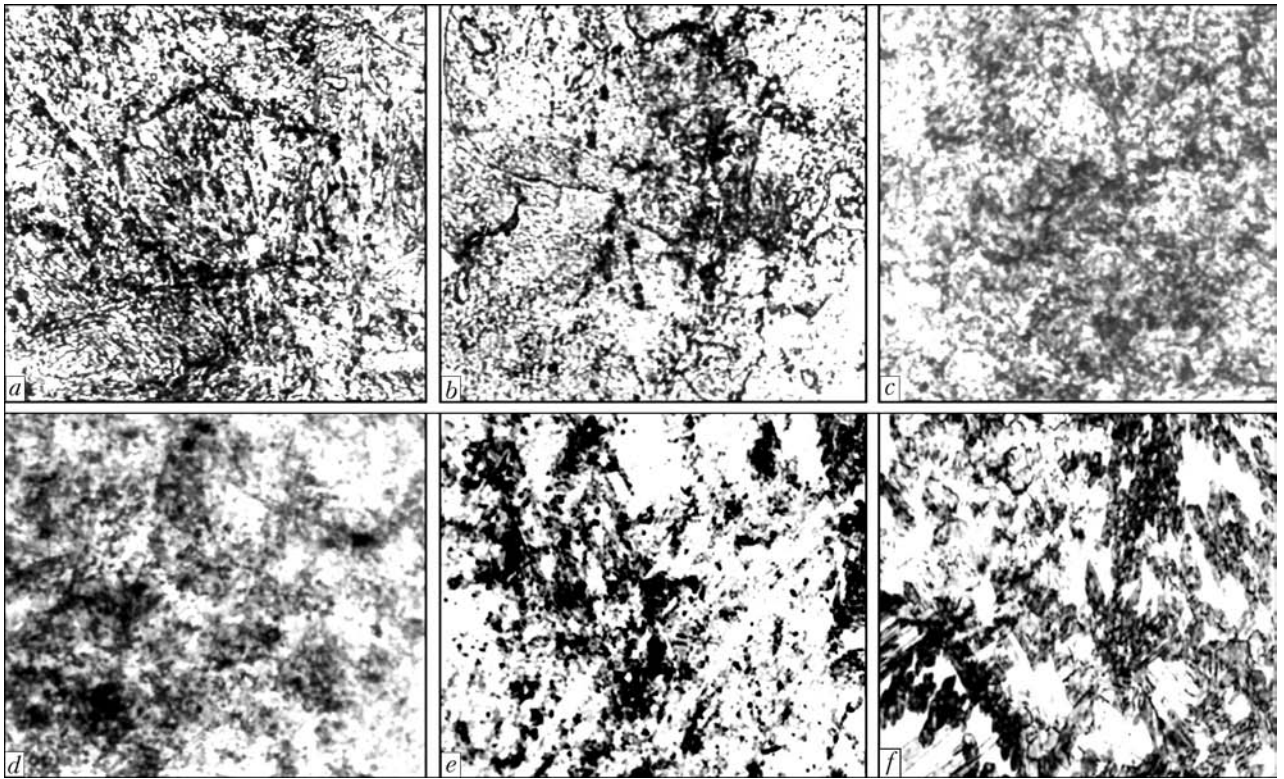


Figure 1. Microstructures ($\times 500$) of metal deposited with flux-cored wire PP-AN130 (*a, b*), PP-AN132 (*c, d*) and PP-AN147 (*e, f*): *a, c, e* – cooling rate of 3; *b, d, f* – 0.018 °C/s

Heat resistance. This is the capability of steel to preserve the structure and properties required for deformation or cutting at working edge heating during operation. Heat resistance of stamping steels is usually characterized by the temperature of two-hour tempering, after which hardness is equal to *HRC* 40 [5]. Nine samples of each type of the deposited metal of $15 \times 20 \times 20$ mm size were made to study the heat resistance. The samples were first subjected to two-hour tempering at temperatures in the range of 200–700 °C. After cooling down the hardfaced surface of the samples was ground and hardness was determined (Figure 2).

It is established that all the types of deposited metal are characterized by a sufficiently high heat resistance – 630–650 °C. However, the best heat resistance is found in the metal deposited with flux-cored wire PP-AN132. The shape of its curve is the same as that of metal deposited, for instance, with flux-cored wire PP-AN130. The difference consists only in that hardness lowering in this type of deposited metal starts at higher tempering temperatures.

In all the three types of deposited metal a slight increase of hardness is observed as a result of tempering in the temperature range of 500–550 °C. Secondary hardening effect is observed as a result of decomposition of residual austenite with formation of martensite and carbides, which is what leads to hardness increase.

Wear resistance at metal-on-metal friction at elevated temperatures. It is known that during hot forming of metals and alloys (rolling, forging, stamping) specific pressure of metal on the tool can be quite

considerable and by some data reaches 300–500 MPa. Metal slipping is always found in the deformation site as a result of its drawing, which alongside high specific pressures leads to wear of the tool working surface at metal-on-metal friction at elevated temperatures. Therefore, determination of deposited metal wear resistance under these conditions is important.

The main test parameters include specific pressure on the tested sample, sample heating and cooling temperature, rate of relative displacement of rubbing elements (friction speed), and kind of material of the fretting ring. Laboratory wear testing at metal-on-metal friction at elevated temperatures by ring–plane schematic was conducted in an all-purpose testing unit [6]. For this purpose samples of $40 \times 10 \times 17$ mm size were made from the hardfaced blanks, the deposited layer thickness being 8–10 mm. During testing the sample was pressed with the hardfaced plane to a rotating ring-counterbody, which was heated by a gas torch. In addition, the sample makes a reciprocal displacement in the vertical plane, sliding over the surface of the rotating ring-counterbody. Testing conditions were as follows: load of 800 N (specific pressure of about 100 MPa); speed of counterbody rotation of 30 rpm; sample oscillation amplitude in the vertical plane of 20 mm; oscillation frequency of 62 min^{-1} ; sample temperature in the fretting zone of 600 °C; testing time of 1 h. Rings of 120 mm diameter from steel 45 were used as the counterbody.

Friction rate in the experiments was equal to 20–22 m/min, which corresponds to modes the most widely accepted in industry at hot forming of metals.

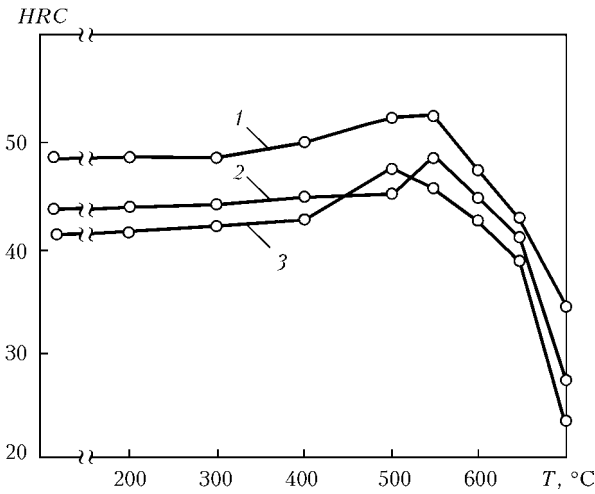


Figure 2. Dependence of hardness of metal deposited with different flux-cored wires on tempering temperature: 1 – PP-AN132; 2 – PP-AN147; 3 – PP-AN130

Fretting ring was heated by oxygas flame. Owing to a strictly controlled flow rate of combustible gas and oxygen, the fretting ring temperature was kept constant at 950–980 °C, and ring temperature was periodically controlled using optical pyrometer.

Results of wear testing at metal-on-metal friction at elevated temperatures are given in Figure 3, *a*. The lowest wear was found in metal deposited with flux-cored wire PP-AN132, the highest wear was found with flux-cored wire PP-AN130. Higher wear resistance of deposited metal of the first type is, apparently, attributable to a higher content of carbon and alloying elements and its higher heat resistance and hardness.

Thermal stability. This is a most important property, which characterizes the resistance of the deposited metal to fire cracking at multiple repetition of heating-cooling cycles. As a rule, the fatigue life of tools for hot forming of metal depends primarily on this property [1, 7, 8].

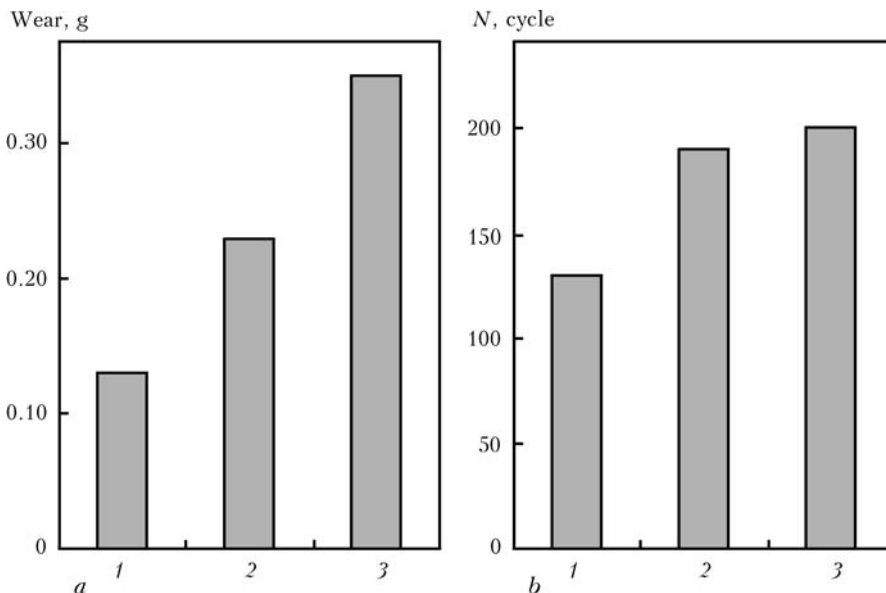


Figure 3. Wear at metal-on-metal friction at elevated temperatures (*a*) and thermal stability (*b*) of metal deposited with different flux-cored wires: 1 – PP-AN132; 2 – PP-AN147; 3 – PP-AN130

Procedure of thermal stability testing should envisage optimum dimensions and shape of the hardfaced sample; temperature and rates of its heating and cooling, close to these characteristics for the hardfaced parts, etc. To assess the thermal stability of materials used for hardfacing the tools for hot forming of metals, a sample should have a sufficient mass, so as to ensure a gradient of temperatures and stresses simulating the actual conditions, during its surface heating.

Thermal stability tests of the deposited metal were conducted in a unit for comprehensive assessment of deposited metal properties [6]. For this purpose 30 × 40 × 40 mm samples were cut out of the hardfaced blanks and the hardfaced surface of the samples was polished. The sample was mounted in the holder of the testing machine with the ground surface up, which was heated by a flame cutter. Uniform heating was obtained on a heated spot of 15–20 mm diameter. Heating was continued for 11 s with cooling by a powerful water jet for 8 s. After stabilization of the testing conditions the maximum sample temperature in the heated spot was equal to 650–700 °C, at cooling it was 60–80 °C. Thermal stability was assessed by the number of cycles of heating-cooling on the surface of a hardfaced sample up to appearance of a net of fire cracks, visible for a naked eye (Figure 3, *b*).

The best thermal stability was found in metal deposited by flux-cored wire PP-AN130, and metal deposited with PP-AN147 wire was somewhat inferior to it. Metal deposited with flux-cored wire PP-AN132 had lower thermal stability.

As is known [5], thermal stability is adversely affected by structural inhomogeneity of steels: presence of carbide (intermetallic) excess phases required for increase of heat and wear resistance. Thermal stability starts markedly decreasing, if their quantity exceeds 10–12 %. Apparently, this can account for the



lower thermal stability of metal deposited with flux-cored wire PP-AN132.

Hot hardness. Under the operating conditions of hot metal forming tools metal hardness at increased temperatures (hot hardness) is highly important. Material resistance to wear depends on its ability to resist plastic deformation, i.e. hardness at elevated temperatures and material ability to preserve hardness for a long time. As a rule, steels containing molybdenum, tungsten, chromium, vanadium have high wear resistance at elevated temperatures, and their initial room temperature hardness is not very important.

Hot hardness of deposited metal of the selected types was studied. Sample heating was performed in a special inductor in vacuum, hardness measurements were conducted at 1 kg load, with 60 s soaking under load. As noted in [7], temperature of forming rolls in the deformation site is equal to 600–650 °C, that is why hot hardness of the deposited metal was determined at this temperature and at 20 °C for comparison (Figure 4).

Deposited metal of all the three types has approximately the same hardness at room temperature. High temperature hardness is different to a greater degree: metal deposited with PP-AN132 wire has hardness on the level of *HRC* 35; for PP-AN147 wire — *HRC* 32; for PP-AN130 wire — *HRC* 30.

Thus, the best heat resistance, hot hardness and wear resistance at metal-on-metal friction at high temperatures is found in metal deposited with flux-cored wire PP-AN132; however, it has the lowest thermal stability. Metal deposited with flux-cored wire PP-AN130 has the best thermal stability, although it is inferior to two other type of deposited metal by other service properties. Metal deposited with flux-cored wire PP-AN147 takes an intermediate position by all the service properties.

CONCLUSIONS

1. Investigations of microstructure of metal deposited with flux-cored wires PP-AN130, PP-AN132 and PP-AN147 showed that at simulation of thermal cycle of arc hardfacing of forming rolls (preheating and delayed cooling after hardfacing) the structure of all the three types of deposited metal consists of martensite, bainite, residual austenite and carbides in different proportions. In all the three types of deposited metal a slight increase in hardness is noted as a result of

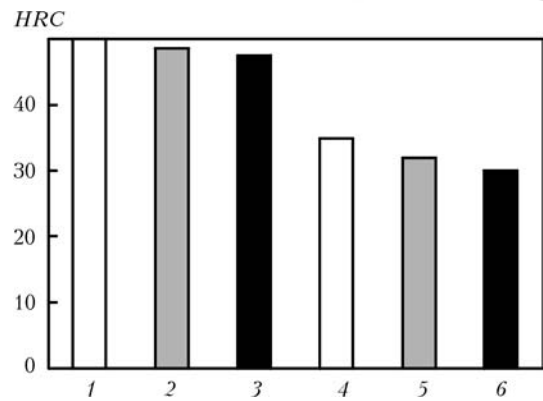


Figure 4. Hardness of metal deposited with different flux-cored wires at temperatures of 20 (1–3) and 600 (4–6) °C: 1, 4 — PP-AN132; 2, 5 — PP-AN147; 3, 6 — PP-AN130

tempering in the temperature range of 500–550 °C. Secondary hardening occurs as a result of residual austenite decomposition with formation of martensite and carbides, which is what leads to hardness increase.

2. Proceeding from the deposited metal properties, flux-cored wire PP-AN130 can be recommended for hardfacing of rolls of bloomings and slabbing and roughing stands of rolling and hoop mills, in which deformation of metal heated up to the highest temperatures takes place. It is rational to use flux-cored wire PP-AN132 for hardfacing forming rolls of leader and roughing stands, in which metal deformation proceeds at relatively low temperatures and there is no need for high thermal stability of the deposited metal, while its wear resistance and hot hardness have a more essential role. Flux-cored wire PP-AN147, which has the most optimum combination of all the service properties, can be recommended for hardfacing heavy-duty rolls of roughing mills in pipe and section rolling mills.

1. Ryabtsev, I.A., Kondratiev, I.A. (1999) *Mechanized arc surfacing of metallurgical equipment parts*. Kiev: Eko-tehnologiya.
2. Kondratiev, I.A., Lazarenko, Yu.N. (1978) Experience of application of large diameter flux-cored wire for mechanized surfacing. In: *Theoretical and technological principles of surfacing. Surfacing consumables*. Kiev: PWI.
3. Frumin, I.I., Ksyondzyk, G.V., Kondratiev, I.A. et al. (1986) Increase in service life and resistance of forming rolls by surfacing methods. *Chyorn. Metallurgiya*, Issue 7, 11–19.
4. Ryabtsev, I.A., Kuskov, Yu.M., Kondratiev, I.A. (2004) Arc and electroslag cladding of mill rolls. *Svarshchik*, 1, 7–10.
5. Geller, Yu.A. (1983) *Tool steels*. Moscow: Metallurgiya.
6. Ryabtsev, I.I., Chernyak, Ya.P., Osin, V.V. (2004) Modular unit for testing deposited metal. *Svarshchik*, 1, 18–20.
7. Frumin, I.I. (1961) *Automatic arc surfacing*. Kharkov: Metallurgizdat.
8. Tylkin, M.A. (1971) *Increase in fatigue life of metallurgical equipment parts*. Moscow: Metallurgiya.



EFFECT OF TIN ADDITIONS ON STRUCTURE AND TECHNOLOGICAL PROPERTIES OF BRAZING FILLER METALS OF THE Ag–Cu–Zn SYSTEM

V.F. KHORUNOV, S.V. MAKSYMOVA and B.V. STEFANIV
E.O. Paton Electric Welding Institute, NASU, Kiev, Ukraine

The effect of tin and silicocalcium additions on structure, melting temperature ranges and spreading of alloy of the Ag–Cu–Zn system was investigated. It was found that cadmium-free brazing filler metals are characterised by good performance and provide strength properties of the joints close to those provided by brazing filler metal PSr-40.

Keywords: brazing, brazing filler metals, cadmium-free brazing filler metal, eutectic, thermal analysis, structure, technological properties

Silver-base brazing filler metals found practical application several thousands years ago. They have become strongly established in modern market of brazing consumables. Silver in its pure form can be applied as a brazing filler metal. However, most of the filler metals are based on eutectic of the Ag–Cu system [1], having a melting point of 779 °C and containing approximately 28 wt.% Cu. Adding zinc to the Ag–Cu system alloys leads to formation of ternary eutectic 56Ag–24Zn–20Cu (point *E* in Figure 1) with a melting point of 665 °C [2].

To decrease their melting point, alloys of this system are doped with the fourth (fifth, sixth) element. Wide acceptance has been received by the Ag–Zn–Cu–Cd system filler metals, which are plentiful in the market. Their different modifications are included both in catalogues of all companies manufacturing brazing filler metals and in standards of industrialised countries [3]. The main advantage of this system of the filler metals is that they have the lowest brazing temperature among a wide range of silver-base brazing filler metals. For example, temperature of eutectic of

this quaternary system (45Ag–15Cu–16Zn–24Cd) is approximately 615 °C [4], whereas the most widely applied brazing filler metal PSr-40 has a solidus temperature of 590 °C and liquidus temperature of 610 °C. These filler metals are used to advantage for brazing different materials, and for the extensively applied iron- and copper-base alloys they provide joints with good mechanical properties.

Meanwhile, the problem of replacing cadmium in brazing filler metals has arisen long ago. The European Parliament and United Europe Consulate Council adopted a directive that prohibits application of hazardous materials, including cadmium, in particular. Tin was chosen as an alternative to it [5, 6].

Study [5] gives data that in alloys of the Ag–Cu–Zn, Ag–Cu–Cd and Ag–Cu–Zn–Sn systems (Figure 2) the solidus and liquid temperatures can be considerably decreased due to a tin addition, compared with the ternary system. However, in this case the melting temperature range is higher. To reach a solidus temperature of the alloys equal to about 630 °C, it is necessary that the silver content of alloy Ag–Cu–Zn–Sn be about 55 wt.%, i.e. a bit higher than in the widely applied filler metals. In opinion of the author of study [5], this may lead to a 15–20 % increase in the cost of work. Later, the similar task was posed in study [6], which, by the way, made a wide use of the data of study [5], in particular data on alloys 1 and 4 (Table 1). It should be noted that the range of brazing filler metals considered in study [7] has been much widened. That study contained the data on strength properties of brazing filler metal in the as-cast state, and compared alloys of the Ag–Cu–Zn, Ag–Cu–Zn–Sn and Ag–Cu–Zn–Cd systems.

It follows from the data given in Table 1 that brazing filler metals of the Ag–Cu–Zn–Sn system are not inferior to the ternary system filler metals and to those containing cadmium, which is very important for their practical application. At this point, one should note the following interesting fact. Filler metals 3–5 (Table 1) have close chemical composition, which corresponds to standard American filler metal BAG-28. At the same time, they are markedly differing

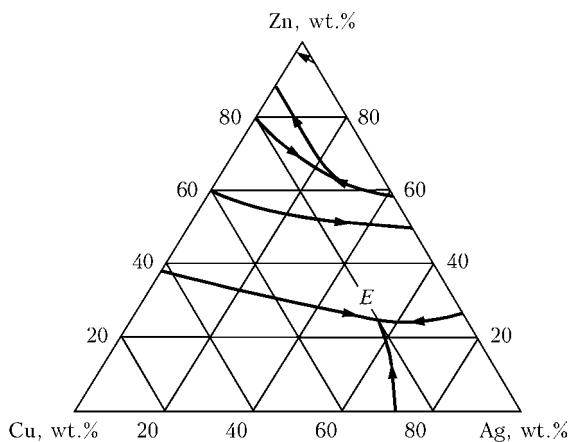


Figure 1. Projection of solidification surface of constitutional diagram for Cu–Ag–Zn system [2]

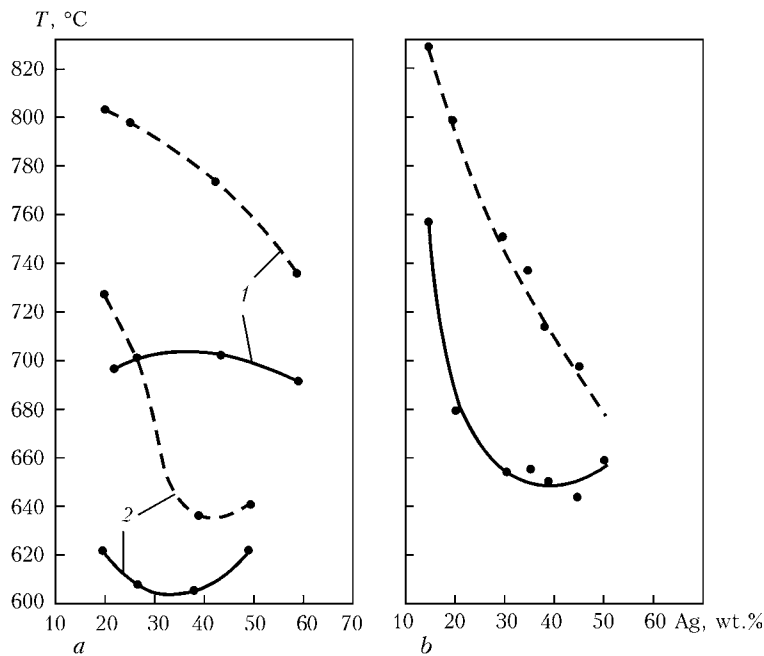


Figure 2. Variations in solidus (solid curve) and liquidus (dashed curve) temperatures in alloys of the Ag-Cu-Zn (1), Ag-Cu-Zn-Cd (2) (a) and Ag-Cu-Zn-Sn (b) systems depending on their silver content

in their mechanical properties, filler metal 5 having the lowest strength, and filler metal 4 having the highest strength among all the alloys investigated. Study [6] gives no explanation to this fact. It gives no strength characteristics of the brazed joints either.

Judging from the ranges of products present in the market, the filler metals under consideration have not yet ousted the cadmium-containing ones. More information on alloys of the Ag-Cu-Zn-Sn system is required to reveal the cause of low popularity of these filler metal in the world market.

The purpose of the present study was to investigate the effect of tin additions (3–10 wt.%) in alloys of the Ag-Cu-Zn system on structure of the latter, spreading area and strength of the resulting brazed joints in steel 12Kh18N10T, as well as on the same parameters with the silicocalcium addition.

The E.O. Paton Electric Welding Institute carried out investigations of the effect of tin on the melting

range, structure and strength of the joints. The charge was made from pure materials (silver of the SrA-1 grade, cathode copper M0k, and zinc of the TsV grade). Allowing for a high pressure of the saturated zinc vapour, the zinc content in the charge was 2 % higher than in the filler metal. Filler metals were melted by high-frequency heating in the graphite crucible, and flux PV200 was used for shielding. First copper and silver were melted, then heating was stopped, and zinc and cadmium were added after the metal temperature decreased to 400–500 °C. To provide a homogeneous melt by induction and mechanical stirring, a filler metal was subjected to repeated short-time heating until it melted down.

Steel 12Kh18N10T 2 mm thick was chosen as a base metal. Billets measuring 100 × 20 × 2 mm were brazed by using gas-flame heating and flux PV209. Overlap was 2 mm. The flux was preliminarily applied to the brazing zone in the form of paste mixed with

Table 1. Chemical composition, melting ranges and strength of brazing filler metals [6]

Number of filler metal	Chemical composition of elements, wt.%					Melting temperature range, °C	Tensile strength in cast state, MPa
	Ag	Cu	Zn	Sn	Cd		
1	30	36	32	2	–	665–755	448
2	35	34	30	1	–	660–740	476
3 (BAg-28)	39	31	28	2	–	645–725	473
4 (BAg-28)	39	31	27	3	–	635–710	497
5 (BAg-28)	40	30	28	2	–	649–710*	406
6 (BAg-1a)	50	15	16	–	19	627–635*	457
7	40	30	28	–	–	–	441
8	45	25	30	–	–	–	425

*The data are taken from study [3].

**Table 2.** Results of tests of brazing filler metals of the Ag-Cu-Zn-Sn system to spreading and shear strength of the brazed joints in steel 12Kh18N10T

Number of filler metal batch	Filler metal system	Spreading area, mm ²	Shear strength, MPa
1	56Ag-22Cu-17Zn-5Sn	130.3	$\frac{242.7-297.9}{267.4}$
2	57.5Ag-22.5Cu-17Zn-3Sn	125.9	$\frac{267.3-288.5}{275.4}$
3	55Ag-21.5Cu-16.5Zn-7Sn	140.9	$\frac{251.4-263.9}{259.5}$
4	55Ag-20Cu-15Zn-10Sn	127.9	$\frac{158.1-214.1}{187.8}$
5	56Ag-22Cu-17Zn-5Sn-0.25SiCa	117.5	$\frac{250.3-277.2}{263.1}$
6	57.5Ag-22.5Cu-17Zn-3Sn-0.25SiCa	119.2	$\frac{284.9-298.8}{290.5}$
7	55Ag-21.5Cu-16.5Zn-7Sn-0.25SiCa	139.2	$\frac{234.5-261.2}{251.1}$
8	55Ag-21.5Cu-15Zn-10Sn-0.25SiCa	152.1	$\frac{168.4-203.0}{183.1}$

water, which was dried before heating. After heating to a melting temperature of the flux, a filler metal preform was placed on the joining zone, and heating was continued till melting of the preform and formation of the joint. The samples after brazing were machined to remove reinforcement, and then tensile tested using the MTS-20 testing machine.

The experiments on spreading of brazing filler metals were carried out according to GOST 23904-79. Filler metal preforms (0.50 + 0.01) g in weight were placed on a plate measuring 40 × 40 mm. The flux was poured from above on the filler metal placed on the substrate. The samples were heated for 3 min in the furnace preliminarily heated to 700 °C. The area of spreading of each filler metal was calculated using the AutoCard 2002 software. Compositions of the investigated filler metals and results of the experiments on spreading and strength of the brazed joints are given in Table 2.

Analysis of the obtained data showed that the area of spreading of filler metals with a different tin content is approximately within the same ranges, i.e. the tin content has an insignificant effect on this characteristic, including in the silicocalcium-containing alloys. Some increase in the spreading area can be noted only at a tin content of 7 wt.%. It follows from Table 2 that strength of the joints decreases with increase in the tin content of a filler metal. While strength of the joints brazed with the filler metal containing 3 wt.% Sn is 275 MPa, that with the filler metal containing 10 wt.% Sn is 187 MPa. Moreover, consistency of the results decreases with increase in the tin content.

The brazing filler metals containing silicocalcium exhibit the same trend: strength of the joints brazed

with the filler metal containing 3 wt.% Sn is 290 MPa, and that with the filler metal containing 10 wt.% Sn is 183 MPa. Consistency of the test results decreases accordingly. At the same time, the data presented show some increase in strength of the joints with a silicocalcium addition to the alloy containing 3 wt.% Sn. In this case, doping with silicocalcium should be considered useful. At a considerable tin content the effect of silicocalcium is levelled. It means that adding it is inexpedient.

New data were obtained from investigation of melting ranges and structures of the considered alloys with a different tin content. Melting ranges of the alloys were determined by using the VDTA-8 unit in the helium atmosphere. Weight of the investigated sample was 1.03 g, and rate of its heating and cooling was 80 °C/min. The samples were heated two times to achieve a good fit of the preform to the crucible bottom and provided reliable data on thermal effects. The thermal effects were fixed on the second heating curve, the solidus and liquidus temperatures of the alloy were also determined from this curve (overcooling prior to solidification has a substantial effect in cooling of the alloy). At the same time, the level of the thermal effects is better reflected on the alloy cooling curves.

Analysis of the obtained data showed that doping with tin has a substantial effect on the phase transformation temperature and melting range. For instance, the composition of alloys with 3 wt.% Sn is practically single-phase (Figure 3, *b*). The solidus temperature is 640 °C, and the liquidus temperature is 690 °C. A hardly perceptible thermal effect takes place at a temperature of 680 °C. It does not show up appreciably even in cooling, i.e. the second phase content is insignificant. Emergence of the thermal effect



Table 3. Chemical composition (wt.%) of alloys determined by thermal analysis

Investigated region	Ag	Cu	Zn	Sn	Si
57.5Ag-22.5Cu-17Zn-3Sn (eutectic)					
Dark phase	32.072	47.222	19.359	1.344	0
Light phase	75.732	6.880	13.305	3.833	0.252
Eutectic	74.127	12.133	12.948	0.711	0.085
57.5Ag-22.5Cu-17Zn-3Sn-0.25SiCa (eutectic)					
Dark phase	18.212	58.161	21.811	1.285	0.528
Light phase	75.835	7.609	13.046	3.333	0.189
Eutectic	73.486	7.144	13.534	5.716	0.120
56Ag-22Cu-17Zn-5Sn					
Dark phase	15.638	59.222	22.458	2.517	0.160
Light phase	74.588	9.837	11.880	3.696	0
Eutectic	69.885 / 68.269	6.400 / 6.867	9.698 / 10.379	13.917 / 14.257	0.091 / 0.219
56Ag-22Cu-17Zn-5Sn-0.25SiCa					
Dark phase	17.153	55.552	24.570	2.486	0.236
Light phase	72.037	8.520	12.320	6.838	0.285
Eutectic	58.129	18.081	14.749	7.846	0.393
55Ag-21.5Cu-16.5Zn-7Sn-0.25SiCa					
Dark phase	17.706	60.295	20.517	1.182	0.298
Light phase	77.668	3.793	10.968	7.274	0.305
Eutectic	74.851	4.467	11.466	8.798	0.423
55Ag-21.5Cu-16.5Zn-10Sn-0.25SiCa					
Dark phase	9.551	64.382	22.305	3.357	0.402
Light phase	76.841	5.075	7.932	10.027	0.963
Eutectic	72.816	6.234	8.343	12.312	0.290

becomes noticeable at a temperature of 480–490 °C, which can hardly be associated with melting of a low-melting point component. Most likely, this is a result of phase transformation in the solid phase, which is indirectly confirmed by the presence of a number of transformations occurring in the solid phase of the Sn–Cu system [7].

The results obtained for the alloy with 5 wt.% Sn are approximately identical to those obtained for the

alloy with 3 wt.% Sn (Figure 3, *a*), i.e. it is almost single-phase in melting and solidification, the thermal effect taking place at a temperature of 490 °C. The insignificant increase of the liquidus temperature is hard to explain. Moreover, the thermal effect in this case is located lower on the cooling curve than for the alloy with 3 wt.% Sn. Strength of the joints decreases to some extent.

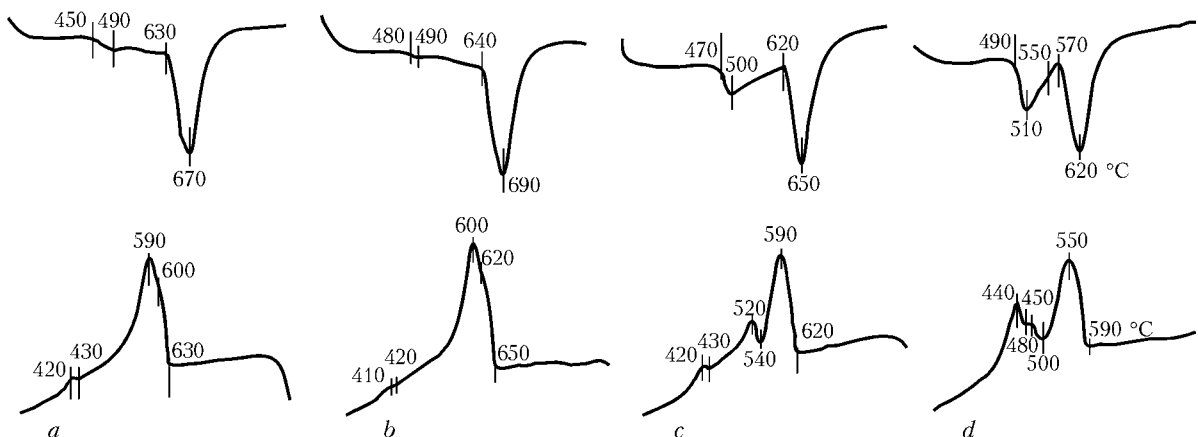


Figure 3. Data of differential thermal analysis of alloys of the 56Ag-22Cu-17Zn-5Sn (*a*), 57.5Ag-22.5Cu-17Zn-3Sn (*b*), 55Ag-21.5Cu-16.5Zn-7Sn (*c*) and 55Ag-20Cu-17Zn-10Sn (*d*) systems

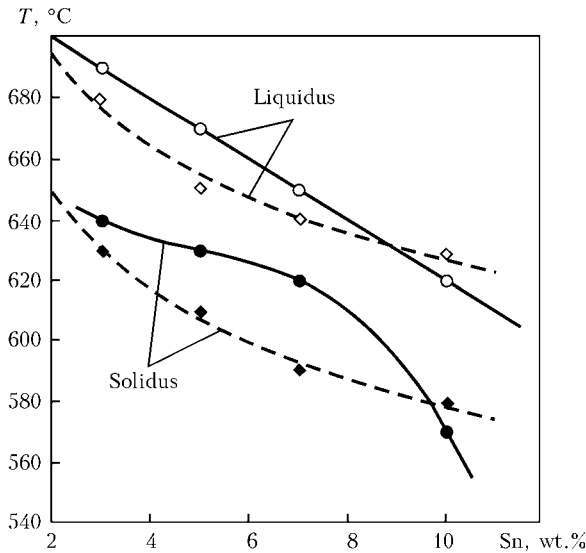


Figure 4. Variations in liquidus and solidus temperatures in alloys of the Ag-Cu-Zn-Sn (solid curve) and Ag-Cu-Zn-Sn (SiCa) (with the silicocalcium addition) (dashed curve) systems

The presence of the two thermal effects emerging at temperatures of 620–650 and 470–500 °C is clearly fixed in the alloy with 7 wt.% Sn. The presence of the third effect can be seen in the cooling curve at a

temperature of 420–430 °C (Figure 3, *c*). Strength of the joints brazed with this filler metal is markedly lower.

The presence of the thermal effect, but in a more explicit form, was fixed in the alloy with 10 wt.% Sn (Figure 3, *d*). Strength of the joints is much lower (approximately by 90 MPa, compared to the joints brazed with the alloy with 3 wt.% Sn). Approximately the same phenomena are fixed in the alloys containing a silicocalcium addition with increase in the tin content as in the alloys without the silicocalcium addition (Figure 4).

Examination of structure and chemical heterogeneity of alloys with 3 wt.% Sn showed that they can be classed with the eutectic structures with a higher or lower content of the primary phase. The silicocalcium addition does not change the general character of structure (Figure 5, *a, b*). The eutectic composition is difficult to identify in a complex structure. However, it is possible to judge on the composition of individual phases. The dark phase (based on copper) contains approximately 32 wt.% Ag, 19 wt.% Zn and 1.3 wt.% Sn (Table 3), and the light phase (based on silver) contains about 6.8 wt.% Cu, 13.3 wt.% Zn and

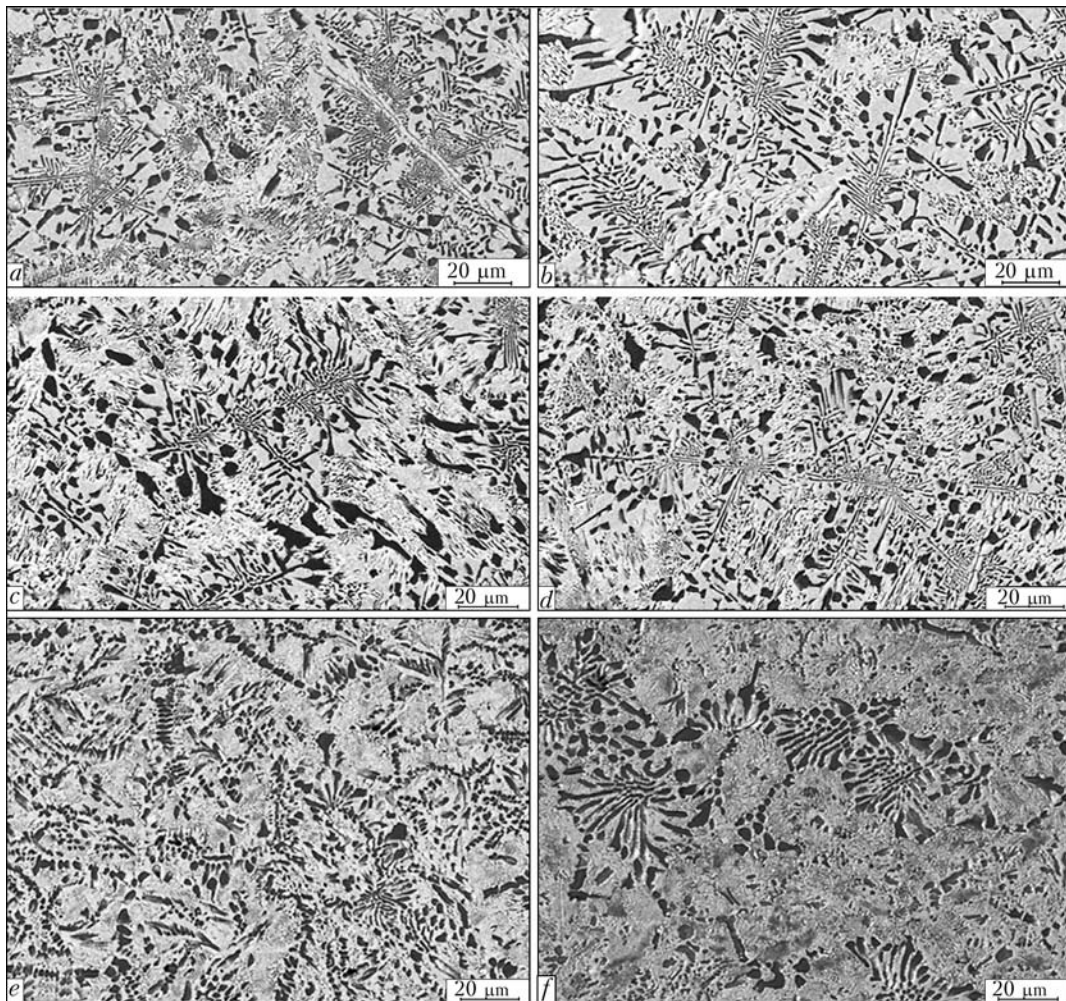


Figure 5. Microstructure of alloys of the 57.5Ag-22.5Cu-17Zn-3Sn (*a*), 57.5Ag-22.5Cu-17Zn-3Sn-0.25SiCa (*b*), 56Ag-22Cu-17Zn-5Sn (*c*), 56Ag-22Cu-17Zn-5Sn-0.25SiCa (*d*), 55Ag-21.5Cu-16.5Zn-7Sn-0.25SiCa (*e*) and 55Ag-20Cu-15Zn-10Sn-0.25SiCa (*f*) systems



3.8 wt.% Sn. The first composition is in a higher temperature range than the second one. Therefore, the first alloy should be a bit more high-temperature one, and should be the first to solidify, which can be seen in Figure 5, *a, b*. The alloys containing tin solidify in almost indiscernible temperature ranges (see Figure 3, *c*). Supposedly, solidification of the alloys occurs as follows. Primary dendrite of the copper-base phase precipitate from the liquid, and then the second phase starts solidifying around the first one in a close temperature range, i.e. solidification of the conglomerate eutectic takes place, and solidification of the normal (lamellar) eutectic begins in the intervals. As the primary crystals are few, the normal eutectic takes a larger part of a section. It should be noted that in some cases the eutectic has a sort of the dendrite stem, and the eutectic colony looks like the «eutectic dendrite». Similar eutectic solidification was noted in filler metal of the Ni–Mn–Cu–Si system [8].

Adding silicocalcium does not have a marked effect on structure of a brazing filler metal, as well as on distribution of elements into structural components.

As noted above, the curves plotted with the help of high-temperature differential analysis for alloys with 3 and 5 wt.% Sn are very similar to each other. The same can be said about structure of these alloys (see Figure 5, *a–d*). It should be noted that the tin content of structural components of alloys with 5 wt.% Sn increases, especially with the silicocalcium addition.

With increase in the tin content to 7 wt.%, the content of the dark high-temperature phase based on copper also grows, and structure as a whole (especially the eutectic component) becomes greatly refined, like in the case with 10 wt.% Sn (Figure 5, *e*). At the same time, the alloys with 10 wt.% Sn and siliconcalcium addition comprise the eutectic regions with coarser grains (Figure 5, *f*). Probably, this depends upon the ingot cooling conditions.

It can be concluded on the basis of the results obtained that the additions of tin to the alloys of the Ag–Cu–Zn system have a less efficient influence than the additions of cadmium. For example, the minimal

achieved liquidus temperature is about 650 °C even in the alloys with 7 wt.% Sn, i.e. it is much higher than in the alloys with a high cadmium content. However, at a tin content of 7 and more than 10 wt.%, the melting range is two-phase and very wide, this deteriorating the technological properties of the filler metal. In addition, strength characteristics of the joints become much worse (see Table 3). It can be stated on the basis of the results obtained that alloys with 3 or maximum 5 wt.% Sn are most suitable for the application. Moreover, the silicocalcium addition should be considered useful.

CONCLUSIONS

1. The investigated compositions of environmentally clean brazing filler metals of the Ag–Cu–Zn–Sn system have structure close to the eutectic one, suitable melting range, and provide good technological properties of the joints.

2. Utilisation of these filler metals instead of those of the Ag–Cu–Zn–Cd system for brazing stainless steels provides the comparable strength values at a tin content of the filler metals equal to no more than 5 wt.%.

3. Filler metals of the system under consideration do not require any changes in heating methods and compositions. They require no special approaches, and can be easily applied under industrial conditions.

1. (1996) *Constitutional diagrams of binary metal systems*: Refer. Book. Vol. 1. Ed. by N.P. Lyakishev. Moscow: Mashinostroenie.
2. Drits, M.E., Bochvar, N.R., Guzej, L.S. et al. (1979) *Binary and multi-component copper-base systems*. Moscow: Nauka.
3. Schwartz, M.M. (1987) *Brazing*. Ohio: Metals Park.
4. (2003) *Reference book on brazing*. Ed. by I.E. Petrunin. Moscow: Mashinostroenie.
5. Roberts, P.M. (1978) Recent developments in cadmium-free silver brazing alloys. *Welding J.*, **10**, 23–30.
6. Timmins, P.F. (1994) The development of Ag-based brazing alloys. *Ibid.*, **10**, 31–33.
7. (1996) *Constitutional diagrams of binary metal system*: Refer. Book. Vol. 2. Ed. by N.P. Lyakishev. Moscow: Mashinostroenie.
8. Khorunov, V.F. (2008) *Principles of brazing of thin-walled structures of high-alloy steels*. Kiev: Naukova Dumka.



PROPERTIES OF THE WELDED JOINTS OF TUBULAR BILLETS PRODUCED BY PRESSURE BRAZE-WELDING WITH A FORMING DEVICE

A.S. PISMENNY, A.S. PROKOFIEV, A.A. PISMENNY, D.P. NOVIKOVA, R.V. YUKHIMENKO, V.V. POLUKHIN, I.I. PTASHINSKAYA and Yu.V. POLUKHIN
E.O. Paton Electric Welding Institute, NASU, Kiev, Ukraine

The paper generalizes the results of assessment of the influence of a forming device on properties of a circumferential butt joint forming in solid-state pressure butt braze-welding of tubular billets. Chemical elements distribution and phase composition were studied in the weld metal and the adjacent zone.

Keywords: welding, pressure butt welding, braze-welding, upsetting, deformation, formation, weld, chemical composition, distribution of elements

Formation of the weld metal in a process of solid-state pressure welding with a high-frequency heating occurs non-uniformly along the entire length of the joint, which shows up in different thickness of the weld. This non-uniformity is caused mainly by a complex character of movement of heated edges in upsetting during their plastic deformation and, in particular, by a non-uniform heating of the edges across the billet section.

The resulting peripheral fillet areas of the weld have a larger width of solidified interlayer of the weld, compared with the internal weld areas, where only common intergrowth grains of the base metal are located instead of the weld metal.

Separate visible fragments of the solidified weld interlayer have size comparable with grain size of the

base metal, as well as the weld exhibits the trend to increase in thickness with distance to the fillet area [1–5].

The E.O. Paton Electric Welding Institute suggested using a forming device in solid-phase pressure braze-welding of pipes to provide the weld with a uniform thickness.

This process of solid-phase butt braze-welding is performed in the following way. The edges of the parts being welded are covered with a mixture of brazing filler metal and activating substances, and the weld zone is shielded by flux. Heating is stopped after the billet edges reach the required temperature, at which melting of activating substances takes place. At the same moment the forming device is placed over the weld plane, and upsetting is performed. Formation of the weld bead occurs with the help of circumferential forming device (Figure 1, clamps and upsetting mechanism are not shown). The welds on tubular samples of diameter 26×2.5 mm from 08kp (rimming) steel (GOST 1050–74) were made by the braze-welding method according to the above-described scheme by using the P-137 UKhL 4 unit designed for pressure welding and brazing of 21.3–60.0 mm diameter pipes under a nominal upsetting force of 4.5 kN.

Heating of the joining zone was carried out with a high-frequency generator. The PVV-100/8000 converter with a speed of 8000 rpm, GVV-100/8000 generator with a frequency of 8000 Hz, and T33-800 UKhL 4 quenching transformer were used.

Chemical compositions of metal of the tubular billets, brazing filler metal and weld metal, which were used for the braze-welding process, are given in the Table. For that the nickel-based brazing filler metal (with $\approx 67.298\%$ Ni) applied prior to the braze-welding process by plasma spraying on edges of the billets and their outer surface near the joining zone was used [6].

X-ray spectral microanalysis was performed with the Comebax device (model SX-50) to examine distribution of main chemical elements across the welded joint. The examinations were carried out with move-

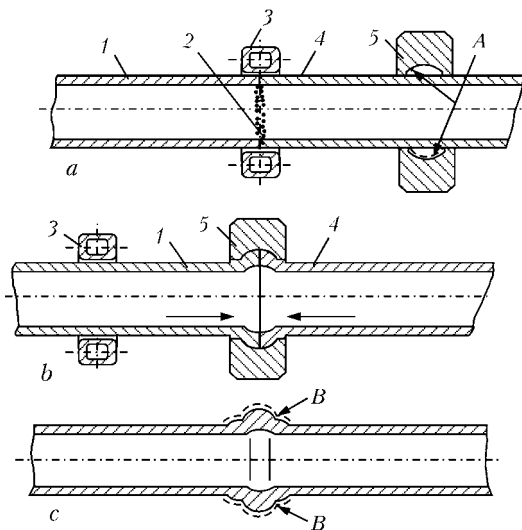


Figure 1. Scheme of the process of induction welding and braze-welding with forced weld formation: *a*, *b* – heating and upsetting process, respectively; *c* – resulting welded joint; 1, 4 – tubular billets; 2 – mixture of brazing and welding consumables; 3 – circular inductor; 5 – forming device; A – forming surface of the device; B – weld bead surface

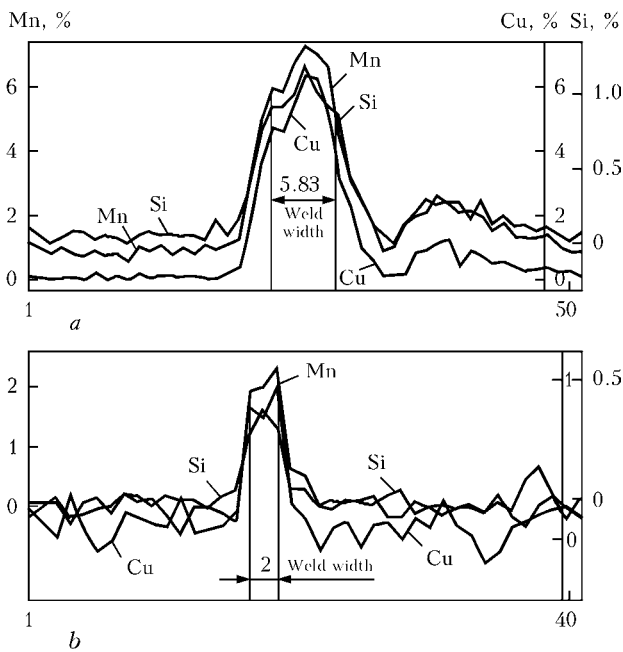


Figure 2. Distribution of Mn, Cr and Si determined in the first (a) and second (b) point in cross section of the joint with the optically revealed area of the weld metal

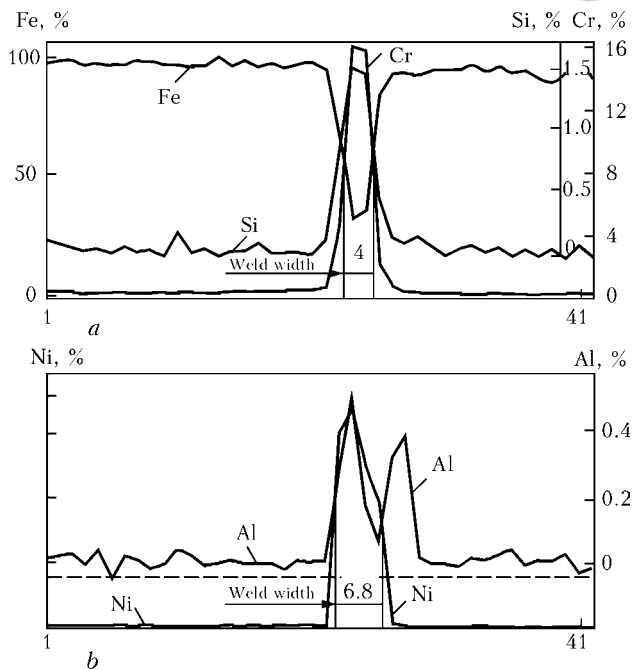


Figure 3. Distribution of Fe, Si, Cr (a), Ni and Al (b) in cross section of the joint with the optically revealed area of the weld metal

ment of the microprobe to a distance of 50 μm (1.02 μm step).

The X-ray spectral microphotographs of distribution of chemical elements in a cross-section of the joint with the optically identified area of the weld 2–7 μm wide are presented in Figures 2 and 3.

The examinations of microstructure were performed in several points on fragments of the weld, where a non-displaced interlayer of the crystallized solid-state phase can be visualized.

The analysis was carried out in four points for seven main chemical elements. Microhardness of the resulting welds and base metal in the near-weld zone was also measured with the help of the LECO microhardness gage M-400 under 25 g loading. Immediately before the welding process the edges of the tubular billets were covered with powdered flux – borax $\text{Na}_2\text{B}_4\text{O}_7$ on a binder.

It can be seen that base of the weld metal in the solidified areas is iron, the content of which due to its diffusion from metal of the billets into the weld exceeded 45 %. The content of iron in a sprayed layer of the brazing filler metal was only 3.7 %.

At the moment of heating shutdown, the formed liquid phase contains primarily components of the sprayed layer of the brazing filler metal. The content

of nickel as a component of the brazing filler metal reduced from 67.298 to 32.172 % in wetting the base metal edges with the liquid phase. However, its content in the base metal of the billet was only 0.25 %.

Thus, an interdiffusion of nickel from the liquid phase into the base metal and vice versa took place.

It is known that the depth of penetration of diffusion fluxes into the base metal in iron to nickel welded joints made in $3 \cdot 10^{-4}$ mm Hg vacuum at a temperature of 1300 ± 10 $^\circ\text{C}$ and pressure of 15 MPa is about 20 μm for a period of welding of 10 min [7].

Application of plastic deformation and a high speed of the braze-welding process (deformation rate $\epsilon \geq 100\text{--}120$ s^{-1}) [8] lead to reduction of both thickness of the weld up to 2–7 μm (see Figures 2, 3) and diffusion zone in the base metal. The content of chromium in the weld metal also increased to 16.772 % (however, originally its content in the deposited brazing filler metal was 14.012 %, and in the base metal – 0.1 %). It is known that chromium, in particular, forms high-resistant alloys and Cr–Ni systems, which are located in the weld zone in a solid-liquid state during welding.

The temperature of the solid-state welding process carrying out (800–950 $^\circ\text{C}$) also promotes formation of compounds of chromium with carbon, silicon and other impurities, in particular, with aluminum.

Distribution of main chemical elements in base metal, deposited brazing filler metal and optically revealed areas of weld metal in welded joints

Investigated area	Al	Si	Cr	Mn	Ni	Fe	Cu	Balance
Base metal	–	0.03	0.1	0.4	0.25	98.735	0.25	0.235
Sprayed brazing filler metal	2.673	2.359	14.012	0.26	67.298	3.736	0.374	9.287
Weld metal	0.381	1.691	16.772	0.339	32.172	45.688	0.439	2.516



HV0.25, MPa

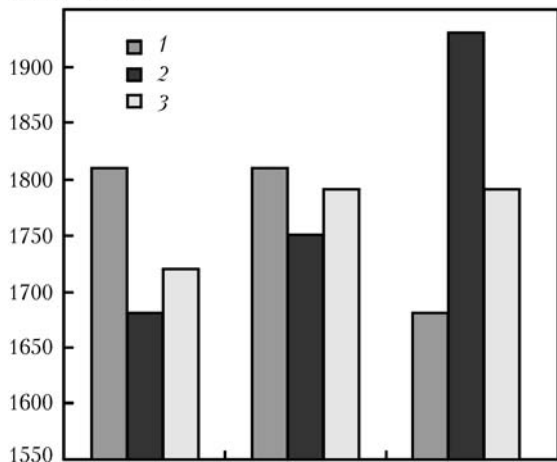


Figure 4. Diagram of distribution of microhardness in welded joint: 1 – weld metal; 2 – base metal; 3 – fusion line

The content of manganese in the weld metal is 0.339 %, which is lower than in the base metal (0.4 %). The content of manganese in sprayed brazing filler metal is even lower, and equals 0.26 %.

Manganese actively interacts with non-metals, i.e. impurities, such as carbon, nitrogen and phosphorus, in heating and formation of the liquid phase.

The data given in the Table indicate to a reduction of the content of impurities in the weld metal, compared with the deposited brazing filler metal. Thus, there was a reduction of the content of silicon from 2.359 % in the deposited brazing filler metal to 1.691 % in the weld metal, and of the content of aluminum from 2.673 to 0.381 %, respectively. The content of other elements, including impurities, decreased from 9.287 % in deposited brazing filler metal to 2.516 % in the weld metal.

Initially, with increase in temperature during heating, the non-metallic impurities dissociate from the compounds containing them. Then they diffuse into the liquid phase, where they form new compounds, including with components of the brazing filler metal, which is accompanied by increase in their content in the liquid phase, with which they are displaced from the weld zone during the upsetting process. The copper content of the weld metal grows. For example, the copper content of the billet base metal is 0.25 %, of the deposited coating is 0.374 %, and of the weld metal is 0.439 %. It is likely that copper diffuses from both base metal edges and deposited coating into the liquid phase, the fragments of which form a fusion line.

Analysis of microhardness of the weld metal and near-weld zone was carried out on samples in order to determine their comparative characteristics by using the known methods [9–14]. Microhardness HV0.25 of the weld metal was 1680–1810 MPa, that of the base metal was 1680–1930 MPa, and of the fusion line was 1720–1790 MPa, respectively.

Figure 4 shows the diagram of distribution of microhardness in a welded joint, based on the obtained data. The spread of the microhardness values from a

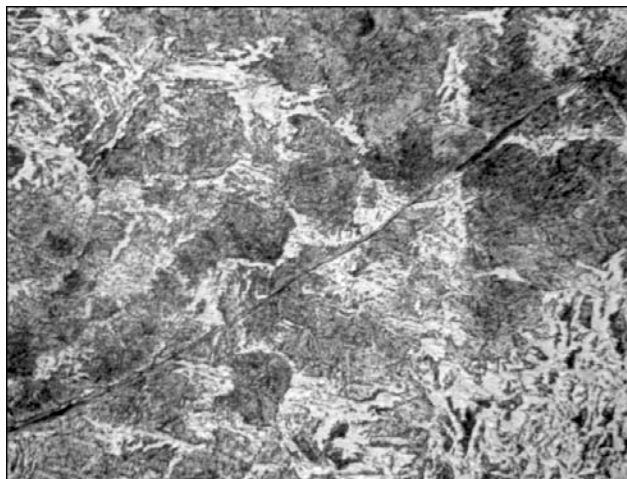


Figure 5. Microstructure (x320) of the weld region up to 3.5 μm thick

mean measured microhardness of the weld equal to HV 1805 MPa amounts to 7 %. These data are indicative of the closeness of strength properties of the weld metal to properties of the base metal [15].

No elements of an activating substance, participating in the diffusion processes in the form of individual quenching structures and brittle phases, were revealed in the weld metal and near-weld zone.

The diffusion processes are activated along the phase contact boundaries in a short period of time upon reaching the melting temperature of the brazing filler metal and shutdown of heating before upsetting.

In upsetting, the internal, least heated deep layers of the base metal, which are situated between the middle and internal diameter of a tubular billet, take part in the weld formation.

The forming device protects the weld face from its exposure to the environment, while the weld formation proper occurs with a thermo-mechanical impact in the form of plastic deformation, followed by solidification under a pressure that is close to the uniform volumetric stressed state, which provides a more homogeneous composition of the weld metal along its entire length.

Sometimes, fragments of the weld interlayer solidified under a pressure can be seen along the length of the formed weld. These are the remainders of metal that was in the solid-liquid state, which were not completely pressed out, were plastically deformed and transformed into a thin weld interlayer (Figure 5).

CONCLUSIONS

1. Application of the forming device leads to a 2–7 μm decrease in the weld thickness and reduction of width of the diffusion zone, compared with the weld formation in a free state.

2. No quenching structures and brittle phases were revealed in the weld metal and near-weld zone.

3. Application of the forming device results in homogenization and formation of uniform phase composition of the weld metal and near-weld zone.



1. Lebedev, V.K., Tabelev, V.D., Pismenny, A.S. (1983) Pressure butt brazing of steel pipelines. *Avtomatch. Svarka*, **9**, 25–27.
2. Lebedev, V.K., Tabelev, V.D., Pismenny, A.S. et al. (1989) High-temperature brazing of tubes for exploration drilling. *Ibid.*, **5**, 28–30.
3. Pismenny, A.S., Shinlov, M.E., Buzhenetsky, A.I. (1995) Application of induction braze-welding for joining of oil range pipes. *Ibid.*, **12**, 35–38.
4. Pismenny, A.S., Prokofiev, A.S. (2002) Press welding of pipes using activating materials. *The Paton Welding J.*, **7**, 19–23.
5. Prokofiev, A.S., Pismenny, A.S., Bondarev, V.A. et al. (2001) Induction braze-welding of no-accessory T-joints in pipes. *Ibid.*, **4**, 43–47.
6. (1989) *Handbook of steels and alloys grades*. Moscow: Mashinostroenie.
7. Larikov, L.N., Ryabov, V.R., Falchenko, V.M. (1975) *Diffusion processes in solid phase welding*. Moscow: Mashinostroenie.
8. Pismenny, A.S., Skachko, Yu.N. (2006) High-frequency heating. Heating of metal in pressure welding. In: *Machine building*. Vol. 3, 4: Technology of welding, brazing and cutting. Ed. by B.E. Paton. Moscow: Mashinostroenie.
9. Davidenkov, N.N., Belyaev, S.E., Markovets, M.P. (1945) Characterization of main mechanical properties of steel using hardness measurement. *Zavod. Laboratoriya*, **10**, 964–973.
10. Sichikov, M.F., Zakharov, B.P., Kozlova, Yu.V. (1947) About determination of mechanical properties without tensile tests. *Ibid.*, **12**, 1463–1471.
11. Kuchuk-Yatsenko, S.I., Kazymov, B.I. (1967) Optimal thermal cycle in resistance butt welding of 12Kh1MF steel. *Avtomatch. Svarka*, **6**, 24–27.
12. Forostovets, B.A. (1972) Peculiarities of joint metal structure in fusion welding. *Ibid.*, **4**, 9–13.
13. Markovets, M.P. (1979) *Determination of mechanical properties of metal by hardness*. Moscow: Mashinostroenie.
14. Gulyaev, A.P. (1989) To problem of mechanical properties of structural steels. *Materialovedenie i Termich. Obrab. Materialov*, **7**, 23–25.
15. Shmykov, A.A. (1956) *Handbook of heat-treater*. Moscow: Mashgiz.

EVALUATION OF STRESS-STRAIN STATE OF DISSIMILAR WELDED JOINTS FROM 10KH13G18D + 09G2S STEELS

A.I. GEDROVICH¹, S.A. TKACHENKO¹ and I.A. GALTSOV²

¹V. Dal East-Ukrainian National University, Lugansk, Ukraine

²Lugansk National Agrarian University, Lugansk, Ukraine

The features of determination of residual welding stresses on full-scale samples from 10Kh13G18D + 09G2S dissimilar steels are considered. A dependence is established between the size of the zone of plastic strains and longitudinal residual welding stresses on the applied technologies of gas-shielded welding, modes and heat inputs. Positive influence of the technology of cold metal transfer on residual stresses and dimensions of plastic strain zones in dissimilar steel joints is conformed.

Keywords: residual stresses, welding modes, heat input, welds, near-weld zone, plastic strain zone, magnetic properties

The cars of diesel-driven and electric trains being used at present time in Ukraine and CIS countries have two doors, car length up to 21.5 m and maximum capacity up to 240 persons. Car bodies are manufactured from low-carbon and low-alloy steels in a form of sheet, bar and plates (including cold bent sections) as well as steel castings separate elements of which, according to statistics, require a repair or change already after 5–6 years of running [1] due to high corrosion.

The main trend of development of a design of the electric and diesel-driven trains of this type is the maximum reduction of structure weight at retention or increase of the amount of seats with simultaneous providing of the necessary technical characteristics [2]. The elements and units of cars are subjected to corrosion, abrasive wear and temperature fluctuations in running along with multiple mechanical and alternating dynamic loads.

Steels having the following mechanical properties: $\sigma_t = 500\text{--}550$ MPa, $\sigma_y = 400$ MPa, $\delta = 21$ % are recommended to use for cars engineering based on experience of running and experimental and theoretic investigations of R&D institutes VNIIZhT and VNIIV.

Low-carbon and low-alloy steels used at present time do not fulfill the requirements mentioned above.

There is a world practice experience of application of stainless chromium-nickel steels of austenite class for skin of cars in transport industry with the aim of reaching more long-term resource of their running.

Stainless nickel-free 10Kh13G18D grade steel [3] was developed and recommended for manufacture of cars by the I.P. Bardin TsNII Chermet (Moscow, Russia) instead of 12Kh18N10T and 08Kh18N10 steels in order to provide the necessary requirements and economy of expensive nickel. This steel is characterized by high ductility in pressing and cavitation resistance, therefore it is good in application for body skin, and more cheap low-alloy higher strength 09G2S steels for framework elements of the body structures of cars. Application of 09G2S steel for framework elements of the body allows reducing the thickness of parts from 3.0–8.0 to 2.5–7.0 mm, and usage of 10Kh13G18D stainless steel in cold-worked state — skin thickness from 2.5 to 1.5 mm. As a result, it is expected that at significant increase of the car dimensions the weight will not change and its life time will increase.

It is well-known that a working capacity of welded structures significantly depends on thermo-mechanical properties occurring in area of the weld, values of



Figure 1. Laboratory unit for welding of the samples from dissimilar steels 10Kh13G18D + 09G2S

plastic strain and level of longitudinal residual stresses σ_x [4, 5], which in the welded joints can reach a yield strength σ_y of a metal to be welded and more, and transverse stresses at two-dimensional stressed state can not be higher than $0.75\sigma_y$ [4]. A purpose of the present paper, therefore, is to investigate the dependences of formation of zones of plastic strains and longitudinal residual stresses in welding of 10Kh13G18D + 09G2S dissimilar steels.

The study was carried out in experimental way. Numerous investigations showed [3–8] that the residual welding stresses, which can exceed the material yield strength in welding of low-carbon structural steels and reach the yield strength [6] in welding of Cr–Mn corrosion-resistant steels, are formed in welded joints and units as a result of effect of welding thermal-deformation cycle. The longitudinal stresses are tensile as a rule and being the result of different level plastic strain in welding heating and cooling [5]. The dependences of their distribution in an active zone are studied well enough and plastic strain in it reaches 1–2 % [4, 5] in welding structural steels (St3, 14G2 and etc.).

The differences in formation of the longitudinal residual stresses σ_x in welding of pearlite steel 09G2S and austenite steel 10Kh13G18D are conditioned by the fact that austenite stainless steels have a low heat conduction coefficient, high coefficient of linear expansion and tendency to hardening. The presence of plastic strain and fields of high residual first-kind

tensile stresses leads to austenite decomposition, i.e. phase transformation and occurrence of α -phase, in the weld zone and near-weld zone according to study [6]. Distribution of the residual welding stresses [6, 7] in this zone can be qualitatively considered on a content of α -phase in the welded joint. In this study a zone of plastic strains on the area of welded joint from the side of pearlite steel was determined on yield bands [4] and longitudinal residual stresses — on a change of magnetic properties of steel (magnetic permeability) [5].

The plates of 125 × 300 × 1.5 mm size (steel 10Kh13G18D), the thickness of which corresponded to the thickness of metal of the car skin, and 125 × 300 × 2.5 (7) mm size plate from steel 09G2S were used for investigations. Higher thickness 7 mm corresponded to the joints of skin with the car body frame. The samples were previously ground and polished. Polished samples were lap assembled and their welding was carried out using semi-automatic machines A-547U and TRS-3200 CMT (Figure 1). At that Sv-08Kh20N9G7T grade welding wire of 1.2 mm diameter and shielding gas mixture (Ar + CO₂) in a «conductor» assembly jig as well as CMT technology were used.

The following conditions were applied in welding by semi-automatic machine: A-547U: $I = 110–120$ A; $U_a = 20–21$ V; $v_w = 17–22$ m/h; $q_w = 3350$ J/cm; and $I = 106$ A; $U = 15.9$ V; $v_w = 38.2$ m/h; $q_w = 1105$ J/cm for TRS-3200 CMT semi-automatic machine.

The zone of plastic strains $Bn2$ (Figures 2 and 3) on 10Kh13G18D austenite steel was etched after welding by Fray etching agent, then after the zone boundaries became apparent the etching agent was washed out with alcohol, the sample was dried and etching by Amberg–Kalling etching agent carried out. After the boundaries of plastic strain became clearly apparent the sample was wiped out by alcohol and dried.

The zone of plastic strains $Bn1$ (see Figures 2, 3) in the area of welded joint from the side of 09G2S pearlite steel was determined on yield bands — Chernov–Luders lines. Longitudinal residual stresses σ_x in

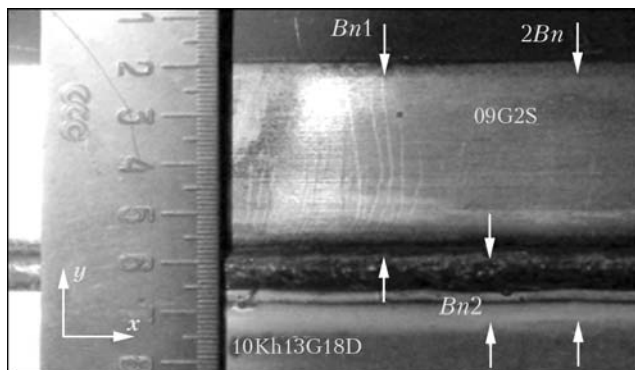


Figure 2. Sizes of the plastic strain zones $Bn1$, $Bn2$, $2Bn$ of a sample of lap welded joint from steels 10Kh13G18D ($\delta = 1.5$ mm) and 09G2S ($\delta = 2.5$ mm) in welding by A-547U semi-automatic machine

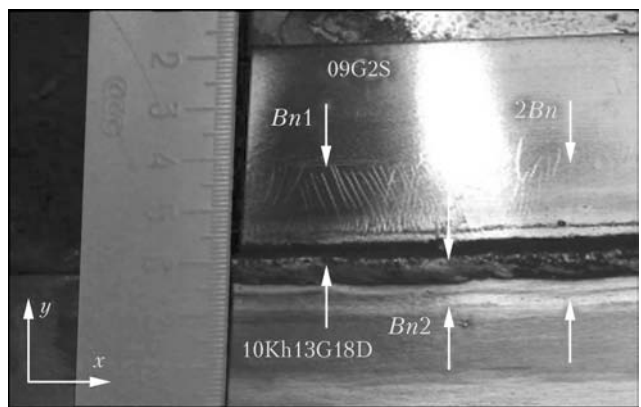


Figure 3. Sizes of the plastic strain zones $Bn1$ and $Bn2$ of a sample of lap welded joint from steels 10Kh13G18D ($\delta = 1.5$ mm) + 09G2S ($\delta = 2.5$ mm) in welding by TRS-3200 CMT semi-automatic machine

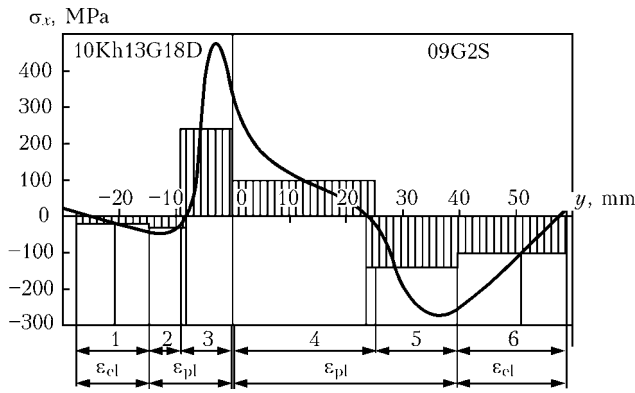


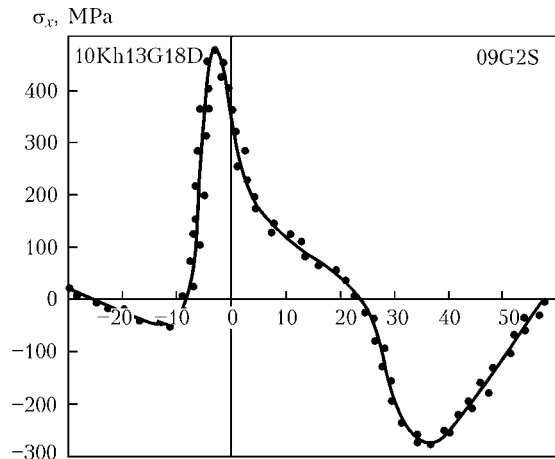
Figure 4. Character stressed zones of the welded joint from steels 10Kh13G18D ($\delta = 1.5$ mm) + 09G2S ($\delta = 2.5$ mm) in welding by A-547U semi-automatic machine (for 1-6 see the text)

10Kh13G18D steel were evaluated according to the procedures of study [5]. The common zone $2Bn$ of plastic strains of dissimilar joint 10Kh13G18D + 09G2S was determined after etching in the central part of the welded joint with a portable binocular microscope MPB-3. An error of measurement made 0.025 mm. Five measurements were performed to calculate the average value. The end areas of 60 mm length were not considered in order to eliminate an influence of end effect. The experiment was repeated three times. The average value of $2Bn$ zone, therefore, was determined on data obtained from 15 observations. Photography was carried out by digital camera.

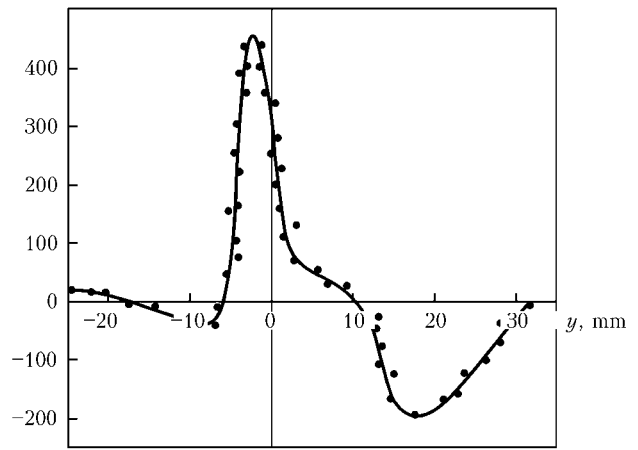
Distribution of longitudinal residual stresses σ_x along the OY axis was determined after the welded joint complete cooling. The tensile stresses appear in austenite steel 10Kh13G18D since it has significantly larger reduction of volume in comparison with 09G2S ferrite-pearlite steel, and compression stresses compensating them (Figure 4) form in the area of ferrite-pearlite steel. The fields of residual stresses in single and dissimilar joints are close to each other and differ only by some displacement of diagram in the direction of steel with smaller heat conduction (in this case in the direction of austenite steel) (Figure 5). These stresses in most cases cannot be relieved by heat treatment and develop a danger of service failure as well as change of structure in time. After making a comparison of the diagram of residual stresses σ_x and sizes of the zone of plastic strains in welded joints obtained in welding of samples by A-547U and TRS-3200 CMT semi-automatic machines, the following conclusions can be done:

- reduction of the level of tensile stresses σ_x by 5.3 % and size of the plastic strain zone $2Bn$ by 45.5 % is observed in samples from 10Kh13G18D ($\delta = 1.5$ mm) + 09G2S ($\delta = 2.5$ mm) steels in welding with semi-automatic TRS-3200 CMT machine;

- reduction of the level of tensile stresses σ_x by 5.3 % and size of the plastic strain zone $2Bn$ by 21.3 % takes place in samples from 10Kh13G18D ($\delta = 1.5$ mm) + 09G2S ($\delta = 7$ mm) steels in welding with semi-automatic TRS-3200 CMT machine.



a



b

Figure 5. Diagrams of residual stresses σ_x in the welded joints from steels 10Kh13G18D ($\delta = 1.5$ mm) + 09G2S ($\delta = 2.5$ mm) obtained with A-547U (a) and TRS-3200 CMT (b) semi-automatic machines

Based on analysis of the plastic strain zones $2Bn$ of the welded joint from 10Kh13G18D ($\delta = 1.5$ mm) and 09G2S ($\delta = 2.5$ mm) and diagrams of residual stresses σ_x in samples welded by A-547U semi-automatic machine (see Figure 4) the following stress zones can be outlined:

1 – zone of compression stresses σ_x (≈ 16 mm) is situated in the HAZ base metal (from the side of austenite steel) and has no plastic strain in welding. The level of maximum compression stresses is -45 MPa, average value is -27 MPa;

2 – zone of maximum compression stresses σ_x (≈ 6 mm). The metal is also situated in HAZ and suffers from the plastic strain in the process of welding cycle. The level of maximum compression stresses is -50 MPa, average value is -40 MPa;

3 – zone of maximum tensile stresses σ_x . The weld and near-weld zone (≈ 9 mm) from the side of austenite steel are situated in the area of plastic strains. The level of maximum tensile stresses is 475 MPa, average value is 250 MPa;

4 – zone of maximum tensile stresses σ_x . The weld and near-weld zone (width of ≈ 23 mm) from the side of ferrite-pearlite steel are situated in the area of plastic strains. The level of maximum tensile stresses is 350 MPa, average value is 100 MPa;

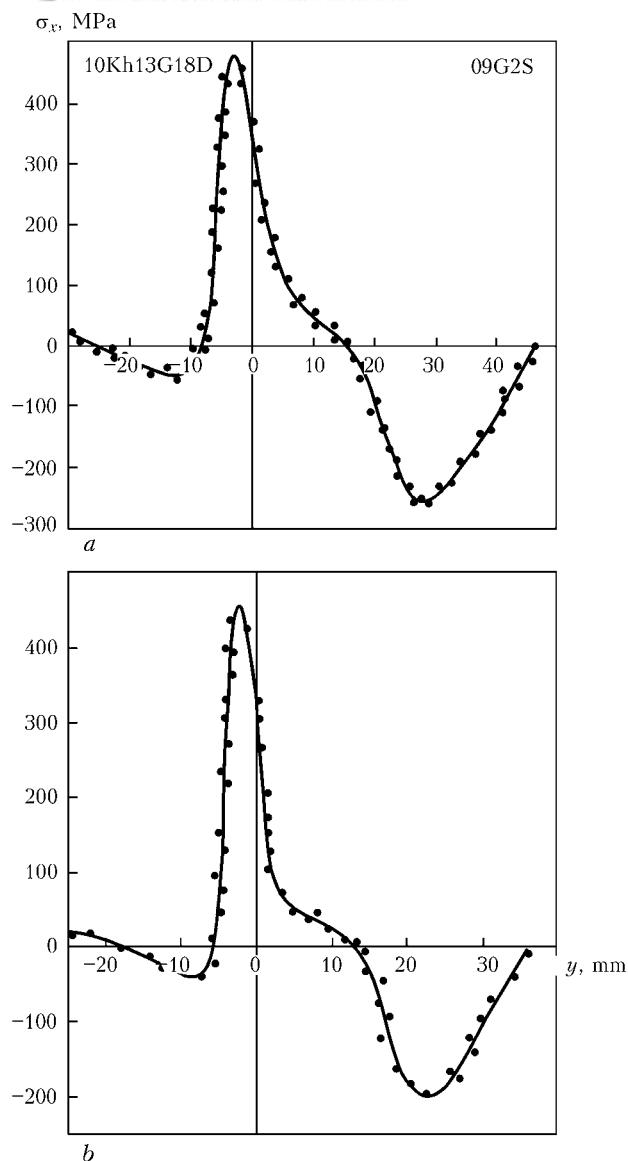


Figure 6. Diagrams of residual stresses σ_x in the welded joints from steels 10Kh13G18D ($\delta = 1.5$ mm) + 09G2S ($\delta = 7$ mm) obtained with A-547U (a) and TRS-3200 CMT (b) semi-automatic machines

5 – zone of maximum compression stresses σ_x (≈ 17 mm) are situated in the base metal which suffers from the plastic strains in the process of welding. The level of maximum compression stresses is -270 MPa, average value is -140 MPa;

6 – zone of compression stresses (≈ 19 mm) are situated in the base metal, which undergoes no plastic strains in welding. The level of maximum compression stresses is -230 MPa, average value is -100 MPa.

It follows from the analysis of obtained experimental data that the maximum tensile residual stresses, which 6.6 % higher over the yield strength

of the material ($\sigma_y = 450$ MPa), are observed in zones 3 and 4. The plastic strain zones are identical to the described above and differ only in sizes of the plastic strain zones and values of stresses in welding of the samples using TRS-3200 CMT semi-automatic machine.

Theoretical calculation on a method described in study [4] was carried out in order to verify integrity of the data obtained as a result of the experiments carried out for determination of the size of zones of plastic strains $2Bn$ which appear in welded joints from dissimilar steels (10Kh13G18D + 09G2S). Data obtained in welding of the samples using semi-automatic machines A-547U and TRS-3200 CMT were taken as a basis for calculation and comparative analysis.

Comparison of the data on the size of plastic strain zones showed that the disagreement between the experiment and theoretic calculation does not exceed 5 %.

CONCLUSIONS

1. Size of the plastic strain zone $2Bn$, which consists of the zone of plastic strain $Bn1$ (HAZ from the side of ferrite-pearlite steel) and $Bn2$ (HAZ from the side of austenite steel), where $Bn1 > Bn2$, was determined in experimental way in welding of dissimilar steels.

2. Presence of significant longitudinal tensile stresses σ_x in HAZ metal from the side of austenite steel and compression stresses in HAZ metal from the side of ferrite-pearlite steel was determined.

3. Advantage of application of CMT technology for achievement of minimum plastic strain zone in welded joints from dissimilar steels was verified in experimental way.

1. Basov, G.G., Golubenko, A.L., Mishchenko, K.P. (2003) Conception for development of type of advanced motorized-car rolling stock for Ukrainian railways. In: *Transact. on problems of implementation and mastering of production in Ukraine of motorized-car rolling stock based on unified intermediate car*. Lugansk: Mashinostroenie.
2. Bereznitsky, V.A., Sergienko, N.I., Shcherbakov, V.P. (2003) Application of stainless and low-alloy steels for cars of diesel- and electric trains of maximum passenger capacity. *Ibid.*
3. Goldshtejn, M.I., Grachev, S.V., Veksler, Yu.G. (1985) *Special steels*. Moscow: Metallurgiya.
4. Gedrovich, A.I. (1998) *Plastic strain in welding*. Lugansk: UUGU.
5. Kasatkin, B.S., Prokhorenko, V.M., Chertov, I.M. (1987) *Stresses and strains in welding*. Kiev: Vyshcha Shkola.
6. Gedrovich, A.I., Tkachenko, A.N., Tkachenko, S.M. et al. (2007) Peculiarities of structure and properties formation in 10Kh13G18D steel fusion zone. *The Paton Welding J.*, 4, 20–24.
7. Sagalevich, V.M., Saveliev, V.F. (1986) *Stability of welded joints and structures*. Moscow: Mashinostroenie.
8. Kurdyumov, G.V., Utevsky, L.M., Entin, R.I. (1977) *Transformations in iron and steel*. Moscow: Nauka.

MAGNETICALLY-IMPELLED ARC BUTT WELDING OF PIPES OF STEEL X70

S.I. KUCHUK-YATSENKO, V.S. KACHINSKY, V.Yu. IGNATENKO, E.I. GONCHARENKO and M.P. KOVAL
E.O. Paton Electric Welding Institute, NASU, Kiev, Ukraine

The paper gives the results of investigation of weldability of pipes of $\text{Ø}168 \times 7$ mm from X70 steel for application in pipelines for various purposes, as well as the results of metallographic and mechanical property investigations of welded joints.

Keywords: *press welding, magnetically-impelled arc, pipe steel X70, pipelines, joint formation, technology of welding*

Over the recent years the investigations are carried out at the E.O. Paton Electric Welding Institute of the NAS of Ukraine for welding pipes and pipelines of up to 219 mm diameter and up to 16 mm wall thickness [1]. Results of investigations showed the feasibility of practical application of magnetically-impelled arc butt (MIAB) welding for pipes and pipelines. The MIAB welding process is characterized by a high efficiency (time of welding is 20–50 s), minimum consumption of pipe parent metal equal to wall thickness, moreover, the auxiliary welding consumables and consumable gas are not required.

The aim of the present work is to investigate the weldability of steel X70 using the MIAB welding method. Pipes of 168 mm diameter and 7 mm wall thickness were used for investigations. This selection was due to demands of different branches of industry and construction for the development of new highly-efficient methods of welding of small-diameter pipes and pipelines. Steel X70 refers to low-carbon steels

with the following chemical composition, wt. %: 0.03 C; 0.156 Si; 1.45 Mn; 0.004 S; 0.004 P; 0.07 Cr; 0.14 Ni; 0.20 Mo; 0.02 V; 0.30 Cu; 0.033 Al; 0.022 Ti; 0.062 Nb; 0.012 As.

Peculiar features of joints formation in MIAB welding, and also main parameters, defining the quality of joints, are described in works [1, 2]. Main technological parameters of welding steel X70 pipes of $\text{Ø}168 \times 7$ mm are the following (Figure 1): time of welding is 34.7 s; upsetting force – 247 kN; pipe shortening – 7.5–7.9 mm; consumed power – 28.7 kW.

To perform the mechanical tests, the sections were cut out from the pipe welded joint. Formation of welded joint on external and internal sides of the pipe is given in Figure 2.

Results of mechanical tests showed that strength and ductile properties of welded joint are at the level of characteristics of the parent metal (Table 1, Figure 3).

Structure of HAZ metal in MIAB welding is mainly similar to the structure of similar joints of pipes made



Figure 1. Welded joint of steel X70 pipes of $\text{Ø}168 \times 7$ mm

Table 1. Mechanical properties of parent metal and welded joint of steel X70 pipes

Test area	σ_y , MPa	σ_t , MPa	KCV ₊₂₀ , J/cm ²
Parent metal	448.9–469.1	528.8–566.8	248.4–265.7
	460.6	551	256.5
Welded joint	411–440	511–556	124.8–283.4
	425.5	533.5	204.1

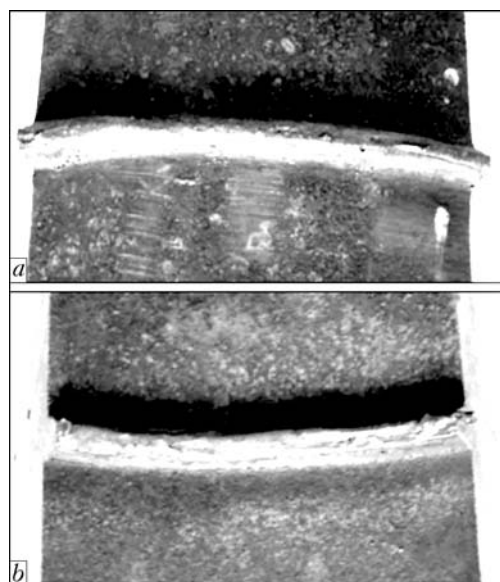


Figure 2. Formation of welded joint on external (a) and internal (b) sides of pipes

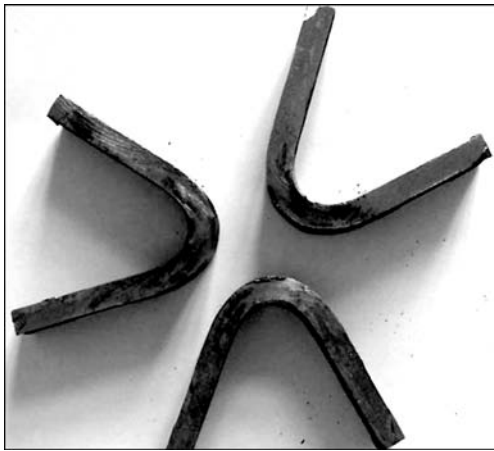


Figure 3. Results of bend tests of welded joint

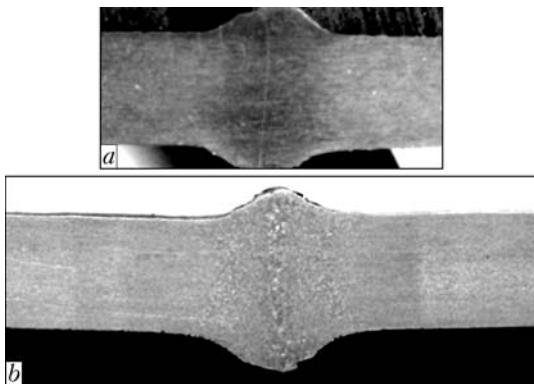


Figure 4. Macrosections of steel X70 welded joints made by MIAB welding (a) and FBW (b)

by the flash-butt welding (FBW), but there are differences in the formation of a central part of the joint. Analysis of macrostructure of joints of steel X70 pipes of $\varnothing 168 \times 7$ mm showed (Figure 4, a) that the HAZ width in MIAB welding is not more than 10 mm, and the width of area of normalization in a middle line is 2 mm. In FBW the width of HAZ and normalization area is 18 and 6 mm, respectively (Figure 4, b). Thus, in MIAB welding the HAZ is much narrower than in FBW that provides the formation of a finer-grain structure.

The area of welded joint of steel X70 was subjected to metallographic examinations. The microhardness of welded joint was measured in the LECO device

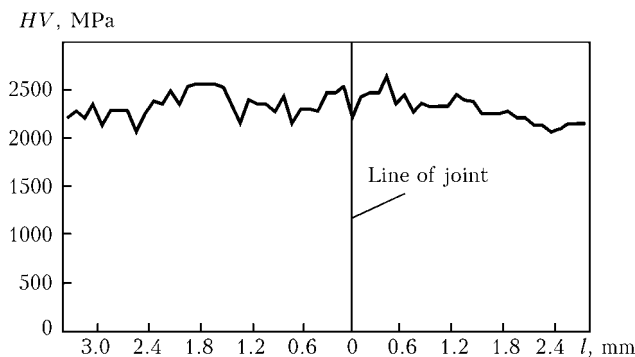


Figure 5. Distribution of microhardness of metal in welded joint zone

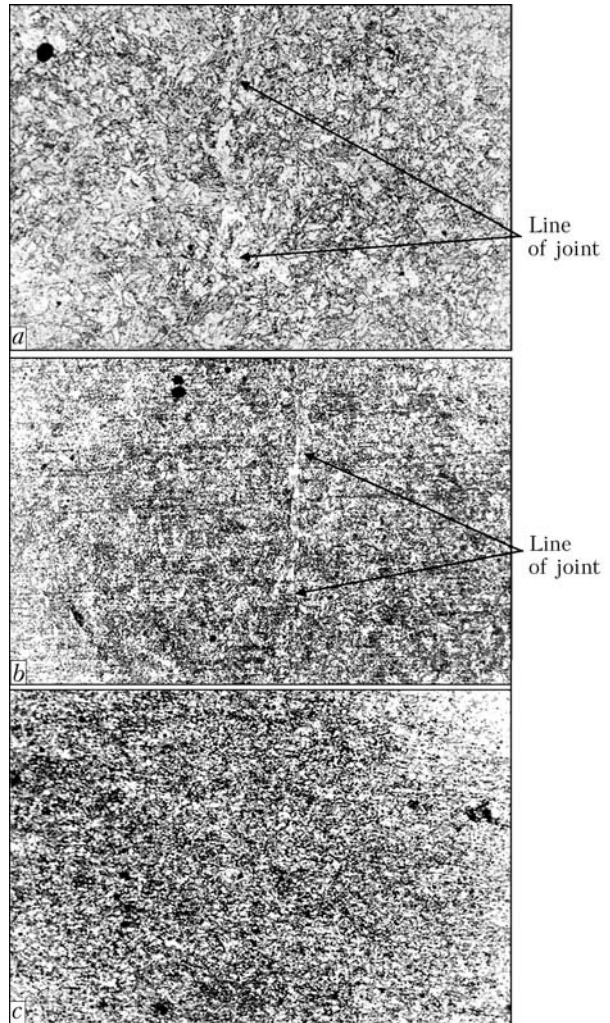


Figure 6. Microstructures ($\times 150$) of welded joint near external edge (a), in central area (b) and parent metal (c)

M-400 at 1 N load and 100 μm pitch. Sample was etched in 4 % HNO_3 solution in alcohol.

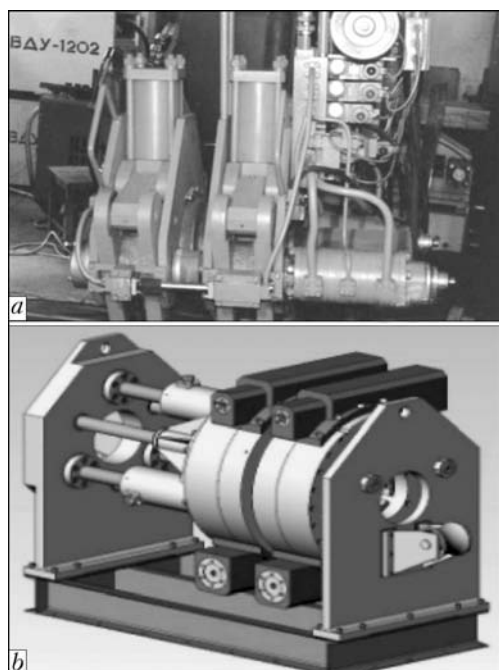


Figure 7. Appearance of machines K-872 (a) and K-981 (b)



It is seen in Figure 5 that there is a negligible increase of hardness in a ferrite band up to *HV* 2450 MPa in the joint, that is higher than the microhardness of the pipe parent metal. In FBW the decrease in microhardness at this region is usually observed.

The joint line represents an intermittent white band of up to 10 μm thickness in a central part of the welded joint and it is widened up to 30 μm to the edges of section sample (Figure 6, *a*). Microhardness of ferrite band of the joint line is *HV* 2050–2450 MPa. Structure of area in a central part of sample is fine-grained (number 8–9 by GOST 5639–82) ferrite-pearlite with hardness of *HV* 2470–2640 MPa (Figure 6, *b*). At the edge of sample the structure is coarser (number 7) with domination of a ferrite component and microhardness of *HV* 2190–2350 MPa (Figure 6, *a*). At the fine grain area the structure is fine-grained ferrite-pearlite with number 10–11 and *HV* 2270–2400 MPa.

The parent metal is fine-grained with domination of a ferrite component (grain number is 10) and *HV* 2130–2360 MPa (Figure 6, *c*).

At the coarse grain area the amount of a pearlite component is increased as compared with that of parent metal and other HAZ regions. This leads to a negligible increase in hardness at this region. Defects in welded joint were not revealed.

The carried out investigations showed that the structure and mechanical properties of joints of pipe steels X70, made by MIAB welding, are very similar to those of FB-welded joints. Therefore, the systems and methods of non-destructive testing and in-process control, accepted in FBW, can be similar.

The machines have been developed for MIAB welding of pipes and pipelines, providing welding in the field and stationary conditions (Table 2).

Machines K-980, K-872, K-981 (Figure 7) are designed for press welding of pipes and different-purpose pipelines and consist of welding head, hydraulic

Table 2. Technical characteristics of machines for MIAB welding

Type of machine	Diameter of pipes to be welded, mm	Wall thickness, mm	Welding efficiency, welds/h	Consumed power, kV·A	Mass, kg
K-980	50–140	3–10	80	80	3500
K-872	89–219	2.5–8.0	60	90	2500
K-981	120–250	3–10	50	160	4500

pumping station, control cabinet with a remote control panel, and arc power source.

The suspended head K-872 is of a tong type, the characteristic feature of which is a separate clamping of pipes being welded. Machine by its design has a possibility of loading and unloading pipes being welded aside [3].

Machines K-980 and K-981 are of a continuous type, the characteristic feature of which is a separate clamping of pipes being welded. Design of machine of a continuous type provides a high accuracy of axial aligning of welded pipes and pipelines [4].

CONCLUSIONS

1. Main conditions of MIAB welding for formation of welded joints of steel X70 are defined.
2. Technology of welding of steel X70 pipes of $\varnothing 168 \times 7$ mm has been developed.
3. Welding equipment and technology of MIAB welding of pipes of up to 250 mm diameter and up to 12 mm wall thickness have been developed

1. Kuchuk-Yatsenko, S.I., Kachinsky, V.S., Ignatenko, V.Yu. (2002) Magnetically-impelled arc butt welding of thick-walled pipes. *The Paton Welding J.*, **7**, 24–28.
2. Fakagi, K., Arashida, F., Sato, S. et al. (1982) Magnetically impelled arc butt welding of town gas pipelines. *Metal Construction*, **10**, 542–548.
3. Kuchuk-Yatsenko, S.I., Kachinsky, V.S., Sakharnov, V.O. et al. *Machine for magnetically-impelled arc butt welding*. Pat. 45449 Ukraine. Valid from 15.04.2002.
4. Kuchuk-Yatsenko, S.I., Kachinsky, V.S., Galyan, B.O. et al. *Machine for butt welding of pipes*. Pat. 200713302 Ukraine. Valid from 29.11.2007.



TECHNOLOGY AND EQUIPMENT FOR MANUFACTURE OF HIGH-PRESSURE CYLINDER BODIES OF SHEET ROLLED STEEL

M.M. SAVITSKY, A.S. PISMENNY, E.M. SAVITSKAYA, S.I. PRITULA and S.K. BABENKO

E.O. Paton Electric Welding Institute, NASU, Kiev, Ukraine

At the E.O. Paton Electric Welding Institute the design and technology have been developed for manufacture of combined high-pressure cylinders with a mass-dimensional factor $M/V \leq 0.65 \text{ kg/l}$ for use in motor-vehicle transport. The cylinder consists of a pressurized body and a strengthening composite sheath. To manufacture the cylinder body, welded of thin-sheet steel, a specialized assembly-welding equipment and technology of precision welding, subsequent inspection and heat treatment of welded joints were developed. Production lines of up to 20,000 and 100,000 cylinders per year with their safety factor above 2.6 were created.

Keywords: arc welding, motor-vehicle cylinders, high pressure, life of equipment, technology of welding, longitudinally- and spirally-welded shells, production lines

The natural gas, namely methane, is one of the most widely-spread and promising energy carriers on the Earth. Its explored reserves approach 10^{12} and predicted ones (taking into account hydrates) approach 10^{15} – 10^{16} nm^3 [1]. Production of gas and its preparation for use are economically and ecologically less expensive as compared with oil, and combustion stipulates the lower (1.5–2.5 times) content of oxides of carbon and nitrogen, as well as aromatic hydrocarbons in combustion products [2]. Moreover, the gas cost is approximately 2 times lower than the cost of benzene, and its application as a motor fuel does not require the change in design of motors and does not exclude the feasibility of their service using gas, benzene or their mixtures [3]. In addition, there are some inconveniences in arrangement of additional charge capacities (high-pressure vessels) on the board of motor vehicle. In this connection, some companies modified the designs of bodies and started the manufacture of motor cars with built-in cylinders.

Requirements for cylinders are rather high [4] and a definite level of technological discipline and mechanization of works is necessary for their production. This is a premise for organizing the highly-technological manufacturing, and the modern rates of motorization of the world and consumption of oil resources allow predicting the challenges for these kinds of manufacturing. Moreover, about 900 mln of registered transport vehicles exhaust up to 60 % of all pollutions into environment. Therefore, at the present stage the application of gas as a motor fuel will make it possible to decrease the pollution of environment and to delay the collapse of automotive industry because of exhaustion of oil reserves, and also to develop the more acceptable solutions, for example, producing fuel, in-

cluding gas, from recovered sources, hybrid motor vehicles, such as «gas–electric energy» and so on.

The problem of gasifying the motor vehicle transport was considered as far back as last century, but these were mainly the pioneering projects which allowed gaining the experience and preparing the base for transition to the wide-scale solutions.

At present, about 9 mln motor vehicles are in service using the natural gas, where a compressed gas is mainly used, as the existing cryogenic tanks for liquefied methane do not guarantee its long-term storage on the board, and most motor vehicles are used at sufficiently large intervals, i.e. there is no alternative to high-pressure cylinders.

At the present stage the steel cylinders, manufactured of all-drawn pipe billet by a hot rolling of edges, found a wide spreading [5]. This technology was tested earlier on cylinders for technical gases and attracted manufacturers by its accessibility and simplicity. However, it was not managed to organize the mass production of these cylinders in Ukraine, because of difficulty in producing the tubular billet without laminations and with small tolerances for wall thickness. Moreover, the formation of bottoms by rolling can be realized only at a definite ratio of diameter to pipe wall thickness. This limits the possibility of manufacture of cylinders of different types and sizes with a stable mass-dimensional characteristic (mass-to-volume ratio M/V) of not more than 1 kg/l.

The further decrease and stabilization of this characteristic was realized in design of metal-plastic cylinder with a welded body of sheet steel, suggested by the E.O. Paton Electric Welding Institute and S.P. Timoshenko Institute of Mechanics [6]. The body consists of a longitudinally-welded shell and two stamped semi-elliptic bottoms, welded to it by circumferential welds, a neck is welded-in into one of these bottoms. As the body is manufactured of low-strength low-alloy steels (shell of steel 09G2SF of 3 mm thickness, and

bottom — of steel 09G2S 6 mm thick), it is strengthened by a load-carrying fiber-glass sheath of a «cocoon» type, made by a scheme of a longitudinal-transverse winding. The cylinder has a stable mass-dimensional characteristic $M/V \approx 0.9$ kg/l, safety factor is not less than 2.6 and withstands up to 40,000 charges.

From the point of view of owners of motor car transport the cylinders of this design have the excessive mass, and from the point of view of manufacturers they require increased expenses for formation of a composite sheath. The further improvement of design was realized using high-strength steels [7]. Here, the semi-spherical bottoms were used, in which the operating stresses are 2 times lower than in a cylindrical part of the body, thus refusing their additional strengthening, and providing the equal strength of all elements of structure by a circular winding of a cylindrical part of the cylinder [8, 9]. This simplified radically the technology and equipment for the sheath formation.

The required safety factor of new cylinders is determined mainly by mechanical properties of steel, which are preset by an initial structure and conditions of metal heat treatment [10]. At static and dynamic loading by internal pressure the problem of equal strength of welded joints was solved for different levels of strength up to 2000 MPa [11]. However, at a low-cycle loading the feasibility of application of this solution was not confirmed [12]. Here, the negative role was played by the imperfection of the joint geometric sizes. As is known, it is very difficult to provide the perfect assembly of edges being welded in assembly of thin-walled elements of the body due to ovality of parts after rolling and stamping. This results in violation of a smooth transition from the weld to the parent metal and probability of formation of high local concentration of stresses is increased, thus leading to the development of microplastic deformation and premature exhaustion of safety factor of metal in confined areas.

The attained amount of cycles of loading (ST SEV 3648–82) [N] is determined by the expression

$$[N] = \frac{1}{n_N} \left[\frac{A}{\left(\sigma_A - \frac{B}{n_\sigma} \right)} \left(\frac{2300 - t}{2300} \right) \right]^2,$$

where n_N is the safety factor by the number of cycles; A , B are the characteristics of material; σ_A is the amplitude of stresses; n_σ is the safety factor by stresses; t is the temperature.

The life of welded joints depends greatly on such geometric parameters, as displacement of edges (Figure 1, *a*) and radius of weld conjugation with parent metal (Figure 1, *b*). This dependence is higher at a lower ductility (elongation δ) of metal. The obtained calculation data are well correlated with results of hydraulic tests of real cylinders (light signs), in which the values of edge displacements and radii of conju-

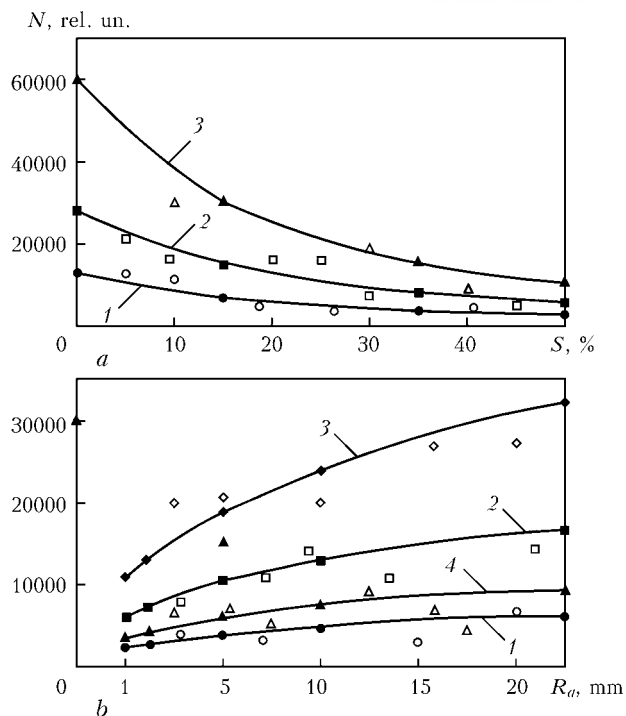


Figure 1. Dependence of cylinder life on geometric parameters of welded joint: displacement of edges (*a*) and radius of weld conjugation with parent metal (*b*) at different levels of metal elongation: 1 – $\delta = 8$; 2 – 12; 3 – 18; 4 – 10%; light signs – real cylinders

gation were determined after depressurization of cylinders in places of fatigue cracks initiation.

To eliminate the diplanation of edges in serial manufacturing of cylinders, the assembly-welding equipment has been developed which allows parts during assembly to be deformed elastically, eliminating the ovality and forming the welded joints with minimum ($\delta \geq 10\%$) displacement of edges (Figure 2). Welding in this equipment is performed on one side per one or two passes (Figure 3, *a*). During the first pass, which is performed with a complete penetration of edges, a load-carrying weld is formed, which is in compliance with chemical composition of the parent metal. During the second pass, the optimum width and weld reinforcement height are provided and, consequently, a necessary radius of its conjugation with the parent metal. For this purpose, the welding of the first pass is made in argon using a special activating flux, which increases the arc penetrability at lowered currents and provides penetration of up to 10 mm thick steel for one pass without edge preparation. This allows preventing the formation of coarse hardening structures in weld and HAZ metal, as well as defects of types of pores, lacks of penetration, lacks of fusion, cracks, and forming the load-carrying welds of I, II classes according to GOST 23055–78 during the first pass, which have chemical composition similar to the parent metal. The second pass is made using a filler wire and can be used for improvement of geometry, structure and ductility of the weld metal. The conformity of weld to the required class of quality is evaluated by 100% X-ray method.

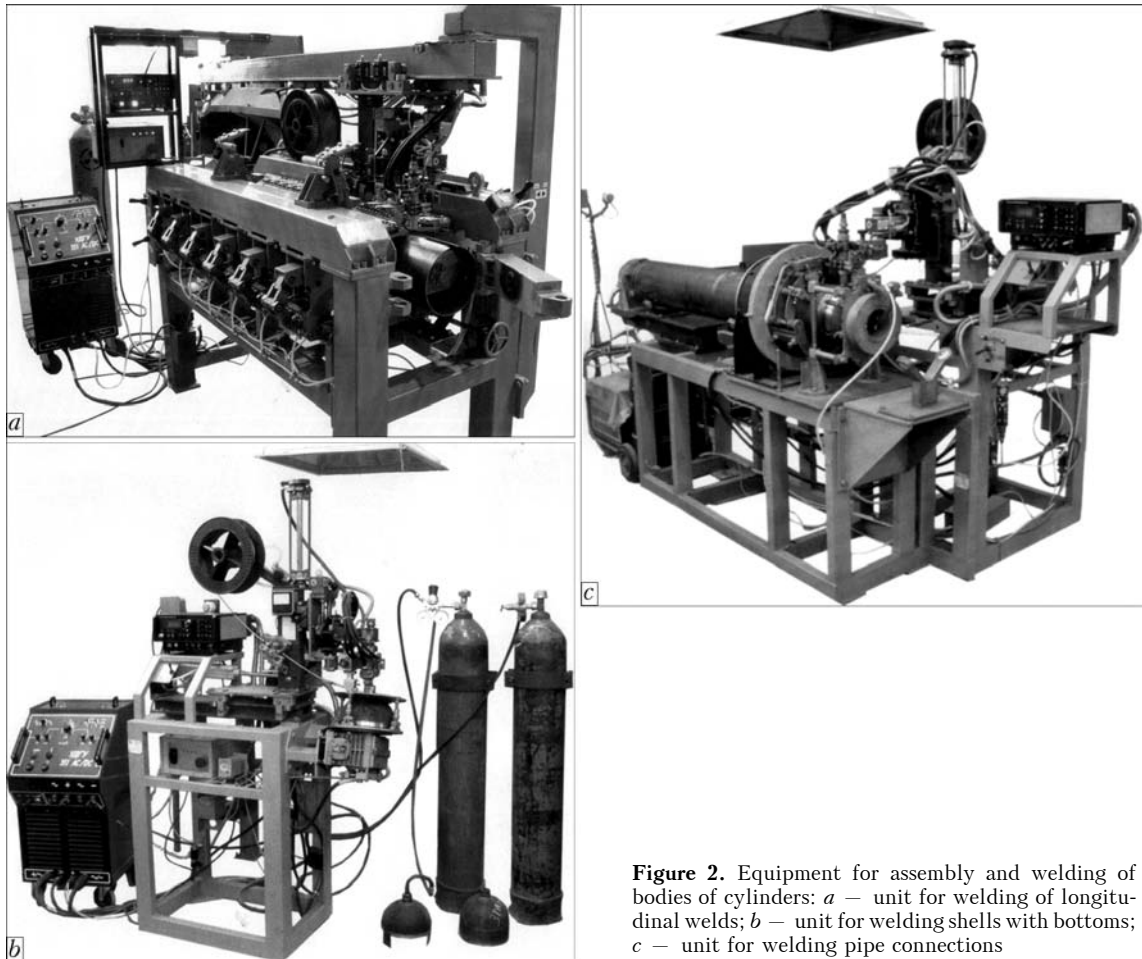


Figure 2. Equipment for assembly and welding of bodies of cylinders: *a* – unit for welding of longitudinal welds; *b* – unit for welding shells with bottoms; *c* – unit for welding pipe connections

The comparative tests carried out by one of the foreign companies showed that the micro-alloy steel joints, made by the above-described technology, are superior to joints, welded by plasma, electron beam, laser, consumable electrode in gas mixtures and non-consumable electrode in argon. They have the higher resistance against the formation of fatigue cracks at a low-cycle loading. As to the medium-carbon steels,

hardened with the formation of martensite, so it occurred in a number of factors, defining the resistance against the fracture of high-strength steel butt joints, that initial structure of metal of weld and HAZ is important here, or rather the fact how this structure can be transformed and approach the structure of the parent metal after final treatment. It was found that if, after postweld treatment of joints of steels of 25SNMVFA or 30KhGSA type, to transform the bainite-martensite structure of weld and HAZ metal, hardened from welding heading, into a relatively equilibrium structure of temper sorbite (Figure 4), then the texture of cast weld metal is disappeared after hardening and austenite grain is refined in the area of HAZ metal overheating. As a result of leveling the differences of structures of parent metal and joint, the service life of cylinders is increased from 1600–1800 up to 25,000–30,000 charges.

The NDT of welded joints is rather important operation in the technological process. The organizing of control using X-ray method requires working places, protected from radiation, financial and temporary expenses, that leads under the conditions of a serial production to the formation of weak points in the production line. A challenging addition to the X-ray inspection in a serial production of high-pressure cylinders is the new method: a shear speckle-interferometry, or shearography [13, 14]. It allows obtain-

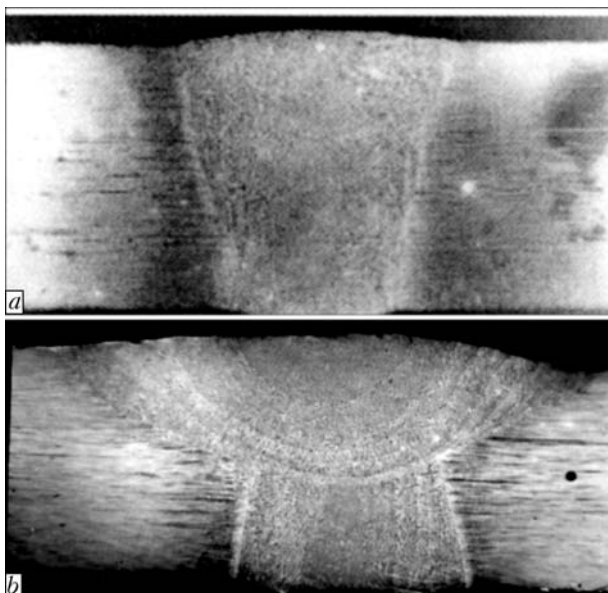


Figure 3. Macrosections of single- (*a*) and two-layer (*b*) welds

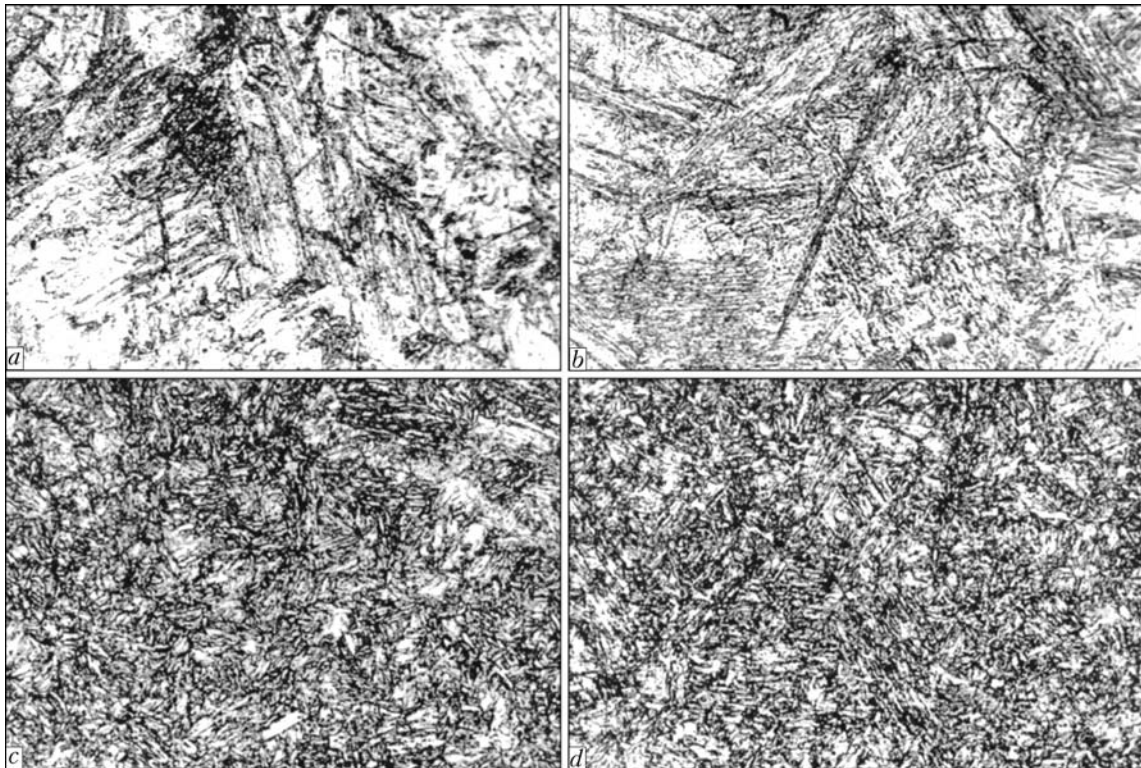


Figure 4. Microstructures ($\times 300$) of metal of weld and HAZ after welding (*a, b*) and local heat treatment (*c, d*)

ing the in-process complete information about technical condition of object being examined and revealing the potentially defect-hazardous places, which then can be selectively controlled by the X-ray method.

The main principle of the shearography is as follows. The cylinder area being examined is subjected to loading by the internal pressure or external heating and then illuminated by a coherent laser beam. The reflected light flow in the interferometer is divided with a shear into two wave fronts, converted into an electric signal and transferred to computer for the processing. The results are recorded on electron carriers and can serve as a target indication for next identification of defect using standard X-ray methods. Evidently, this method can be also applied for evaluation of cylinders condition at their periodic inspection. Speckle-patterns, recorded during initial inspection, can be compared with patterns, obtained after a definite period of service and, thus, to determine the service life of cylinders.

As the investigations showed [14], it is possible to reveal at elasto-deformed state of the object not only defects, recorded in X-ray inspection, but also local concentrations of stresses, usually not-shown on radiograms, but influencing the life and reliability of the cylinders.

Basing on the developed designs of combined cylinders, complex of technologies and a non-standard equipment, a production line of assembly, welding, inspection and heat treatment of cylinder bodies of sheet steel (Figure 5, *a*) and also formation of a composite sheath has been created. The line of this type allows organizing the updated production of combined

cylinders with a longitudinally-welded shell of efficiency up to 24,000 cylinders per a year. The mass-dimensional characteristic of these cylinders is about 0.65 kg/l. The production cost of cylinders is 2 and more times lower than the cost of similar cylinders of foreign production.

The drawbacks of a longitudinally-welded shell are usually the probability of location of physical and geometric imperfections of a longitudinal weld along the generatrix, and also non-balancing of rigidity and residual stresses in spite of the fact that the level of operating stresses from radial forces in shell is 2 times higher than those from axial forces. To eliminate these drawbacks, the technology envisages the preliminary bending of edges, mechanical-heat treatment of joints and subsequent calibration of the shell. As a whole, this allowed providing the equal strength of all the areas of the shell and increasing the uniformity of distribution of operating stresses in them, however, leading to the increase in amount of technological operations.

A spirally-welded shell is subjected to the influence of the above-mentioned factors to a less degree, as the vectors of radial stresses are not normal to the weld plane, and the zones of an increased rigidity and elasto-plastic deformations are not concentrated in one plane [15] that eliminates the required calibrations. Besides, the combination of operation of formation and welding of butt in a single mechanism allows eliminating the bending of edges and intermediate transporting operation.

To shorten further the cycle of manufacturing, to reduce the cost and to increase the rates of manufacture

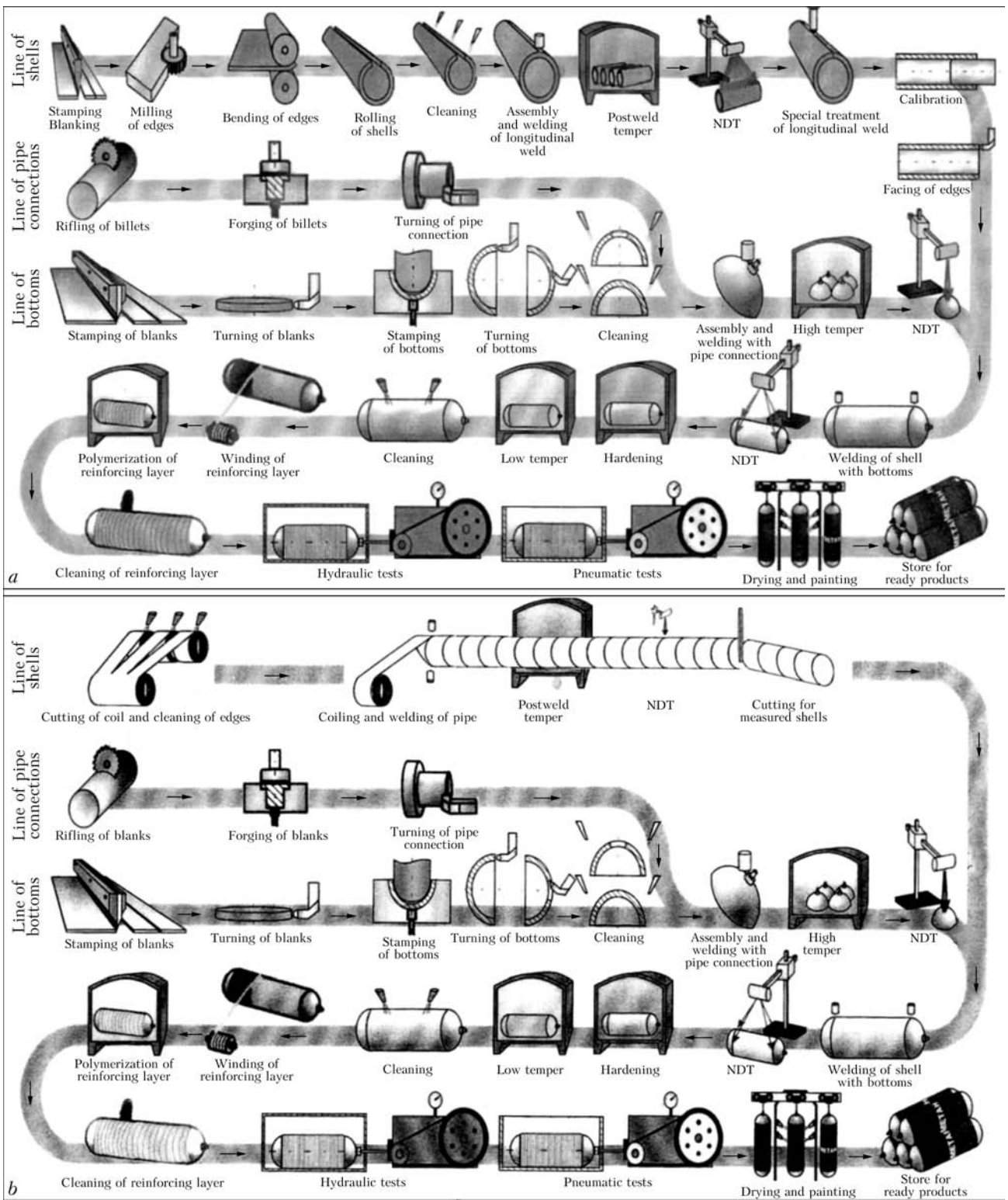


Figure 5. Technological line of manufacture of cylinders with longitudinally- (a) and spirally-welded (b) shells

of cylinders, the production line of the second type is also offered (Figure 5, b), the distinguished feature of which is the possibility of application of high-efficient method of high-frequency welding [16].

Equipment has been designed and passed trials in welding of special-purpose pipes. The equipment arrangement into the line of cylinders production makes it possible to combine up to five technological opera-

tions in one unit, including formation, welding and heat treatment of tubular billet and to refuse three more operations as being not required. As a heat source, the welding arc can also be used at a some decrease in speed of tubular billet manufacture. This will allow balancing the load of all the elements of the line under the conditions of small-serial production or instable demand for products. Under the conditions

Diameter of pipes being welded depending on thickness and width of billet strip

Pipe diameter, mm	Wall thickness, mm	Strip width, mm
75–100	0.5–1.5 (2.5)*	100
100–200	0.8–2.0 (3.0)	100
200–250	0.8–2.5 (3.5)	200
300–700	1.0–3.0 (4.5)	200, 300, 500 (depends on unit type)

*At 260 kW power of generator of high-frequency current.

of a large-serial or mass production, it is rational to apply the high-frequency welding, the main characteristics of which are given in the Table.

At present the industrial technology has been developed and designing documentation has been worked out for the equipment for welding of spirally-welded pipes of diameter from 75 up to 700 mm under the shop conditions. Mock-ups of bodies of different-purpose cylinders, manufactured of these pipes and tested, gave a positive result. The appearance of the mock-up of the cylinder body after tests using internal pressure is presented in Figure 6.

The main technical characteristics of equipment in the condition of high-frequency welding are as follows:

Welding speed, m/min	30–40
Speed of pipe output, m/min	8–12
Efficiency, kilometer of pipes per shift	1.0–1.5
Power of generator of high-frequency current, kW	160–250
Capacity of electric drives, kW	8
Length of pipes, m	any
Voltage of electric equipment supply (50 Hz), V	380
Materials to be welded	steel, aluminium
Area occupied by welding line, m ²	150–200

It should be noted in conclusion that the design, technologies of welding and heat treatment, as well as non-standard assembly-welding equipment developed at the E.O. Paton Electric Welding Institute, make it possible to manufacture combined welded cylinders with a stable mass-dimensional characteristic $M/V = 0.65 \text{ kg/l}$ and service life of more than 15,000 charges. According to TU 28.2-05416923-072:2005 a series of cylinders was manufactured with a safety factor (ratio of pressure of depressurization P_{depr} to operating pressure P_{op}) equal to more than 2.6, which is preserved stable after 15,000 charges.

To organize the serial production of cylinders with a longitudinally-welded shell, the production line of the first type can be used. When necessary to provide the mass production of cylinders, it is rational to use

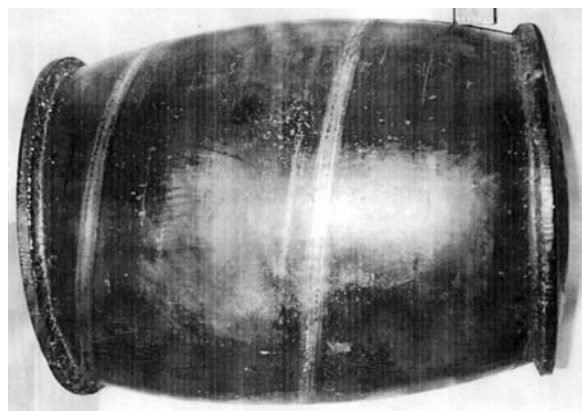


Figure 6. Appearance of mock-up of body of spirally-welded cylinder after tests using internal pressure

the line of the second type, based on manufacture of a spirally-welded shell.

- Karp, I.M., Eger, D.O., Zarubin, Yu.O. et al. (2006) *State-of-the-art and prospects of development of oil and gas complex*. Kyiv: Naukova Dumka.
- Matsuyama, K. (2007) Trend of automobile vehicles and the joining technologies. *Riv. Ital. Saldatura*, **5**, 683–693.
- Volkov, V., Kaplun, S.V., Zerya, A.V. (2007) New step in application of compressed natural gas as a motor fuel. *Avtozaprav. Kompleks + Alternat. Topливо*, **6**, 57–58.
- (2001) *Agreement on principles of technical regulations uniformity for complex vehicles, equipment objects and parts being mounted and/or used on wheel vehicles and on conditions of potential recognition of official statements issued on the base of these regulations*: UNO, E/ECE/TRANS/505. Rev. 2/Add tog 12 June 2001.
- Sakhatov, R.M. (2009) Shatterproof metal-composite cylinders BMK-300V and others. *Avtozaprav. Kompleks + Alternat. Topливо*, **4**, 51–54.
- Polevoj, V.A., Ozerov, V.I., Savichenko, A.A. et al. (1992) Structure and technology of production of metal-plastic cylinders. *Gazovaya Promyshlennost*, **11**, 30–31.
- Paton, B.E., Savitsky, M.M., Kuzmenko, G.V. (1994) Prospects of application of high-strength medium-alloy steels in high-pressure motor transport welded cylinders. *Avtomatich. Svarka*, **3**, 4–9.
- Savitsky, M.M., Kulik, V.M., Lupan, A.P. et al. *Combined cylinder*. Pat. 44793 Ukraine. Publ. 15.03.2002.
- Savitsky, M.M., Kulik, V.M., Savichenko, O.O. et al. *Cylinder*. Pat. 82000 Ukraine. Publ. 25.02.2008.
- Pokrovskaya, N.G., Petrakov, A.F., Shalkevich, A.B. (2000) Current high-strength steels for aircraft engineering products. *Metallovedenie i Term. Obrab. Metallov*, **3(2)**, 23–26.
- Savitsky, M.M. (1991) Weldability of high purity alloy steels. In: *Proc. of Int. Seminar on Metallurgical Requirements of Producers and Consumers to Weldability of Welding Products*. Kiev, 10–15.
- Kurkin, S.A. (1976) *Strength of pressurized welded thin-wall vessels*. Moscow: Mashinostroenie.
- Lobanov, L.M., Pivtorak, V.A., Olejnik, E.M. et al. (2003) Electron shearography as a new method for diagnostics of materials and structures. *V Mire Nerazrush. Kontroliya*, **4**, 67–69.
- Olijnyk, O.M. (2004) *Nondestructive testing of machine-building structures by electron shearography method*: Syn. of Thesis for Cand. of Techn. Sci. Degree. Iv.-Frankivsk: NTU Nafty i Gazy.
- Pismenny, A.S., Polukhin, V.V., Polukhin, V.I. et al. (2005) Production and application of thin-walled spirally-welded pipes. *The Paton Welding J.*, **9**, 29–32.
- Pismenny, A.S. (2008) *High-strength steel of metal products*. Ed. by B.E. Paton. Kiev: PWI.

MODERN EQUIPMENT FOR SHIPBUILDING

P. SEYFFARTH

Ingenieurtechnik und Maschinenbau GmbH, Rostok, Germany

Experience of IMG GmbH (Rostok, Germany) in development and manufacture of modern automated lines for cutting and marking of shaped sections for shipbuilding and related industries is described. The lines provide high precision of part manufacturing and processing speed, this allowing payback of their procurement costs within a year and a half.

Keywords: plasma cutting, shipbuilding, shaped sections, automatic lines, equipment, marking, manufacturing accuracy

Modern shipbuilding and other related industries require a high degree of automation. The known Ingenieurtechnik und Maschinenbau GmbH (IMG), Rostok, Germany, uses automated processes of cutting, welding, assembly and transportation. In addition to automated lines for manufacturing flat and bent panels, the Company is also equipped with lines for making micropanels, automated lines of shaped section cutting, cranes and other vehicles, as well as welding gantries to make butt and fillet joints. Starting from 2005, the Company pays a lot of attention to introduction of powerful industrial lasers. It is the world leader in the field of application of ytterbium fiber lasers in shipbuilding.

IMG fulfills orders of more than 50 large shipyards of the world (USA, China, Korea, Australia, Turkey,

Canada, France, Great Britain, Finland, Italy, etc.). It is also known in Russian Federation. Here its equipment is operating in Admiraltejskaya Shipyard, Baltijsky Zavod, northern shipyards, etc. The first automated panel line was mounted by IMG Company in «Krasnoe Sormovo» Shipyard in Nizhny Novgorod in 2005.

One of the examples of the Company's modern equipment is a flow line for automatic cutting of shaped sections. Shaped section cutting line (Figure 1) with numerical program control (NPC) is designed for automated cutting and marking of shaped sections, which are used in shipbuilding, and includes the following elements: equipment for automatic material feed (accumulation tables for material with chain conveyors; roller conveyors; automatic processing devices for robotic plasma cutting of end cuts and



Figure 1. General view of NPC line for shaped section cutting

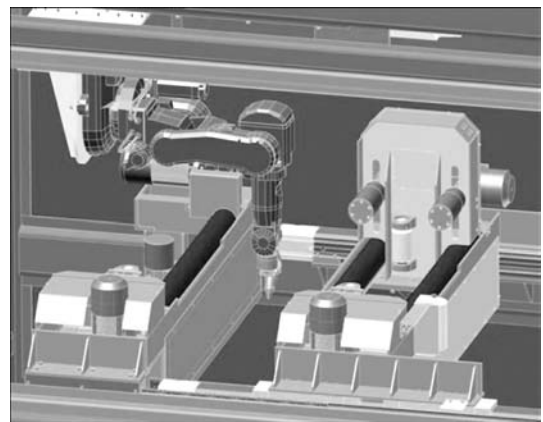


Figure 2. Appearance of the cutting device

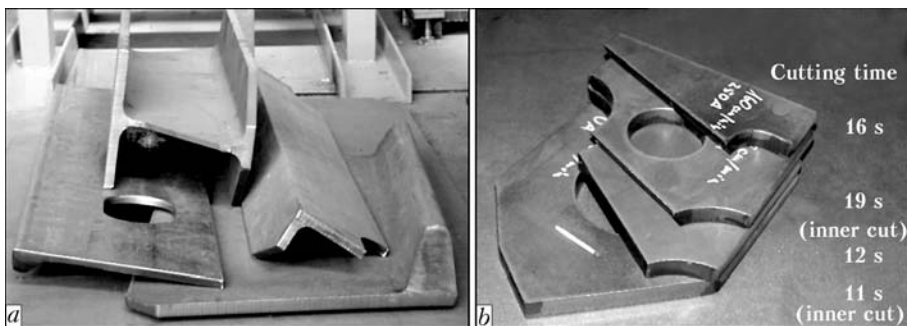


Figure 3. End cuts (a) and inner cuts of different types with or without edge preparation (b)

inner cuts (dales) (Figures 2 and 3), as well as alphanumeric marking of blanks (Figure 4).

Equipment for shaped section sorting after cutting includes a manipulator for blank warehousing, sorting gantry for loading 3 to 12 m sections and cartridges for finished shaped parts. Operation with a pivot arm and sorting gantry is more adaptable to fabrication and faster compared to bridge crane.

Equipment for development of control programs with NPC ensuring automatic mode of operation of shaped section cutting line (Figures 5-7) is divided into hardware (programming, file storage and program starting) and software (generation of programs of cutting with NPC and line operation).

NPC line for cutting shaped sections is complex equipment for making parts from shaped sections. Interfacing with shop sections in the plant is achieved as follows. At the input information is received about the shaped sections supplied for cutting (transmitted from the plant system of production planning); about geometry of pipe section cutting (received from CAD system); about shaped blanks used as initial material for shaped section cutting; about empty cartridges for

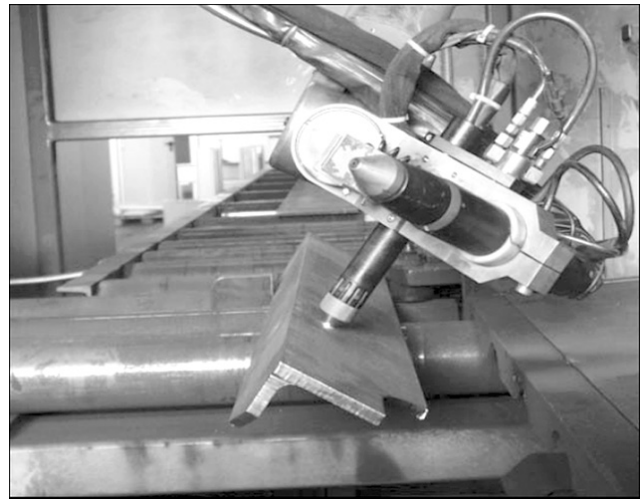


Figure 4. Marking by a plasma or jet method

finished shaped sections after cutting. At the output information is provided about cartridges filled with shaped sections for their transportation, as well as shaped section types made by cutting (feedback to production planning system).

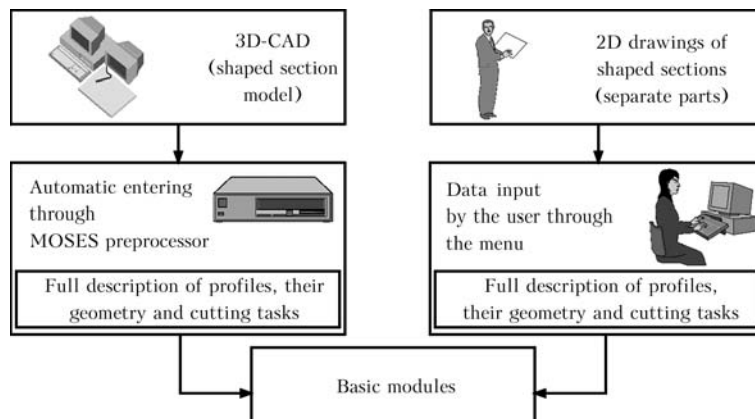


Figure 5. Entering and preparation of data for program generation

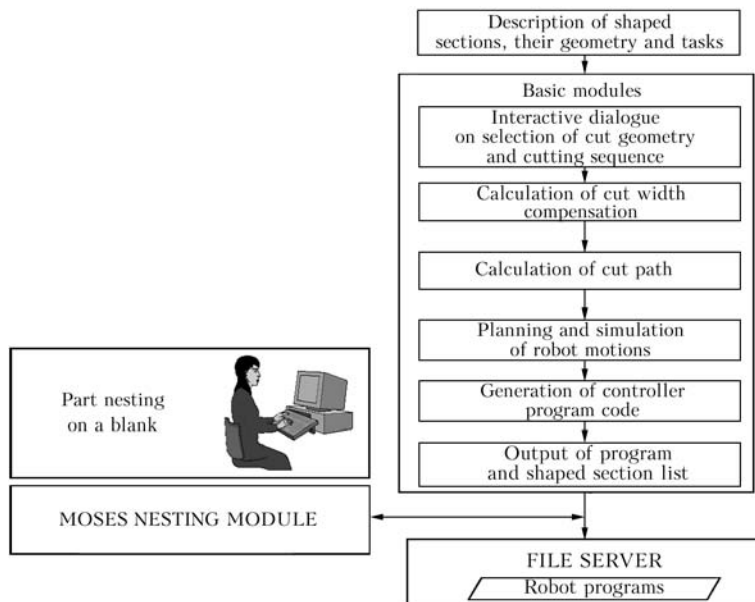


Figure 6. Schematic of the program for shaped section processing

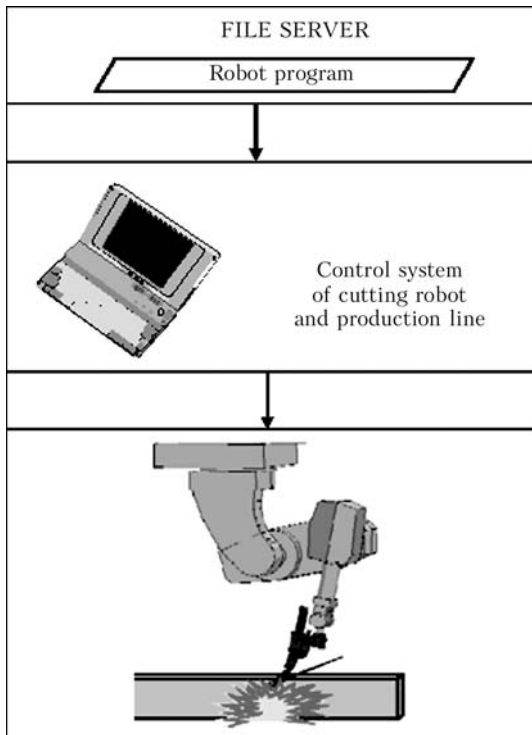


Figure 7. Use of cutting programs

Shaped section processing line (Figure 8) fulfills the following main functions: laying of shaped section stacks or individual shaped sections on a chain conveyor; intermediate storage of blanks on the chain conveyor and feeding them to charging roller table; blank feeding to cutting chamber; automatic fulfillment of the working task of production preparation department in the cutting chamber: cutting along the length (end cuts); cutting out dales; application of alphanumeric marking with paint using a marking

ing care should be taken to keep 200 mm distance between them. After laying the shaped sections, their fully automated processing starts: feeding individual shaped sections from chain conveyor to hoisting conveyor, and then to roller conveyor, along which the section moves to the cutting chamber; intermediate accumulation of shaped sections on the roller conveyor and their subsequent transportation to the cutting chamber; shaped section feeding by roller conveyor located in front of the cutting chamber and its fastening for processing, shaped section position being controlled by a device of length measurement located in front of the cutting chamber; if required the measurement system issues a signal on position correction using a cutting robot; making end and inner cutouts in the blanks using robotic plasma cutting (see Figures 2 and 3), during which the shaped section remains in the cutting chamber in the fixed position; marking of shaped blanks before the cutting chamber by the jet method (see Figure 4); displacement of shaped section to the loading table for approximately 500–3000 mm. Finished parts can be dumped or loaded manually, and they can be placed into a box by a rotating beam crane; they can be placed into a box by the shop crane, or transferred to the grinding section. Shaped section transportation for approximately 3000 and 13,000 mm is performed by a transportation roller conveyor and chain conveyor, which also has the role of intermediate accumulator. Transportation by the sorting gantry, shaped section laying into cartridges and their transfer to the grinding section can also be performed. Then shaped sections are laid into cartridges by the shop crane and transferred to the grinding section, the shop crane requiring availability of a magnetic crossbeam.

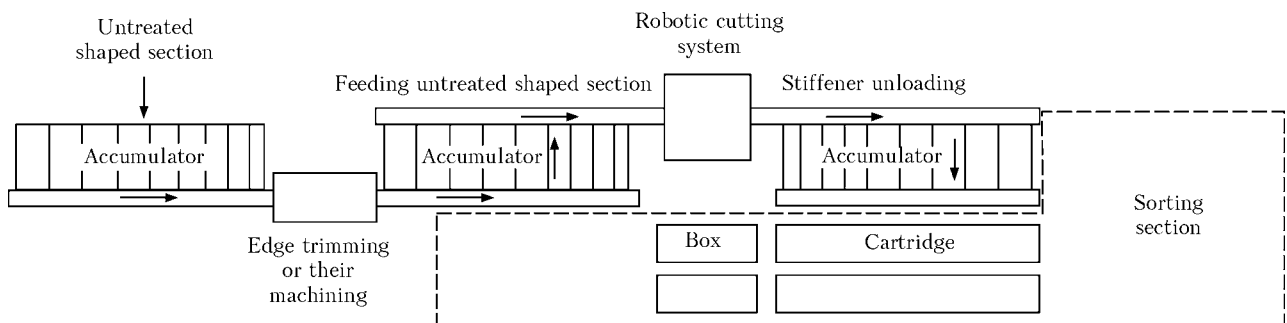


Figure 8. Diagram of shaped section treatment line

device; automatic transportation of shaped sections to discharging; shaped section sorting by cartridges with ridge-like posts in the pre-set technological sequence.

Operator (or two operators) using the crane available in the shop, moves the body of shaped blanks into the line working zone onto a chain conveyor. Conveyor design facilitates for the operator the task of laying and positioning the shaped sections. At lay-

Thus, accuracy of part manufacture, and their processing speed many times exceed the technologies of shaped section preparation used so far. This allows eliminating the bottlenecks in the technological process. Note that owing to a high efficiency of automatic cutting line the investments into its introduction are paid back within a year and a half.

CLEANING AND ACTIVATION OF WELDED SURFACES DURING EXPLOSION WELDING

L.B. PERVUKHIN¹, O.L. PERVUKHINA¹ and S.Yu. BONDARENKO²

¹Institute of Structural Macrokinetics and Materials Science, RAS, Chernogolovka, RF

²Altai State Agrarian University, Barnaul, RF

Absence of the cumulative effect in explosion welding of large-sized samples and commercial size plates in the modes used in commercial production is experimentally proved. The mechanism of cleaning and activation of surfaces ahead of the contact point is proposed, based on the hypothesis of formation of thin layers of low-temperature plasma in the welding gap on the interface between the shock-compressed gas and surfaces being welded. It is suggested that formation of strong bonds between atoms of the joined metals in explosion welding should be regarded as a three-stage process.

Keywords: explosion welding, welded surface, oxides and contamination, cleaning, activation, cumulative jet, plasma flows, contact point, three-stage process

For explosion welding, similar to any other solid-phase pressure welding process, the most important is the condition of materials being welded, which depends on mechanical and chemical properties of the base and cladding layers, quality of preparation and roughness of surfaces being welded.

In keeping with the currently accepted theory of joint formation in explosion welding, it is believed that under the conditions of slanting collision self-cleaning occurs, as a rule, as a result of cumulative jet formation [1–3], which removes a layer of metal from the surfaces being welded together with the oxides and contamination, and carries them out of the welding gap in the form of a cloud of dispersed particles. Then the juvenile surfaces are compressed under the impact of the detonation products up to formation of a metal bond. The process of metal joining in explosion welding is accompanied by an abrupt increase of temperature in the joint zone, which is indicated by the presence of «cast structures» – zones, in which material melting occurs during welding. It should be noted that the cumulative jet proper was observed only during special experiments in the modes, markedly different from those applied in explosion welding of steels. It was not possible to obtain a cumulative jet experimentally, even at a symmetrical schematic at a low angle of collision (20° for steel, and 30° for aluminum), and the presence of a cloud of dispersed particles in front of the contact point was recorded in the photos [4], and a wavy joint line was formed.

A doubt as to the determinant role of cumulation in joint formation in explosion welding is expressed in [5, 6]. In [4] a conclusion was made about «...formation of a reverse mass flow (cumulation) is not a mandatory condition for joint formation in explosion welding, and, similar to wave formation, it is only indirectly related to it». Explosion welding is considered to be solid-phase pressure welding, and metal adhesion – a particular case of topochemical reactions

in pressure welding, which are characterized by a three-stage nature of the process of formation of strong bonds between the atoms of the joined metals; establishing physical contact; activation of contact surfaces; volume development of interaction. Authors of [7] state that explosion welding is characterized by a two-stage nature of the process of joint formation – physical contact and activation of contact surfaces due to plastic deformation. However, despite the doubts as to existence of the reverse flow under explosion welding conditions, the process of joint formation, as well as the energy balance, are considered allowing for the presence of the cumulative effects.

This paper deals with the issue of existence of the cumulation process, and in its absence – issue of existence of mechanisms, which can lead to cleaning and activation of the surface to be welded.

Processes occurring in front of the contact point were studied using the method of traps: a trap consisting of two pre-scraped steel sheets, assembled at an angle with an initial gap equal to welding gap, was mounted on large-sized samples and sheets of commercial size (Table 1) from the end face, opposite to the start of the process. The above method allows recording on samples and sheets of commercial size the presence of particles flying out of the welding gap with shock-compressed gas (SCG), without changing the explosion welding conditions. This method was successfully applied in investigation of processes running in the welding gap in welding titanium to titanium [8] and titanium to steel [9].

Before the start of experiments, published experimental and theoretical data of various authors were used to determine the anticipated thickness of the coating on one of the trap plates in the presence of the cumulation process (see Table 1). Calculations were performed proceeding from the condition that material, removed by the cumulative process from the surface of the plates being welded, is deposited on the trap surface without taking into account the lateral projection of particles:

$$h = \frac{h_{\text{rem}} S_{\text{sheet}}}{S_{\text{trap}}}, \quad (1)$$

**Table 1.** Thickness of coating layer on the surface of one of the traps

Welded material (atmosphere)	Sample size, mm	Trap size, mm	Calculated data, μm			Experimental data
			[9]	[5]	[10]	
Steel–steel (air)	500×1200	250×500	48	528	192	Absent
Steel–titanium (air)	500×1200	250×500	48	528	192	20–80 μm
Steel–steel (air)	1400×5900	250×1400	236	2600	944	Absent
Steel–titanium (argon)	2700×2800	250×2700	112	1232	448	Same

where h_{rem} is the thickness of metal removed from the welded sheet surface, μm ; S_{sheet} is the sheet area, mm^2 ; S_{trap} is the trap area, mm^2 .

At equal width of the sheet being welded and the trap this ratio becomes

$$h = \frac{h_{\text{rem}} l_{\text{sheet}}}{l_{\text{trap}}}, \quad (2)$$

where l_{sheet} is the sheet length, mm; l_{trap} is the trap length, mm.

At calculation of the thickness of the layer which should be deposited on the trap plates, experimental data of [4, 10] were taken as the basis, and at the same time assessment by the hydrodynamic cumulation theory was performed [11].

Calculations of the anticipated coating thickness showed that in explosion welding of large-sized samples and sheets of commercial dimensions, coating thickness should be 48–2600 μm (see Table 1).

Experimental investigations by trap method showed that in steel welding to titanium in air a deposited layer of 20–80 μm thickness is present on the plate surfaces, which consists of a mixture of partially melted titanium oxides. However, experiments did not reveal on the trap surface the presence of particles, flying out of the welding gap in welding of large-sized sheets and samples of steel to steel and of steel to titanium in argon.

Thus, results of the conducted experiments showed that no cumulative effect was recorded in explosion welding of steel to steel and to titanium in argon in welding modes accepted in commercial production of bimetal.

During explosion welding, a SCG region forms in the welding gap ahead of the contact point. Let us consider its thermal impact on the surfaces being welded at a distance from the beginning of plate collision by a procedure described in [12]. Thermal flow from gas to plate surface has the following form:

$$q = \text{St} \rho u c_p (T_{\text{SCG}} - T_0), \quad (3)$$

where St is the Stanton number; ρ is the gas density; u is the mass velocity of gas beyond the shock wave front; c_p is the gas heat capacity; T_{SCG} is the SCG temperature; T_0 is the initial temperature (293 K).

Stanton number at turbulent flowing of the gas flow around the plates is equal to

$$\text{St}_t = \frac{1}{8 \left(2 \lg \frac{a_p}{k} + 1.74 \right)^2}, \quad (4)$$

where a_p is the distance between the plates (welding gap), mm; k is the average size of surface roughness, mm.

At a constant thermal flow from gas into metal the plate surface is heated by the following law:

$$T_s = \frac{q}{2\lambda} \sqrt{6at} + T_0, \quad (5)$$

where λ , a are the heat conductivity and thermal diffusivity of welded plate material; t is the time.

Calculations made for welding steel (contact point velocity $v_c = 2500$ m/s; $a_p = 8$ mm; $k = 0.08$ mm) showed that the maximum temperature to which the metal surface is heated under the condition of an infinite length of 1 m wide sheet is not higher than 600 °C. Therefore, impact of only the SCG on the surfaces being welded is insufficient for their cleaning and activation.

In this connection, we considered the processes of cleaning and activation by analogy with metal rolled stock cleaning by plasma based on the following hypothesis: thermal ionization of gas with formation of thin layers of low-temperature «cold» plasma occurs on the interphase ahead of the contact point in the welding gap at supersonic (5–6 Makh) flowing of SCG over the surfaces being welded [13].

Under the impact of the plasma flow all the known metal oxides and other chemical compounds dissociate, ionize and evaporate (sublimate) from the surface being welded. Positive ions of metals, formed as a result of dissociation of oxides and their ionization, return to the cleaned surface, and oxygen atoms form the simplest gaseous compounds of O_2 , CO_2 and H_2O , which are removed from the welding gap. Note that scale and rust are not the cleaning byproducts, these are exactly the gasified carbon dioxide gas and water molecules. Oxide dissociation results in an abrupt improvement of activation of the surfaces being welded ahead of the contact point.

Similar processes occur in plasma-arc cleaning of metal rolled stock (Table 2). At energy density of $1 \cdot 10^3$ W/ m^2 the thermal flow will be equal to $1 \cdot 10^3$ J/($\text{m}^2 \cdot \text{s}$), and the temperature will reach $(5-10) \cdot 10^3$ K, here the cleaning speed will be 4.5 m/min [12]. By the data of [13], the heat flow from gas into metal in explosion welding is equal to $1 \cdot 10^8-1 \cdot 10^9$ J/($\text{m}^2 \cdot \text{s}$) at brightness temperature of $(5-8) \cdot 10^3$ K in the welding gap, depending on welding mode, and by the data of [15] – from $1.3-1 \cdot 10^9$ to $4.1-1 \cdot 10^{10}$ J/($\text{m}^2 \cdot \text{s}$). Evidently, plasma-arc cleaning speed is incommensurably lower than at explosion welding, but the thermal flow in the latter case is

Table 2. Calculated parameters of plasma cleaning of metal rolled stock

Cleaning method	$T \cdot 10^{-3}$, K	Energy density, W/m ²	Time of plasma action, s	Thickness of removed layer, μm
Plasma-arc [14]	5–10	$1 \cdot 10^3$	5–10	200–300
Shock plasma [12]	5–8	$1 \cdot 10^8$ – $1 \cdot 10^{10}$ [12, 15]	$2.4 \cdot 10^{-5}$ – $1.12 \cdot 10^{-4}$ (at detonation rate 2000–2500 m/s)	5–7 [10, 16]

$1 \cdot 10^6$ times greater, and the removed layer thickness is just 5–7 μm .

In [10, 16] by measuring the mass loss it was established that for modes usually applied in commercial production of bimetal, a layer of 5–7 μm thickness is removed from each of the welded surfaces. If we consider the area of the real surface along a line enveloping the microroughnesses at abrasive cleaning $HR_z 40$, the surface size will increase several times. Quantitative assessment of the real surface area along the microroughness envelope was performed proceeding from the average step of microroughness S_m and its profile height R_z according to GOST 2789–73. Therefore, at loss of a layer of 5–7 μm thickness, a layer not more than 0.3–0.5 μm thick is removed from a unit of the real surface, which is equal to thickness of films on the metal surface, removal of which through dissociation ensures cleaning and activation of the surface.

Conducted investigations and calculations allow suggesting the following mechanism of joint formation in explosion welding. After SCG has reached certain points on the surface to be welded, material heating and formation of «cold» plasma at supersonic flowing begin, and cleaning from oxides and contamination and surface activation occur under the cold plasma impact. Proceeding from the dimensions of SCG region the time of plasma impact is equal to approximately $1 \cdot 10^{-6}$ s. Clean and active surfaces come into contact in the collision point and form a joint, its formation going on beyond the contact point and being accompanied by intensive plastic deformation.

Thus, explosion welding is characterized by running in the above-mentioned sequence of the three-stage process of formation of strong bonds between the atoms of metals being joined: cleaning and activation of contact surfaces ahead of the contact point in SCG region under the impact of a plasma flow; formation of physical contact in the collision point; volume interaction and joint formation beyond the contact point.

Explosion welding quality is determined primarily by processes running ahead of the contact point, namely cleaning and activation of the surfaces being joined.

The proposed hypothesis led to an important conclusion, namely, in order to produce a strong joint at the start of the explosion welding process, prevent formation of initial lacks-of-penetration and regions of lower strength, it is necessary to provide the required SCG parameters and formation of a plasma layer for cleaning and activation of the surfaces being welded.

CONCLUSIONS

1. It is shown that at explosion welding as a result of the impact of a plasma flow cleaning of the surfaces

being welded from oxides and organic contamination and their activation ahead of the contact point occur through oxide dissociation, sublimation of contamination and ionization. Positive ions of metals formed as a result of oxide dissociation, partially come back to the cleaned surface, and atoms of oxygen, nitrogen, and carbon form the simplest gaseous compounds of CO_2 and H_2O type, which are removed from the welding gap by SCG.

2. The following sequence of the three-stage process of formation of strong bonds between the atoms of the joined metals in explosion welding is suggested: cleaning and activation of contact surfaces by SCG and thin plasma flows; formation of physical contact in the collision point; volume interaction with joint formation and plastic deformation beyond the contact point.

- Gelman, A.S., Chudnovsky, A.D., Tsemakhovich, B.D. et al. (1978) *Explosion cladding of steel*. Moscow: Mashinostroenie.
- Deribas, A.A., Zakharenko, I.D. (1975) On surface effects at oblique collisions of metal plates. *Fizika Goreniya i Vzryva*, 11(1), 151–153.
- Wittman, R.H. (1973) The influence of collision parameters on the strength and microstructure of an explosion welding aluminium alloy. In: *Proc. of 2nd Int. Conf. on Use of Explosive Energy in Manufacturing Metallic Materials of New Properties* (Marianske Lazne, CSSR, 1973), 153–158.
- Deribas, A.A. (1980) *Physics of explosion strengthening and welding*. Novosibirsk: Nauka.
- Otto, G. (1964) Aspect relating to the central institute for industrial research. In: *NATO Proc.* (Oslo, Norway, 1964), 1435–1441.
- Babul, W. (1968) *Niektore problemy laczenia wybuchowego*. Warszawa: IMP.
- Lysak, V.I., Kuzmin, S.V. (2005) *Explosion welding*. Moscow: Mashinostroenie.
- Pervukhina, O.L., Berdychenko, A.A., Pervukhin, L.B. et al. (2006) Influence of atmosphere composition on formation of bonding between titanium and steel in explosion welding. In: *Transact. on Explosion Welding and Properties of Welded Joints*. Volgograd: VolgGTU.
- Pervukhina, O.L., Pervukhin, L.B., Berdychenko, A.A. et al. (2009) Features of explosion welding of titanium to steel in a shielding atmosphere. *The Paton Welding J.*, 11, 18–22.
- Konon, Yu.A., Pervukhin, L.B., Chudnovsky, A.D. (1987) *Explosion welding*. Ed. by V.M. Kudinov. Moscow: Mashinostroenie.
- Baum, A.F., Orlenko, P.P., Stanyukovich, K.P. et al. (1975) *Explosion physics*. Moscow: Nauka.
- Ishutkin, S.N., Kirko, V.I., Simonov, V.A. (1980) Investigation of heat effect of shock-compressed gas on the surface of collision plates. *Fizika Goreniya i Vzryva*, 6, 69–73.
- Bondarenko, S.Yu., Pervukhina O.L., Rikhter, D.V. et al. (2009) Determination of the parameters of shock-compressed gas in the welding gap ahead of the contact point in explosion cladding. *The Paton Welding J.*, 11, 39–41.
- Senokosov, E.S., Senokosov, A.E. (2005) Plasma arc surface cleaning of metallic parts. *Metallurg*, 4, 44–47.
- Ashaev, V.K., Doronin, G.S., Ermolovich, E.I. et al. (2006) Application of methods of explosion welding and heat treatment of metals in production of multilayer armor compositions with higher bullet-proofness and viability. In: *Transact. on Armament, Automation, Control*. Kovrov.
- Gelman, A.S., Pervukhin, L.B., Tsemakhovich, B.D. (1974) Study of some problems of surface cleaning in explosion welding process. *Fizika Goreniya i Vzryva*, 2, 284–288.

8th INTERNATIONAL CONFERENCE ON BEAM TECHNOLOGY-2010

The 8th International Conference and Exhibition on Beam Technology STRAHLTECHNIK 2010 took place on 13–15 April 2010 at the Schweisstechnische Lehr- und Versuchsanstalt (SLV) Halle GmbH, Germany. The Conference was organised by the German Welding Society (DVS), SLV Halle GmbH and GSI. The sponsor support in holding the Conference was rendered by the known German companies manufacturing welding equipment: PRO-BEAM, FOCUS and CLOOS.

Approximately 100 participants came from 10 different countries, i.e. Germany, Bulgaria, China, Finland, France, Great Britain, Austria, Slovakia, Ukraine and the USA.

Schweisstechnische Lehr- und Versuchsanstalt (SLV) Halle GmbH celebrates its 80th anniversary in the year 2010. No doubt, the successful highlight of the anniversary was the International Conference on Beam Technology STRAHLTECHNIK 2010 held in Halle from 14 to 15 April 2010, which has been conducted by SLV Halle GmbH since 1996, and meanwhile established as an international forum of new developments in the field of the laser and electron beam technology. The event taking place on a three years basis united professionals from all over the world, who exchanged their experience about the latest developments in the field of beam methods and technology in industrial application. In lectures and poster presentations new ideas, paths of development and results in the field of the laser and electron beam technologies were presented and discussed, as well as impulses for the use of the processes were given.

The guests of honour were Prof. Dr.-Ing. Ulrich Dilthey, President of the International Institute of Welding (IIW), and Mr. John Bruskotter, President of the American Welding Society (AWS).



Section meeting

Most of the papers were dedicated to the issues of practical application of laser and electron beam welding. 15 lectures covered peculiarities of utilisation of laser and hybrid welding technologies. Among them were the lectures on orbital hybrid welding of pipes, application of hybrid welding in ship building, laser welding of BMW car doors, laser welding of dissimilar metals etc. The most complete and precise idea of the Conference can be obtained from the below list of the lectures and poster presentations.

Part 1: Solutions for the Field of Beam Technology

- Ing. *H.-J. Seilkopf*, Burg, Germany «EB and laser beam technologies for turbine construction: Experience and expectations»;
- *C. Punshon*, Cambridge, UK «Application of local vacuum EB welding and new steel development for fabrication of large offshore structures».

Part 2: Beam Welding in Industrial Application I

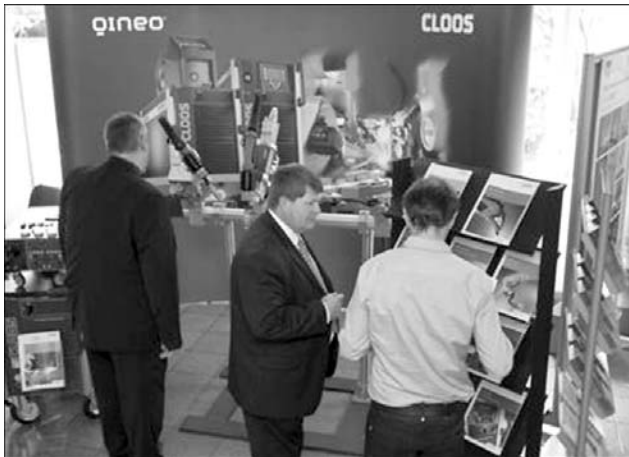
- Prof. Dr.-Ing. *P. Hoffmann*, Erlangen, Germany «Highly productive laser units for complex welded assemblies»;
- Dipl.-Ing. *A. Backhaus*, Aachen, Germany «Electron beam welding of titanium aluminides with a high portion of niobium»;
- Prof. Dr.-Ing. *S. Keitel*, Halle, Germany «Laser based girth welding technologies for pipelines – GMAW gets support».

Part 3: Basic and Further Development of Laser Beam Processes and Techniques

- Dr. *H. Staufer*, Wels, Austria «Increased welding speed and efficiency using the laser hybrid tandem welding process»;
- Dr. *O. Marten*, Pfungstadt, Germany «Qualification of focusing and imaging systems for industrial laser processing with brilliant beam sources in the multi-kilowatt range»;
- *I. Semyonov*, Kiev, Ukraine «Modelling of metal evaporation and plasma formation at pulsed laser processing»;
- *C. Thomy*, Bremen, Germany «Gap tolerant laser GMA hybrid welding of thin plates using the single mode fiber laser»;
- *I. Tomashchuk*, Le Creusot, France «Numerical modelling of dissimilar laser welding of copper to stainless steel».

Part 4: Beam Welding in Industrial Application II

- Dr.-Ing. *A. Gumenyuk*, Berlin, Germany «Orbital welding in pipeline construction – New possibilities by the application of high power lasers»;
- *A. Scherz*, Munich, Germany «Laser beam welding of aluminum doors in the large scale production on the new car generation of the BMW Group»;



Acquaintance with «CLOOS» exposition



Visit to «Josch Strahlschweisstechnik GmbH»

- Prof. Dr.-Ing. habil. *P. Seyffarth*, Rostock, Germany «Laser hybrid welding in ship building using high performance fiber lasers»;

- Dr. *P.I. Petrov*, Sofia, Bulgaria «Parameters used for electron beam welding — A comparative study»;

- *C. Paul*, Haiger, Germany «Laser beam GMA hybrid welding of large plate thicknesses at industrial application».

Part 5: Basic and Further Development of Electron Beam Processes and Technique

- Prof. Dr.-Ing. habil. *R. Zenker*, Freiberg, Germany «Multi spot technique and multi process technologies for welding and surface treatment using electron beam — State of the Art»;

- *Xichang Wang*, Beijing, China «Application of electron beam surf-sculpt technology during composites materials joining»

- Dipl.-Wirt.-Ing. (FH) *M. Streiber*, Dresden, Germany «Electron beam unit for thermal and non-thermal processes»;

- *B. Dance*, Cambridge, UK «Electron beam characterisation: «beam probing». A study of practical beam analysis at high and low powers for EB welding process control».

Poster presentations

- *B. Dance*, Cambridge, UK «Surface structuring using power beams; a review of recent laser and EB process developments»;

- Dipl.-Ing. *R. Weber*, Buseck, Germany «Wire feeding systems for laser beam applications»

- Dipl.-Phys. *F.-H. Rogner*, Dresden, Germany «Cold cathode electron beam sources a new possibility of cost efficient welding tools»;

- Dipl.-Ing. *M. Mavany*, Aachen, Germany «Enhancement of application of the laser-GMA hybrid welding by HyDRA-welding»;

- Dipl.-Ing. *T. Waschfeld*, Halle, Germany «Laser beam welding for the automotive industry — Nissan R35 GT-R»;

- Dipl.-Ing. *C. Schwalenberg*, Halle, Germany «Welding of titanium by using laser beam technology».

In keeping with tradition, the Conference was accompanied by a technical exhibition, where renowned suppliers and developers of beam technological equipment and processes demonstrated their achievements. The Conference participants visited expositions of a number of companies, such as Josch Strahlschweisstechnik GmbH in Teicha and PRO-BEAM Technologies GmbH in Halle, as well as took part in the festive reception at the State Museum of Prehistory with a visit to the Sky Disk of Nebula exposition.

Eruption of Eyjafjallajökull volcano in Iceland delayed departure of the Conference participants, but could not affect the general positive imperative of the event.

The Conference proceedings (papers in English and German) are available at the library of the E.O. Paton Electric Welding Institute.

Ing. I.L. Semyonov

XIV INTERNATIONAL SPECIALISED EXHIBITION «WELDING-2010»

XIV International Exhibition on welding and related processes «Welding-2010» was held from 18 till 21 May at Exhibition Complex «Lenexpo» (St.-Petersburg). This Exhibition has a more than 40 years' experience, and is considered, by right, one of the most representative events in the post-Soviet space. Its popularity is predetermined by the fact that St.-Petersburg is a city with an enormous research and industrial potential, a major centre of ship building, power machine building, motor-car construction and transport, and a recognised cultural centre.

Today St.-Petersburg and the North-West region of Russia make up the major welding engineering consumption market. In this connection, the Exhibition is the most important event, which meets challenges of further development of welding production in Russia and promotes upgrading of the Russian industrial sector and accelerated transition to a higher level of technological advancement.

The Exhibition was organised by Open Joint Stock Company «Lenexpo» with the assistance of the National Welding Committee of the Russian Academy of Sciences, National Agency for Control and Welding, Alliance of Welders of St.-Petersburg and North-West Region of the Russian Federation, known exhibition company «Messe Essen GmbH» (Germany), and Society of Machine Builders of China. Official support was rendered by the Government of St.-Petersburg, Russian Union of Manufacturers and Entrepreneurs, and Russian Chamber of Commerce and Industry. The Exhibition took place in a super-modern pavilion with a floor area of about 9000 m².

The main goal of the Exhibition was to establish numerous and mutually beneficial contacts to ensure successful commercial application of advanced innovation technologies, widening of volume of automation and robotisation of technological processes, and improvement of training of professional staff, specialists and welding operators.

About 200 companies from Belarus, Hungary, Germany, Italy, China, Russia, USA, Ukraine, Finland, Czechia, Switzerland and Sweden took part in the Exhibition. Among them were the leading Russian

and world manufacturers of welding equipment and consumables, R&D organisations, small businesses and trade missions. Many companies chose particularly St.-Petersburg and Exhibition «Welding» to hold their presentations and first shows of their welding equipment and technological processes. Among the participants were the leading Russian manufacturer of welding equipment «RPC «Engineering-Technological Service» (NPF ITS), ESAB (Sweden), «Abicor Binzel», «Svarohnaya Tekhnika» (Russia), «Lincoln Electric» (Russia), «Dukon» (Russia) – official dealer of «Lorch», «Dalex», «Fimer», Elma Tech, «Translas», «Koike», «Shtorm» (Russia), Russian and CIS offices of EWM (Germany) and «Blueweld» (Italy), «Thermal Dynamics» (USA), «Polysoude» (France), «ARGUS Pipeline Service» (Russia), «Kron SPb» – representative of «Oerlicon», «Air Liquide Welding», FRO, SAF in Russia, and «World of Welding» – representative of «Sol Welding» (Italy), etc. As already noted, partners of «Lenexpo» in organising the Exhibitions were Messe Essen and Society of Machine Builders of China. International pavilion «Essen Welding Pavilion» was arranged at the Exhibition. It comprised expositions of 12 companies from Germany, Hungary, Italy and USA, including one of the leaders of the world welding equipment market – «Carl Cloos Schweissttechnik GmbH», which specialises in production of robotic welding and cutting systems, development of new high-productivity processes and equipment, such as for hybrid laser-arc welding.

Of high interest to visitors was exposition of Company «MTI» (USA), which is the world leader in manufacture of friction welding machines. Equipment of the Company covers all currently existing types of friction welding: inertia, continuous drive, linear and rotation. They are used to advantage in agricultural machine building, aircraft engineering, aerospace engine construction, motor car construction, oil and gas industry, defence, and for making bimetal joints.

19 companies demonstrated their developments at the national booth of China. Among them were 9 companies from the Tianjin province, which presented





advanced welding technologies, equipment and consumables.

One should note wide-scale advances of China's manufacturers of welding consumables. For example, Company «Tianjin Bridge» (founded in 1957) is one of the 40 largest enterprises in this province and one of the largest manufacturers of welding consumables in China with an annual sales volume of 600,000 t. The range of products includes 350 types of welding consumables produced under the «Bridge» trade mark.

Company «Tainjin Sainteagle Welding» produces a wide range of rutile electrodes for low- and medium-carbon steels, electrodes providing decreased content of diffusible hydrogen in deposited metal, electrodes for welding low-temperature and heat-resistant steels, and gas-shielding electrode materials for tungsten-electrode welding without extra argon shielding.

Ukraine was represented at the Exhibition by the Kramatorsk Factory for autogenous equipment «DONMET», Odessa Open Joint Stock Company «Zont» (subsidiary in Russia – «Avtogenmash Ltd.» in Tver), Kakhovka Factory for electric welding equipment (agency in Russia – Closed Joint Stock Company «Kakhovka», Belgorod), Simferopol Motor Factory, E.O. Paton Electric Welding Institute of the NAS of Ukraine, Ilnitsky Factory MSO, and Factory «Artyom-Kontakt».

Special activity was noted at the booth of the E.O. Paton Electric Welding Institute. Many visitors expressed interest in modern developments of the Institute, specific places of their application, and innovation projects of the last years. Positive estimates were said about the publication of the Institute – «Avto-matcheskaya Svarka» Journal, owing to the possibility of obtaining from it the most diverse information on topical problems of welding production, acquaintance with novelties, as well as abstracts from the leading profiled world journals.

International Scientific-and-Technical Conference «Advanced Technologies and Development of Welding Science and Practice» was held during the Exhibition on 19–20 May. Papers «Evaluation of Residual Life of Welded Structures» by N.P. Alyoshin (Russia), «Advanced Welding Technologies and Related Processes» by K. Middeldorf (Germany), «Development and Application of Standards in the Field of Welding Production» by A.I. Chuprak, «Russian Welding Electrodes in a Period of General Recession» by Z.A. Sidlin (Russia), etc. were presented at the Conference and arose much interest.

The work in the presentation zone of the Exhibition followed a special program. It included presentations «ESAB Solutions for Welding and Cutting to Increase Efficiency in Ship Building» by ESAB, demonstration of Russian novelties – developments of AVTOVAZ, master classes for advanced training of welders by using adapted simulators (Nevsky Polytechnic Lyceum), Russian-German cooperation on innovations in welding industry – application of welding simulators at training centres of Germany and Russia, energy-saving technologies and environmental protection in welding production, new welding consumables, issues associated with development and application of technologies and equipment, and fine arts in welding.



An interesting initiative of the Exhibition organisers was holding a forum of young welders – meeting of young welding specialists from technical institutes of higher education and vocational colleges, as well as graduates of secondary schools with leading welding specialists. The «Welding. Process Application Fields» film was demonstrated, papers were presented on application of welding under the water, in space and in medicine, presentations were made by heads of welding chairs of the St.-Petersburg institutes, winners of the city competition of welders were awarded, and concert was arranged within the framework of the forum, the goal of which was to acquaint young people with a range of up-to-date welding equipment and help them to get an idea of the new joining technologies.

Summarising, it should be noted that the Exhibition left a favourable impression. It became a real tool for development and improvement of manufacturing, allowed a wide information exchange, strengthening of scientific and business cooperation and establishing new contacts. Also, it gave impetus to creative explorations.

Prof. V.I. Lipodaeu, PWI

FIFTH INTERNATIONAL CONFERENCE «MATHEMATICAL MODELLING AND INFORMATION TECHNOLOGIES IN WELDING AND RELATED PROCESSES»

The 5th International Conference «Mathematical modelling and information technologies in welding and related processes» (MMITWRP-2010) took place in vil. Katsiveli (Crimea, Ukraine) at House of Creativity of Scientists of the NAS of Ukraine in May 25–28, 2010. It was organized by the National Academy of Sciences of Ukraine, E.O. Paton Electric Welding Institute of the NASU and Local Charity Foundation «Welding Community».

More than 60 specialists from Ukraine, Russia, Germany and Austria took part in the Conference work. The Conference was organized in the form of plenary and poster sessions, working languages of the Conference were Russian and English.

32 papers were presented during a period of the plenary session. The Conference was opened by academician of the NASU V.I. Makhnenko with review paper «Prospects of development of mathematical modelling and information technologies in welding and related processes» (E.O. Paton Electric Welding Institute of the NASU, Kiev, Ukraine), in which the results of mathematical modelling were considered ap-

Mathematical models and calculation algorithms of the heat, mass and electric transfer processes taking place in welding and special electrometallurgy processes were investigated in oral and plenary papers. The problems of modelling of the process of electrode metal drop formation; computational investigation of the effect of pulse laser-arc heat source on metal and other problems were also discussed.

The abstracts of papers together with program of the Conference work were published to the beginning of the Conference. Proceedings of the Conference will be published to the end of 2010. The collection of papers mentioned above as well as Proceedings of First–Fourth International Conference can be available from editorial board of «The Paton Welding Journal».

The Program and Organizing Committees of the Conference express their gratitude to the academicians of the NAS of Ukraine I.K. Pokhodnya and V.I. Makhnenko for permanent attention and support of young scientists which prepared approximately half of all papers, presented at the Conference.



plicable to such welding problems as solidification of liquid pool; two-phase zone theory; stability of microstructure of the primary solidification; criteria of weldability of modern steels and alloys; development of critical technologies in welding and related processes; prediction of a period of safe operation of welded units.

Modern means of mathematical modelling and possibilities of standard commercial packages were discussed in the paper.

The Conference was held in creative and friendly atmosphere and was concluded by a trip of the participants of the Conference to the peak of Ai-Petri mountain with visiting of Uchan-Su waterfall and walking along the sea-front in Yalta.

The next sixth international conference will be held in last decade of May, 2012.

Dr. A.T. Zelnichenko, PWI



SESSION OF THE SCIENTIFIC COUNCIL ON NEW MATERIALS AT THE NATURAL SCIENCES COMMITTEE OF THE INTERNATIONAL ASSOCIATION OF THE ACADEMIES OF SCIENCES

The 15th Session of the Scientific Council on New Materials at the Natural Sciences Committee of the International Association of the Academies of Sciences (IAAS) took place on 26–27 May 2010 in Kiev at the E.O. Paton Electric Welding Institute. The subject matter of the Session was «New Processes for Production and Processing of Metallic Materials».

Over 100 scientists and specialists in the field of materials science from academies of sciences, institutes of higher education and enterprises of Belarus, Kazakhstan, Russia and Ukraine took part in the Session of the Scientific Council.

The first day of the Session, 26 May, was dedicated to meetings of the sections on copper-base and polymeric materials, and the plenary session took place on 27 May. This allowed discussing at the plenary session some proposals and remarks on further activities of the Scientific Council put forward in the course of the sections.

The plenary session of the Scientific Council was opened by Prof. B.E. Paton, Chairman, President of IAAS, President of the NAS of Ukraine and Director of the E.O. Paton Electric Welding Institute. He said that the plenary session of 2010 would cover a wide range of problems in the field of materials science. 21 papers were submitted to the plenary session, from which the most interesting 12 papers were selected for presentation. A large number of papers are indicative of an increasing interest to the Scientific Council on New Materials.

Prof. B.E. Paton introduced participants to the program and agenda of the plenary session, at which the papers were to be presented by scientists from Belarus, Kazakhstan, Russian Federation and Ukraine.

Prof. E.N. Kablov, Academician of the Russian Academy of Sciences (All-Russian Scientific Research Institute of Aviation Materials – VIAM, Moscow, RF) presented paper «Advanced Technologies for Manufacture of Parts from a New Generation of Heat-Resistant Alloys». He noted that brazing is widely used now in aircraft engineering. About 50 grades of tin, lead, copper, silver, nickel and titanium based brazing filler alloys are employed in aviation for brazing different components. Part of these filler alloys can be made only in the form of powders. VIAM launched a unit that allows manufacturing the high-

quality powder filler alloys on industrial scales. Associates of the Institute developed fundamentally new technologies for thermomechanical treatment of hard-to-deform heterophase alloys, providing formation of regulated structures with increased ductility at optimal temperature-rate deformation parameters. Also, the methods were developed for production of castings with directed and single-crystal structures.

Paper «Electron Beam Technology for Production of Micro- and Nanosized Powders of Inorganic Materials» by Prof. B.A. Movchan (E.O. Paton Electric Welding Institute, Kiev, Ukraine), Academician of the NAS of Ukraine, was dedicated to new technologies for manufacture of micro- and nanosized powders of inorganic materials. The International Centre for Electron Beam Technologies of the E.O. Paton Electric Welding Institute built an electron beam unit for production of solid- and liquid-phase substances with nanoparticles of inorganic materials. The developed technology allows controlling the composition, shape and structure of nanoparticles of inorganic materials, mostly different oxides.

Prof. V.E. Panin (Institute of Strength Physics and Materials Science, Siberian Branch of the Russian Academy of Sciences, Tomsk, Russia), Academician of the Russian Academy of Sciences, dedicated his paper «Topical Problems of Nanostructuring of Surface Layers of Structural Materials and Their Welded Joints» to investigation of the effect of nanostructuring of surface layers on strength and service properties of materials. Deposition of nanostructured coatings provides increase not only in strength but also in ductility of steel, leads to increase of fatigue strength in cyclic tests to alternating bending, as well as improvement of wear resistance and thermal stability of treated materials.

Prof. N.P. Alyoshin (Research and Education Centre «Welding and Inspection» at the N.E. Bauman Moscow State Technical University, Moscow, RF), Academician of the Russian Academy of Sciences, told about advantages and drawbacks, as well as prospects of development of acoustic methods for non-destructive testing.

Paper «Scientific Bases of Production of Nanometallic Materials» by Prof. S.A. Firstov (Institute for Problems of Materials Science, Kiev, Ukraine), Academician of the NAS of Ukraine, focused on the prob-



lems to be addressed by scientists in transition from materials with microcrystalline structure to materials with nanocrystalline structure, as well as properties of materials with such a structure. If before the improvement of strength properties of structural materials was provided mainly by development of alloys with new chemical and phase compositions, new ways of improving properties of structural materials have been outlined in the last years, consisting in targeted formation of nanocrystalline structure in these materials.

«Development of High-Strength Titanium Alloys for Marine Engineering» was the subject of the paper by associates of CRISM «Prometej» (St.-Petersburg, Russia), which was presented by Dr. B.G. Ushakov. Alloys intended for manufacture of structures operating in sea water should have high corrosion resistance, good weldability and high mechanical properties, in particular, ductility in pressure treatment. Such alloys were developed as a result of completion of a large scope of research. New materials based on titanium of the 5V type feature an increased level of strength characteristics and optimal combination of service properties (fracture toughness, resistance to elasto-plastic deformations, creep resistance).

Prof. V.I. Dubodelov (Physico-Technological Institute of Metals and Alloys, Kiev, Ukraine), Corresponding Member of the NAS of Ukraine, talked about application of electromagnetic effects and an ingenious

MHD technique in new processes of production of parts from non-ferrous metals, steel and cast iron.

The paper by associates of the Institute for Metal Physics of the NAS of Ukraine (Kiev), presented by Prof. V.F. Mazanko, considered the abnormal transfer phenomenon under external effects on metals and methods for its practical application. It is the opinion of the authors that this phenomenon can be used for pulse pressure welding methods, thermochemical-mechanical treatment, modification of surface layers of metal, repair of worn-out surfaces, production of coatings with different properties: corrosion- and wear-resistant, anti-emissive and decorative, and with amorphous and nanostructured state.

Participants of the session during discussions had the opportunity to share opinions on the presented papers and state-of-the-art in the field of development of new materials in their countries, estimate activities of the Scientific Council on New Materials, and express wishes on their improvement. Annual sessions of the Scientific Council on New Materials of IAAS allow preserving and developing creative contacts between scientists of different countries, and promote intensification of information exchange between them.

It is scheduled to hold the next Session of the Scientific Council on New Materials of IAAS in May 2011 at the E.O. Paton Electric Welding Institute.

Dr. I.A. Ryabtsev, PWI



SPECIALIZED FORUM «PATON EXPO 2010»

On June 1–3, 2010 the traditional specialized industrial forum «PATON EXPO 2010» was held at «KievExpoPlaza» Exhibition Center. The Forum included the following exhibitions: «Welding. Related Technologies», «Pipeline Transportation», «Non-Destructive Testing», which were organized by TC «E. O. Paton Electric Welding Institute» of the NAS of Ukraine and «Association OKO» with the support of the NAS of Ukraine, companies «Naftogaz Ukrainy», «Ukrtransgaz», Association of Industrial Armature Engineering of Ukraine, and Society of Welders of Ukraine. Forum sponsor was «Technology Transfer Center Ltd.» of the E.O. Paton Electric Welding Institute.



B.E. Paton, President of the NAS of Ukraine, General Director of STC «E.O. Paton Electric Welding Institute», O.T. Draganchuk, Director of MSMA Research Institute, N.V. Zasulsky, President of Kiev Chamber of Commerce, as well as representatives of Chambers of Commerce of a number of foreign countries, N.A. Androshchuk, Executive Director of Association of Industrial Armature Engineering of Ukraine, V.G. Fartushny, President of the Society of Welders of Ukraine, M.V. Bekker, Chief Engineer of «Ukrtransgaz», Ambassadors Extraordinary and Plenipotentiary of Italy and India in Ukraine participated in the Opening Ceremony.

Displays of about 50 companies from Ukraine, Russia, Iran, Austria, Italy and Poland were on show in the three exhibitions. Exhibitors of «Welding. Related Technologies» Exhibition included the booths of PWI, PWI DB, two pilot plants (PPWE and PPWC), STC «Seproz», known manufacturers of welding equipment and consumables, such as Fronius-Ukraine, DONMET Plant of Autogenous Equipment, Zont, Fronius Electrode, Binzel Ukraine, Zaporozhsteklodyly, etc.



Participants of «Non-Destructive Testing» Exhibition included «Association OKO», uniting leading local developers and manufacturers of NDT means (UkrNIINK, Ultrakonservis and Promprilad), and ONIKO which is the official representative of GE Inspection Technologies, Magnaflux, AGFA and SONY companies in Ukraine.

Achievements of Italian enterprises were presented in Mipa Italy booth (production of equipment for arc welding and thermic cutting, stainless and aluminium welding wires and rods, as well as flux-cored wires).

Scientific-Technical Conference «Integrated Approach to Solving the Problems of Non-Destructive Testing of the Main Pipelines, Pipeline Fittings: Technology of Diagnostics, Welding, Surfacing, Repair» was held within the framework of the Forum.



In conclusion it should be noted that the annual «Welding. Related Technologies» Exhibition traditionally is the main profile exhibition in Ukraine. During three days its visitors could become familiar with modern developments and range of manufactured specialized equipment and consumables.

*Prof. V.N. Lipodaev
Dr. A.T. Zelnichenko, PWI*

SUBSCRIPTION FOR «THE PATON WELDING JOURNAL»

If You are interested in making subscription directly via Editorial Board, fill, please, the coupon and send application by fax or e-mail.

The cost of annual subscription via Editorial Board is \$324.

Telephones and faxes of Editorial Board of «The Paton Welding Journal»:

Tel.: (38044) 287 6302, 271 2403, 529 2623

Fax: (38044) 528 3484, 528 0486, 529 2623.

«The Paton Welding Journal» can be also subscribed worldwide from catalogues of subscription agency EBSCO.

SUBSCRIPTION COUPON	
Address for journal delivery	
Term of subscription since	200 till 200
Name, initials	_____
Affiliation	_____
Position	_____
Tel., Fax, E-mail	_____



ADVERTISEMENT IN «THE PATON WELDING JOURNAL» (DISTRIBUTED ALL OVER THE WORLD)

«АВТОМАТИЧЕСКАЯ СВАРКА»

RUSSIAN VERSION OF «THE PATON WELDING JOURNAL» (DISTRIBUTED IN UKRAINE, RUSSIA AND OTHER CIS COUNTRIES)

External cover, fully-colored:

- First page of cover (190×190 mm) – \$700
- Second page of cover (200×290 mm) – \$550
- Third page of cover (200×290 mm) – \$500
- Fourth page of cover (200×290 mm) – \$600

Internal cover, fully-colored:

- First page of cover (200×290 mm) – \$400
- Second page of cover (200×290 mm) – \$400
- Third page of cover (200×290 mm) – \$400
- Fourth page of cover (200×290 mm) – \$400

Internal insert:

- Fully-colored (200×290 mm) – \$340
- Fully-colored (double page A3) (400×290 mm) – \$570
- Fully-colored (200×145 mm) – \$170

- Article in the form of advertising is 50 % of the cost of advertising area
- When the sum of advertising contracts exceeds \$1000, a flexible system of discounts is envisaged

Technical requirement for the advertising materials:

- Size of journal after cutting is 200×290 mm
- In advertising layouts, the texts, logotypes and other elements should be located 5 mm from the module edge to prevent the loss of a part of information

All files in format IBM PC:

- Corell Draw, version up to 10.0
- Adobe Photoshop, version up to 7.0
- Quark, version up to 5.0
- Representations in format TIFF, color model CMYK, resolution 300 dpi
- Files should be added with a printed copy (makeups in WORD for are not accepted)